

Environmentally Responsive Hydrogels:
Development and Integration with Hard Materials

by

Prithwish Chatterjee

A Dissertation Presented in Partial Fulfillment
of the Requirements for the Degree
Doctor of Philosophy

Approved November 2015 by the
Graduate Supervisory Committee:

Lenore Dai, Co-Chair
Hanqing Jiang, Co-Chair
Mary Laura Lind
Hongbin Yu
Hongyu Yu

ARIZONA STATE UNIVERSITY

December 2015

ABSTRACT

Environmentally responsive hydrogels are one interesting class of soft materials. Due to their remarkable responsiveness to stimuli such as temperature, pH, or light, they have attracted widespread attention in many fields. However, certain functionality of these materials alone is often limited in comparison to other materials such as silicon; thus, there is a need to integrate soft and hard materials for the advancement of environmentally responsive materials.

Conventional hydrogels lack good mechanical properties and have inherently slow response time, important characteristics which must be improved before the hydrogels can be integrated with silicon. In the present dissertation work, both these important attributes of a temperature responsive hydrogel, poly(N-isopropylacrylamide) (PNIPAAm), were improved by adopting a low temperature polymerization process and adding a silicate compound, tetramethyl orthosilicate. Furthermore, the transition temperature was modulated by adjusting the media quality in which the hydrogels were equilibrated, e.g. by adding a co-solvent (methanol) or an anionic surfactant (sodium dodecyl sulfate). Interestingly, the results revealed that, based on the hydrogels' porosity, there were appreciable differences when the PNIPAAm hydrogels interacted with the media molecules.

Next, an adhesion mechanism was developed in order to transfer silicon thin film onto the hydrogel surface. This integration provided a means of mechanical buckling of the thin silicon film due to changes in environmental stimuli (e.g., temperature, pH). We also investigated how novel transfer printing techniques could be used to generate patterned deformation of silicon thin film when integrated on a planar hydrogel substrate. Furthermore, we explore multilayer hybrid hydrogel structures formed by the integration

of different types of hydrogels that have tunable curvatures under the influence of different stimuli. Silicon thin film integration on such tunable curvature substrates reveal characteristic reversible buckling of the thin film in the presence of multiple stimuli.

Finally, different approaches of incorporating visible light response in PNIPAAm are discussed. Specifically, a chemical chromophore- spirobenzopyran was synthesized and integrated through chemical cross-linking into the PNIPAAm hydrogels. Further, methods of improving the light response and mechanical properties were also demonstrated. Interestingly, such a system was shown to have potential application as light modulated topography altering system

DEDICATION

To Mom and Dad

For your love and support

ACKNOWLEDGMENTS

During the journey of my graduate study I have been very fortunate of meeting and collaborating with some outstanding people who I would like to acknowledge for their invaluable contribution. First and foremost, I would like to extend my deepest gratitude to Prof. Lenore Dai, for being such a wonderful mentor. Her deep passion for research and commitment to excellence are some of the many traits that have deeply motivated me. I am thankful for her support, patient guidance and constant encouragement towards my work. I feel fortunate for having this opportunity of working under her able tutelage and wish to carry forward the valuable scientific and professional skills I have gained from her. Next, I would like to thank Prof. Hanqing Jiang for his guidance and advice. I have been inspired by his infectious passion for research and am sincerely thankful for all the thought provoking discussions I had with him. I would also like to extend my warmest regards and thank my thesis committee members, Prof. Mary Laura Lind, Prof. Hongbin Yu and Prof. Hongyu Yu for their valuable suggestions and comments on this work.

I would like to take this opportunity to thank past and present members of Prof. Dai's research team who have provided a stimulating environment for research. Special thanks to Haobo Chen, Dr. Mingmeng Zhang, Elizabeth Nofen and Stella Nickerson for their help in various parts of this dissertation work. I would also like to extend my special gratitude to Yuping Pan and Dr. Teng Ma for their valuable help with the gel-silicon integration project. I have also been fortunate of collaborating with some gifted undergraduate and graduate students-Annie Dai, Onkar Ghag and Eric Stevens- who have made integral contributions for many sections of this dissertation work and I am grateful for their hard work. I would also like to extend my warmest regards to past and present

members of Prof. Hanqing Jiang's research group for their help and support in many projects, especially Xu Wang and Wenwen Xu.

Last but not the least, I would like to thank my wonderful friends who have made my stay at Tempe truly memorable, especially Sayantan Das, Nilesh Badwe, Priyanka Badwe, Sudhanshu Shekhar Singh and Kaushik Sridhar. Most importantly, I would like to thank my family and friends back in India for believing in me to take this path. I am especially grateful to my dad and mom for showering tremendous love and always motivating me to achieve more. Special thanks to my sister and grandmother for their love, I feel truly blessed for having such wonderful people in my life.

Finally, I sincerely acknowledge the external financial support provided by the National Science Foundation and American Chemical Society Petroleum Research Fund and also gratefully acknowledge the use of facilities of the Leroy Eyring Center for Solid State Science at Arizona State University.

TABLE OF CONTENTS

	Page
LIST OF TABLES	ix
LIST OF FIGURES	x
CHAPTER	
1 INTRODUCTION	1
2 BACKGROUND AND MOTIVATION	5
2.1 Environmentally Responsive Hydrogels	5
2.1.1 Classification and Applications	5
2.1.2 Swelling Kinetics and Thermodynamics	20
2.2 Strategies of Integrating Soft and Hard Materials.....	26
2.3 Motivation of Work	33
2.3.1 Tuning the Transition Temperature and Mechanical Properties of Poly(N- isopropylacrylamide)	33
2.3.2 Incorporation of Visible Light Response in Poly(N-isopropylacrylamide) Hydrogels	36
2.3.3 Integration of Environmentally Responsive Hydrogels with Silicon	39
3 EXPERIMENTAL METHODOLOGY	42
3.1 Materials	42
3.2 Synthesis of Macroporous and Microporous PNIPAAm Hydrogels	42
3.3 Preparation of PNIPAAm/PAA Bilayer Hydrogels.....	43
3.4 Bonding of Silicon to PNIPAAm Hydrogels	43

CHAPTER	Page
3.5 Synthesis of Light Responsive Hydrogels.....	44
3.5.1 Physical Approach	44
3.5.2 Chemical Approach	44
3.6 Materials Characterization	45
4 RESULTS AND DISCUSSIONS	48
4.1 Tuning the Swelling Kinetics of PNIPAAm Hydrogels	48
4.1.1 Dependence of Synthesis Technique on Morphology and Swelling Kinetics	48
4.1.2 Dependence of Synthesis Conditions on Mechanical Properties.....	50
4.2 Tuning the Transition Behavior of Poly(N-isopropylacrylamide) Hydrogels	54
4.2.1 Effect of Co-Solvent	54
4.2.2 Effect of Surfactant	60
4.3 Integration of Poly(N-isopropylacrylamide) Hydrogels with Silicon	65
4.3.1 Development of Adhesion Mechanism between Hydrogels and Silicon..	65
4.3.2 Response Properties of Silicon Integrated with Hydrogels	69
4.3.2.1 Buckling Behavior of Non-Patterned Silicon Thin Film on Hydrogels	69
4.3.2.2 Buckling Behavior of Patterned Silicon Thin Film Integrated on Planar Hydrogels.....	72
4.3.2.3 Buckling Behavior of Silicon Thin Film on a Curved Bilayer Hydrogels with Tunable Curvature	78

CHAPTER	Page
4.4 Incorporation of Visible Light Response in Poly(N-isopropylacrylamide)	85
4.4.1 Comparison of Physical and Chemical Approaches	85
4.4.2 Increasing the Response and Mechanical Properties	95
4.4.3 Application of Light Responsive Hydrogels in Tactile Devices	102
5 SUMMMARY AND FUTURE WORK.....	104
5.1 Summary	104
5.2 Future Work	106
REFERENCES	109
APPENDIX	
A PYRROLE-BASED POLY(IONIC LIQUIDS) AS EFFICIENT STABILIZERS FOR FORMATION OF HOLLOW MWCNT PARTICLES	130

LIST OF TABLES

Table	Page
1. Comparison of LCST and Heat Absorption of the Macroporous and Microporous Thermo-Responsive PNIPAAm Gels During Heating and Cooling Cycles	85
A1. PIL-ICP Polarity Importance in Dispersing MWCNT in Various Solvents (Stable Dispersion Denotes Greater Than 6 Month Stability).....	143

LIST OF FIGURES

Figure	Page
2.1	Major Classification of Environmentally Responsive Hydrogels: (a) Schematic Representation of Transformation of Hydrogel From Hydrophobic to Hydrophilic, (b) Examples of Ph, Temperature and Light Responsive Hydrogels7
2.2	Structures of Some Temperature-Sensitive Polymers, (a) Poly(N-Isopropyl acrylamide), (b) Poly(N,N-Diethylacrylamide) (PDEAAM) ,(c) Poly(NIPAAm-Co-BMA)8
2.3	Schematic of UCST and LCST Phase Diagram : (a) Lower Critical Solution Temperature (LCST) Phase Diagram (b) UCST Type Phase Diagrams 10
2.4	Classification and Types of Ph Responsive Hydrogel: (a) Schematic Representation of the Swelling and De-Swelling of Ph Responsive Polymers, Compositional Reversibility of: (b) Anionic and, (c) Cationic Hydrogels in Response to Solution Ph Changes (d) Ph Responsive Hydrogel Application In Drug Delivery. Adopted and Modified From (Gupta, Vermani, and Garg 2002, Koetting and Peppas 2014)15
2.5	Classification and Application of Light Responsive Hydrogels: (a) Light Responsive Hydrogels Classified according to the Responsive Wavelength, (b) “Smart” Microchannel Based On IR Responsive Hydrogels,, (c) UV Responsive Hydrogels Utilized in Controlled Drug Delivery Application. Adopted From (Mura, Nicolas, and Couvreur 2013, Lo, Zhu, and Jiang 2011) 18

Figure	Page
2.6	22
<p>Different Stages of Hydrogel Transition: the Swollen Phase of the Gel (Left) is dominated by Polymer-Solvent interactions obtaining the best Mixing of the Polymer Chains and the Aqueous Solution. the Shrunken Phase of the Hydrogel (Right) is Determined by Polymer-Polymer-interactions, which Remove Solution Out of the Gel. (Adopted From (Richter et al. 2008)</p>	
2.7	24
<p>Different Diffusion Processes :(a) Case I Diffusion (b) Anomalous Diffusion, (c) Case II Diffusion. Adopted From (Rossi and Mazich 1991)</p>	
2.8	30
<p>Steps In A Soft Lithography Process (a) PDMS Mold is Prepared, (b) PDMS Mold Isoaked in A Solution (c) PDMS Mold is Pressed On the Desired Solution (d) PDMS is Peeled off and the Pattern is Revelaed On the Surface</p>	
2.9	32
<p>Example of Soft and Hard Material Integration (a),(b) Wrinkles in Hard/Soft Matter: Buckling Pattern Developed On Ultrathin Silicon (Hard)Due to Release of Pre-Strained PDMS (Soft) Substrate, (c) Health Monitoring Tattoo (d) Hemispherical Electronic Eye Mimicking the Eye of Bee</p>	
4.1	49
<p>SEM and Confocal Microscopy For Morphology Studies of Pnipaam Hydrogel: (a), (b) Macroporous Hydrogel with Average Pore Length of ~ 50μm; (c), (d) Microporous Hydrogel with Average Pore Length ~ 1 μm</p>	
4.2	51
<p>Mechanical Properties of Macroporous and Microporous Hydrogel: (a) Comparison of Re-Swelling Rate of the Hydrogels; (b) Gap Change in Rheometer For Macroporous and Microporous Hydrogels; (c) Rheometer Analysis of Macroporous and Microporous Hydrogels; D)Instron Compressive Analysis of Water Saturated Hydrogels.....</p>	

Figure	Page
4.3 DMA Analysis of Dry Hydrogel: (a) Macroporous Pnipaam Hydrogel; (b) Microporous Pnipaam Hydrogel.....	53
4.4 Transition Temperature and Enthalpy Change During Transition of Pnipaam Hydrogel with Variation of Methanol Percentage: (a)DSC thermograms of Macroporous Hydrogel; (b) DSC Thermograms of Microporous Hydrogel; (c) Comparison of LCST with Change in Porosity and Change of Solvent; (d) Comparison of Heat of Fusion with Change in Porosity and Change of Solvent	57
4.5 Effect of Methanol Concentration On the Swelling Ratio and Rheological Properties (a) Comparison of Swelling Ratio Between Macroporous and Microporous Hydrogel Under Different Methanol Concentration (b) Rheometer Analysis of Macroporous Hydrogel Equilibrated with 20 % Methanol Concentration.....	59
4.6 Transition Temperature and Enthalpy Change During Transition of Pnipaam Hydrogel with Variation of Surfactant Concentration: (a)DSC Thermograms of Macroporous Hydrogel; (b) DSC Thermograms of Microporous Hydrogel; (c) Comparison of Transition Temperature with Change in Porosity and Change of Surfactant Concentration; (d) Comparison of Heat of Fusion with Change in Porosity and Change of Surfactant Concentration	63
4.7 Effect of Surfactant On the Mechanical Properties and Swelling Ratio (a) Rheometer Analysis of Macroporous Gel Equilibrated with 10 Mm; (b) Swelling Ratio Under Different SDS Concentration	64

Figure	Page
4.8 (a) Layer-Assembled Structure of the Pnippaam/PDMS Integrated with Silicon Nanoribbons. (b) Schematics of the Hydrogel Swelling/Shrinking Drivable Silicon Thin Ribbons.	66
4.9 (a) XPS Spectra of the Pnippaam-Based Hydrogel. the Exact Value of Binding Energies and their Chemical State of the Corresponding Elements At Each Peak Are Labelled. the Inset is Core-Level Spectrum of the C in (a) (Blue Line is From the Raw Data); (b) Formation of Pnippaam-Based Gel Integrated with TMOS.	67
4.10 Buckling Pattern On Silicon Ribbons Integrated with Thermoresponsive Pnippaam Hydrogels: i) After Transfer Printing, ii) 2 min after Immersion into Hot Water (45 °c), iii) 4 min, iv) 6 min, v) 8 min, vi)10 min, and vii) 12 min	70
4.11 Hydrogel and Silicon Thin Film Integration (a) Schematic of The Hydrogel Swelling/Shrinking Drivable Silicon Thin Ribbons, (b) Layer-Assembled Structure (c) Demonstration of The Thin Si Diamond Network Structure Becoming Buckled When The Hydrogel Substrate Shrinks.....	70
4.12 Schematic Showing of the Process of Integrating Thin Silicon Ribbon (300 Nm Thick) with Pnippaam Gel: A UVO Mask Was Used to Control the Buckling Pattern.....	73
4.13 Environmental Scanning Electron Microscopy Images of Controlled Buckling Pattern of the Integrated Silicon On Pnippaam Hydrogel: (a) (Mask:	

Figure	Page
30 μm Active – 90 μm Inactive) Wavelength $68.5 \pm 6.3 \mu\text{m}$; (b) Close-Up Image of the Pop-Up Structure; (c) (Mask: 30 μm Active – 190 μm Inactive) Wavelength $142.6 \pm 6.8 \mu\text{m}$	74
4.14 Material Characterization of Pnipaam Hydrogel: (a) Rheological Testing of the Hydrogel; (b) DSC Capturing LCST Behavior of Gels and Quantifying Heat Absorption During Transition	76
4.15. Bilayer Hydrogels with Tunable Curvature: (a) Pictorial Representation of a Bilayer Hydrogel; (b) Finite Element Modeling of Bilayer Gels depicting the Various Stages of Swelling; (c) Ph Responsiveness of the Bilayer Hydrogel, Top Layer is the Pnipaam Hydrogel (Temperature Sensitive) and Bottom Layer is Co-Polymer of Acrylic Acid and Pnipaam Hydrogel (Ph Sensitive)	79
4.16. Responsiveness of Silicon Thin Film Integrated with Bilayer Hydrogel: (a) Effect of Ph (Ph= 10); (b) Buckling of Silicon Ribbons At the Edges (Scale Bar $50\mu\text{m}$); (c) Flat Silicon At the Center (Scale Bar $50\mu\text{m}$); (d) Pictorial Representation of Buckling Under Influence of Temperature; (E) Horizontal View of Buckling Under Influence of Temperature $> 32 \text{ }^\circ\text{C}$ and Ph= 10 (Scale Bar $100\mu\text{m}$)	81
4.17 Rheological Characterization of Bottom Layer (Ph Sensitive): G^* As A Function of Strain At Constant Frequency of 1 Hz Under Different Ph Conditions	82

Figure	Page
4.18 Environmental Response of the Bilayer Hydrogel: (a) DSC Capturing LCST Behavior of Top Layer and Measuring Heat Absorption During Transition; (b) Linear Dimension Change of Bottom and Top Layer of Gels with Ph.....	83
4.19 Effect of Laser Light (488 Nm) on different Hydrogels as Function of Time (2 Minutes) (a) Cross-Linked Pnipaam with No Chromophore and (b) Pnipaam with A 2% Chlorophyllin (c) Illustration Depicting the Effect of Light on the Electrons of Chlorophyllin and there Imminent Release of Heat Energy	86
4.20 Chemical Structure of Spirobenzopyran and Light Responsive Behavior: (a) Chemical Structures and Isomerization of Spirobenzopyrans Due to Light Irradiation, (b) UV Spectroscopy of Spirobenzopyran under Different Conditions.....	91
4.21 Effect of Light On Spirobenzopyran-PNIPAAm Hydrogels As Function of Time: Confocal Image and Effect of 488 Nm Laser on co(Spirobenzopyran-PNIPAAm) Hydrogels Morphology; (Left) Shows Initial Pore Size of the Hydrogel Network and (Right) Shows Increase of Pore Size After Laser Light is Irradiated For 2 Seconds, (Inset) Bulk Co(Spirobenzopyran-PNIPAAm) Hydrogel Demonstrating Bulk Change in 30 Seconds On Account of White Light	92

Figure	Page
4.22 (a),(b) Effect of Chromophore Content On the Visible Light Response of PNIPAAm, (c) UV Spectra of Spirobenzopyran Molecule and Hydrogel Integrated with Spirobenzopyran	94
4.23 Effect of Low Temperature Synthesis On Pore Size and Swelling Ratio (a),(b) SEM Microscopy For Morphology Studies of Spirobenzopyran - Pnipaam Hydrogel with Average Pore Length of ~ 30μm, (c) Re-Swelling Ratio of Spirobenzopyran Based Pnipaam Hydrogels Synthesized Through Low Temperature Polymerization Process	97
4.24 Effect of Acrylic Acid On the Re-Swelling Behavior of Spirobenzopyran Hydrogels	99
4.25 Light Responsive Hydrogel As Tactile Displays, (a) Schematic Illustration of the Photolithographic Setup Used in the Test, (b) Time Lapse of the Pattern Developed On the Hydrogel	101
4.26 Light Responsive Hydrogel As Tactile Displays, (a) Schematic Illustration of the Photolithographic Setup Used in the Test, (b) Time Lapse of the Pattern Developed On the Hydrogel	103
4.27 Light Responsive Hydrogel As Potential Candidate For Pixelated Tactile Device, (a) Schematic of Light Responsive Hydrogel in Fixed Channels, (b) Preliminary Light Responsive Hydrogels Demonstrating Shrinkage of the Hydrogel in the Z-Direction,(c) Hydrogel Synthesized in A Mold and Exposed to Light in Different Sections.....	103

Figure	Page
A1	FTIR Spectra of the Synthesized Polypyrrole-Based PILs with their Respective Chemical Structures Below Each Curve, From the Top Down, PPy-Br (Green), Ppy-PF ₆ (Red), and Ppy-Tf ₂ N (Blue)138
A2	MWCNTS Dispersed in Water without (a and c) and with (b and d) the PPy-Br Stabilizer. A and B: Macroscopic Stability 8 hr After Dispersion (Insets Left) and Corresponding Confocal Images with 25 mm Scale Bars, C and D: TEM Images of the CNT Dispersions with 5 mm and 500 nm Scale Bars, respectively140
A3	(a) Schematic Showing the Proposed Interaction Between the PIL-ICP Hybrid Stabilizers and the Surface of A MWCNT. (b) TGA Scans Showing the Comparative Degradation of the Synthesized PIL-ICP Hybrid Powders. (c) TGA Scans Showing the Comparative Degradation of the Respective Dried PIL-CNT Dispersions with the Pristine MWCNTs, Showing the Interaction Between the Two Materials.....145
A4	Confocal Images of the Pickering Emulsions Showing the CNT-Stabilized Droplets. (a) PPy-Br / CNT / Water, (b) PPy-PF ₆ / CNT / Acetonitrile, (c) Ppy-Tf ₂ N / CNT / Acetonitrile146
A5	SEM Images of the Formed Hollow Particles from the PPy-Br / CNT / Water Pickering Emulsions. Inset is A Schematic Showing the Morphology of the CNT Shell147

Figure	Page
A6	Confocal Images Depicting Si Incorporation in the CNT Stabilized Hexane Droplets, (a),(c) Hexane Droplets in Water Phase, (c),(d) Silicon Dispersed in Hexane Phase150

CHAPTER 1

INTRODUCTION

Each individual material (soft or hard) possesses unique properties and it is often desirable to combine these materials to exploit complementary characteristics. One of the successful examples in the integration of soft and hard materials has been in the field of soft lithography, which allowed for printing of discrete features on hard materials (Xia and Whitesides 1998c, Kane et al. 1999, Unger et al. 2000). The integration of soft and hard materials, especially incorporating thin films, could have potential applications in the field of flexible electronics, which has garnered increasing attention in recent years. This is primarily accredited to the large number of applications that require systems to be highly conformable and able to withstand a significant amount of strain without compromising functionality.

Conventional semiconducting materials such as silicon are essentially considered to be rigid. However, when the thickness of silicon is decreased to around 500 nm or less, it can be made flexible without damaging the properties of the material (Jiang, Sun, et al. 2007, Khang, Rogers, and Lee 2009, Sun and Rogers 2007). This characteristic has enabled such thin materials to be integrated with elastomeric substrates to assume different shapes (Kim et al. 2008, Ko et al. 2008, Rogers, Someya, and Huang 2010). However, the challenge with elastomeric substrates is that there is always a mechanical force required to drive the desired change. Such limitation can be overcome by the use of “smart” materials, which have a stimulus responsive behavior. In this work, the approach of environmentally responsive hydrogels as substrates is investigated.

Environmentally responsive materials have become popular in many of the active research pursuits to produce novel “smart” materials. A few noteworthy applications have been in the areas of drug delivery (Gupta, Vermani, and Garg 2002, Peppas 1997, Qiu and Park 2012), oil clean up (Atta et al. 2006, Ummadisingu and Gupta 2012), actuators (Bassik et al. 2010, Harmon, Tang, and Frank 2003, Richter et al. 2004), sensors (Gerlach et al. 2005, Liu et al. 2003), and novel devices. In spite of their potential usefulness, the idea of employing hydrogels in modern electronics is still a relatively new field. The main reason has been the lack of electrical properties of these materials in addition to integration and packaging challenges. One unique possibility of harnessing the advantages of both “smart” soft material and hard semi-conducting materials simultaneously is through integrating them together by devising special processes via an intermediate elastomeric layer.

A key issue in the development of environmentally responsive hydrogels as “smart” substrates is to understand and devise means to optimize both the responsiveness and the mechanical properties. Presently, most conventional hydrogels demonstrate slow responsiveness and low mechanical properties which render them unattractive to many such applications. With a view of improving the response properties, the synthesis technique of hydrogels has been studied here. Interestingly, the dependence of the surface morphology, particularly the pore size on the response behavior of environmentally responsive hydrogel has been revealed. Also, the controllability of response behavior would be an advantage in expanding the hydrogel application in this field. Previously, modifying the response behavior has been achieved by focusing on particular synthesis method with varying monomer ratio (Zhang et al. 2010, Yoo et al. 2000, Chen and Hoffman 1995b). Although, these studies are useful they are limited to a particular application. A broader and more useful

technique could be the use of other additives which facilitates the controllability of the response behavior, example surfactant or co-solvent. Both these cases, that is the improvement and controllability of the response behavior has been studied in this report with respect to poly(N-isopropylacrylamide), a popular thermo-responsive hydrogel. These studies would definitely enhance the hydrogels' appeal for integration with other hard functional materials.

This dissertation work is divided into three major parts, firstly, we explore means to improve and understand the thermal and mechanical properties of thermo-responsive hydrogels. In the second part we explore the idea of controlling the buckling pattern of thin film silicon integrated with both flat and curvilinear hydrogel substrates. Finally, incorporation of visible light response to poly(N-isopropylacrylamide) hydrogels is discussed. This thesis is structured as follows. Chapter 2 provides the background and motivations on the main topics discussed in this thesis perspective; primarily focusing on the basic mechanism of different common types of environmentally responsive hydrogels based on their thermodynamics and kinetic properties. Furthermore, a quick overview of past efforts made in hard/soft material integration is discussed with emphasis on the motivation and immense potential of incorporating both hard and "smart" substrate in a particular system. Chapter 3 illustrates the basic methodology for synthesizing both conventional and fast response thermo-responsive hydrogel with emphasis on different synthesis conditions. Also we discuss mechanism of developing adhesion and integration of environmentally responsive hydrogel with thin film silicon. Lastly, we discuss in detail various methods of incorporating light response properties into PNIPAAm. In Chapter 4, we first discuss and compare two types of hydrogel synthesis techniques along with method of modulating the transition

temperature of thermo-responsive hydrogels by the presence of co-solvent and surfactant in the solvent media. Secondly, the controlled response of thin film silicon, with respect to patterned and non-patterned silicon ribbons, integrated on both planar and three-dimensional substrate is discussed. Lastly, as extension of the previous work we discuss different mechanism of incorporating light response properties in a thermally responsive hydrogel. Furthermore, methods of improving the mechanical properties and response time of light responsive hydrogel have also been studied. This new type of hydrogel is being proposed to be used as a tactile display and for such purposes preliminary results based on such a system have been detailed, whereby the material so synthesized was used in a soft mold to obtain a binary response system. Chapter 5 is a summary of work for integrating soft thermo-responsive hydrogels with thin film silicon and also controlling the response of this integrated structure. Moreover, the synthesis of multi-functional PNIPAAm hydrogels with emphasis on visible light response is summarized. Finally, few improvements as part of future work is proposed, with regards to usage of ionic liquids as transition temperature modulating co-solvent and other methods of grafting spirobenzopyran on tough hydrogels.

CHAPTER 2

BACKGROUND AND MOTIVATION

2.1 Environmentally Responsive Hydrogels

2.1.1 Classification and Applications

Hydrogels constitute a group of polymeric materials having a hydrophilic structure which renders them capable of absorbing and holding a large volume of water. Chemical crosslinks or physical linkages (e.g. chain entanglement, van der Waal forces, and crystallite formulations) provide the hydrogels unique swelling behavior and three-dimensional structure (Peppas, Bures, et al. 2000, Peppas, Huang, et al. 2000, Hoffman 2002). The importance of hydrogel was first realized in late 1950s when Wichterle et al. demonstrated the remarkable properties of poly(2-hydroxyethyl methacrylate) (PHEMA) hydrogels and further used it as a soft contact lens (Wichterle and Lim 1960). Later, other biomedical applications of hydrogel was proposed such as cell encapsulation by Lim and Sun in 1980 (Lim and Sun 1980). Since then hydrogels have been vastly explored and abundantly adopted in many diverse applications such as high absorbing wound dressing, (Balakrishnan et al. 2005, Razzak and Darwis 2001) to purposes of environmental significance, e.g. waste oil recovery (Zolfaghari et al. 2006). Most of the commercial applications of hydrogels have been in the area of environmentally non-responsive hydrogel, where the gel substrates are popular replacement of conventional materials such as plastic and glass owing to their superior absorption properties and also due to their unique biocompatible nature.

Environmentally responsive hydrogels are a subgroup of hydrogels which have unique properties of responding to external perturbations such as temperature, pH, light, electric and magnetic field etc. by demonstrating large volume transitions. Although such molecules were first discovered pretty early in 1950 by Kuhn et.al, (Kuhn and Hargitay

1951, Kuhn et al. 1950) the true potential of these was realized much later in 1980s by the pioneering work of Tanaka and co-workers(Tanaka 1978, Tanaka et al. 1982). Since then many unique applications have been studied using these materials, e.g. intelligent pumps (Qu et al. 2006), sensors (Hart and Abass 1997), oil-spill cleanup (Xue et al. 2011) etc. Although a vast variety of application have since been proposed, most of the discussions pertaining to the applications and development of environmental responsive hydrogels have mostly focused on bio-medical application such as self-regulated drug delivery systems.

Since its initial discovery, many different environmentally responsive hydrogels have been formulated and proposed. These different polymer chemistry of the environmentally responsive hydrogels can then be classified into many different subgroups, such as; based on source (natural or synthetic), polymeric composition (homo-polymer, copolymer or multi-polymer interpenetrating network), crystal structure (amorphous, crystalline, or semi-crystalline), ionic nature (non-ionic, ionic or amphoteric), or stimulus responsive nature (temperature, pH, light etc.). Among the various groups of classifications, stimulus responsive characteristic is the most prevalent method of categorizing a hydrogel. Here we would be discussing three types of environmental responsive hydrogel that have been mostly used during the course of this work-temperature, pH and light. Figure 2.1 demonstrates some of the popular hydrogel molecules of each type.

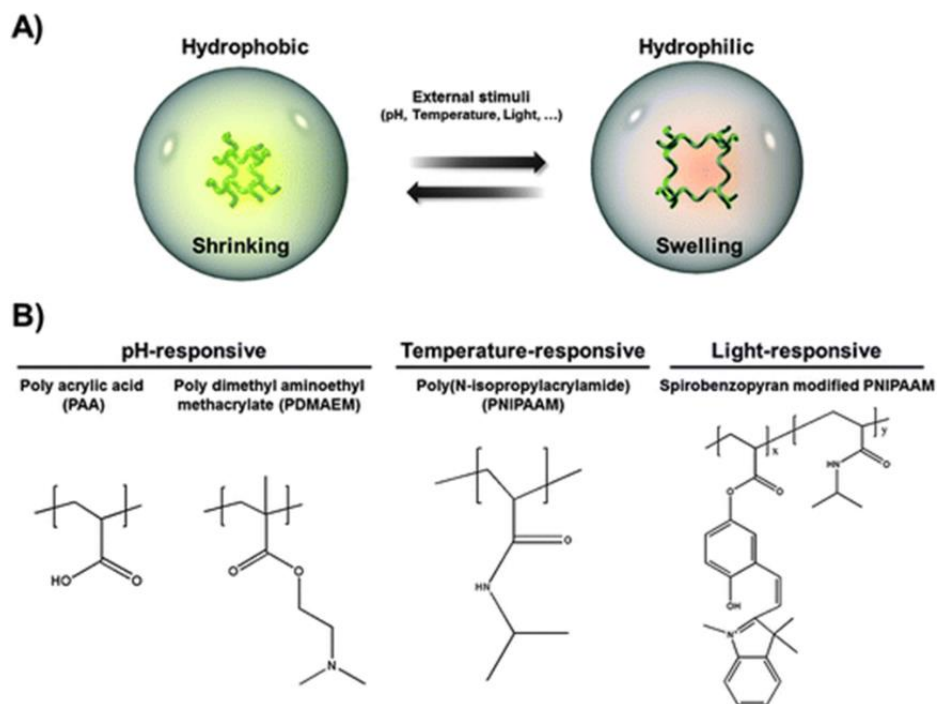


Figure 2.1. Major classification of environmentally responsive hydrogel: (a) Schematic representation of transformation of hydrogel from hydrophobic to hydrophilic, (b) Examples of pH, temperature and light responsive hydrogel. Adopted from (Kang et al. 2013).

Temperature Responsive Hydrogels

Temperature responsive hydrogels are probably the most commonly studied class of environmentally responsive hydrogels. Compared to other environmentally responsive hydrogels temperature responsive hydrogels are more attractive due to the ease of controllability of the trigger force, i.e. temperature. Among the many potential application of such “smart” material, the potential use of these in drug delivery has been the most discussed and explored. The response to temperature stimulus makes such materials an ideal option for smart drug delivery for uniquely targeting cells with higher functioning temperature than the normal physiological temperature; example cancer cells (Sanyal et al. 2011, Schmaljohann 2006, He, Kim, and Lee 2008a).

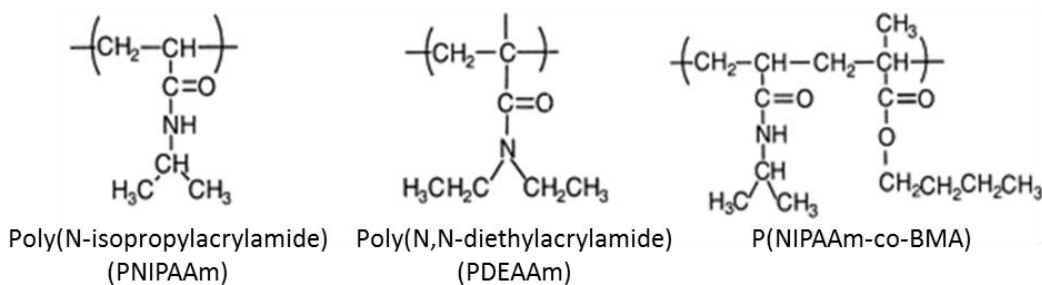


Figure 2.2. Structures of some popular temperature-sensitive polymers, (a) Poly(N-isopropylacrylamide), (b) Poly(N,N-diethylacrylamide) (PDEAAM), (c) Poly(NIPAAm-co-BMA)

Major breakthrough have been done in this field by developing newer and versatile hydrogel polymers which are both benign as well as provide protection to the efficacy of drug from hostile environments, e.g. the presence of enzymes and low pH in the stomach. Apart from biomedical applications, temperature responsive properties have been used for

sensor (Guenther et al. 2007), actuators (Harmon, Tang, and Frank 2003), temperature controlled microfluidics pump (Harmon, Tang, and Frank 2003) and other novel applications.

Many hydrogels of both natural and synthetic origin exhibit a temperature-responsive phase transition property. The common characteristic among these temperature responsive compounds is the presence of one or more hydrophobic groups, such as methyl, ethyl and propyl groups along with a hydrophilic group such as an amide (Figure 2.2). Therefore, switching of hydrophilic to hydrophobic character of the molecule and vice versa is dependent on the interplay of the dominant interaction of the above two groups with solvents; e.g. water. Among the various temperature responsive hydrogels available, poly (N-isopropylacrylamide) and poly (N,N-diethylacrylamide) (PDEAAm) are the most well-known and extensively studied. The transition temperature of both these hydrogels being close to both ambient room temperature and physiological temperature makes them an attractive option for diverse applications. Recently, many natural thermo-responsive polymers based on polysaccharides such as gelatin,(Klouda and Mikos 2008) dextran,(Zhang, Wu, and Chu 2004) chitosan,(Ruel-Gariepy et al. 2002) etc. have also been developed because of their bio-compatibility. The bio-compatibility of these molecules could make them a stronger candidate for human drug test trials.

There are various mechanisms to explain the functioning of different thermo-responsive hydrogel and for some it is still a topic of debate. In general, when a polymer is dissolved in water, there are three types of major interactions that take place between polymer-polymer molecules, between polymer -water and among water-water molecules itself. In the case of hydrogel network, the swelling or shrunken nature is dependent on the strength of these individual interactions. Certain thermo-responsive polymer molecules, at

a specific temperature which is called as the lower critical solution temperature (LCST), exhibit shrinkage due to the reduction of the polymer-water interaction, resulting in an overall hydrophobic behavior and discontinuous de-swelling of the polymer network. This observation could be better explained thermodynamically, by the famous Gibbs free energy theorem and concept of free energy of mixing. For polymers exhibiting such LCST behavior, the free-energy of mixing becomes suddenly negative, making the polymer-water association unfavorable and supporting the polymer-polymer interactions. The negative free energy (ΔG) enabling the phase transformation is attributed to the higher entropy term (ΔS) with respect to the increase in the enthalpy term (ΔH) in the thermodynamic relation $\Delta G = \Delta H - T\Delta S$. Therefore, such a process is entropically driven as the water molecules exhibit greater randomness after the phase transformation. Such a phenomenon is not only restricted to hydrogel but can also be seen in polymer micelle packing and coil to helix transition of other molecules.

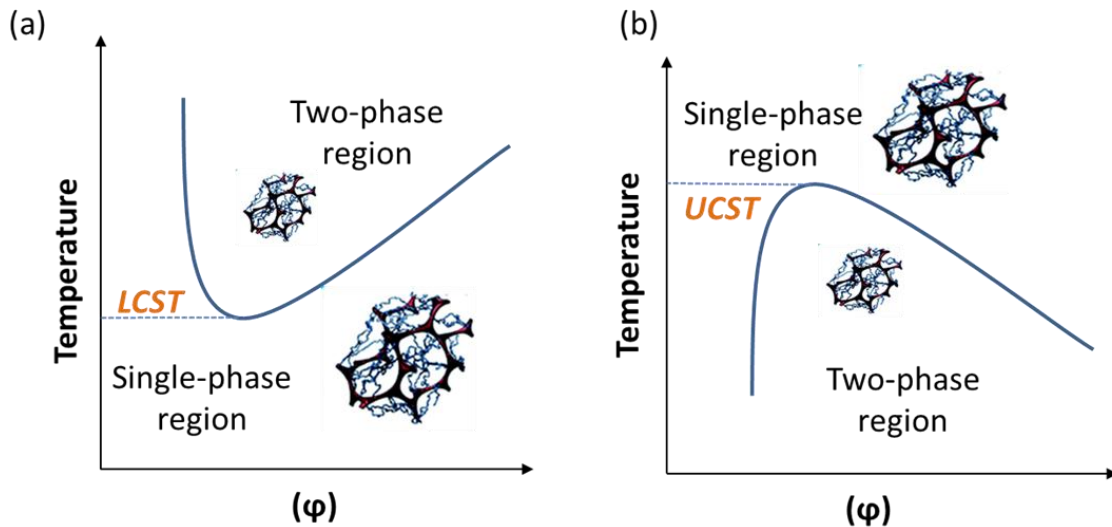


Figure 2.3. Schematic of UCST and LCST phase diagram : (a) Lower critical solution temperature (LCST) phase diagram (b) UCST type phase diagrams

Contrasting LCST phenomenon there are certain polymers that demonstrate the property of upper critical solution temperature which is in opposite to the more conventional LCST behavior. Polymers that exhibit such a property demonstrate an enhanced swelling ratio with increase above a certain temperature. Although pretty rare, most examples of UCST are seen in hydrogels which have an interpenetrating network (IPN) of certain polymer chains, such as polyacrylamide (PAAm) and poly(acrylic acid) or poly(acrylamide-co-butyl methacrylate) crosslinked with N,N'-methylenebisacrylamide (MBA), etc.(Katono et al. 1991) At low temperature, such IPN hydrogels are in the deswelled state due to competitive intermolecular complexes formed via hydrogen bonding between the polymer chains itself. However, as the temperature increases, the hydrogen bonds are disrupted due to the water molecule's kinetic energy and subsequently result in swelling due to de-tangling of the polymer chains, thus allowing hydration, or dominant water-polymer interaction. Unlike LCST, UCST behavior is an enthalpically (ΔH) driven process as the gibbs free energy is negative due to the increase in the absolute enthalpy content, while the change in entropy is reduced. Both these interesting phenomenon could be better explained with a phase diagram which represents the separation of the phases. LCST and UCST are the respective critical temperature points below and above which the polymer and solvent form strong interactions as shown in Figure 2.3.

Beyond synthetic and natural thermo-responsive hydrogels, many of the thermo-responsive hydrogels are modified by conventional cross-linking of different monomers to make it suitable for particular application. Functionalization of natively thermo-responsive hydrogels with more or less hydrophobic constituents would shift the LCST to lower or

higher temperature respectively. For example, Lyon demonstrated that adding of hydrophobic group such as tert-butyl acrylamide to conventional poly(N-isopropylacrylamide) based microgel significantly reduces the transition temperature.(Keerl and Richtering 2007) Similarly, acidic or basic groups, such as acrylic acid or N-(3-Dimethylaminopropyl) methacrylamide (DMAPMA) increase the hydrophilicity of the hydrogel as well as impart pH responsive properties to the hydrogel.(Kim, Bae, and Kim 1997, Das et al. 2010) Interestingly, the swelling characteristics that are swelling ratio of the co-polymerized molecules are also markedly different from the original polymer. Apart from cross-linking methods and addition of other monomers during synthesis, the transition temperature of the thermo-responsive hydrogel is a strong function of the medium as well. This is an exciting characteristic and has been studied in the course of this thesis work to develop methods to adjust and control the transition temperature without changing the polymer chemistry.

pH Responsive Hydrogels

pH responsive hydrogels, are unique systems which respond to changes in pH or electrolyte concentration by demonstrating difference in solubility or volume. Most of the pH responsive hydrogels are able to achieve these unique swelling properties through exchange of protons or hydroxyl ions present in the solution. The pendant acidic (e.g. carboxylic or sulphonic acid) or basic (e.g ammonium salts) groups that are attached on the polymer network are responsible for such discontinuous volume transition at a specific pH (Figure 2.4a). Popular pH responsive hydrogels such as poly(N,N'-dimethylaminoethyl methacrylate) demonstrate reduction of size in basic media (Figure 2.4 b). On the other

hand, hydrogel such as poly(acrylic acid) which are of acidic nature demonstrate discontinuous swelling at high pH while shrink when the medium is of acidic nature (Figure 2.4 c).

Figure 2.4d is a description of the volume transition in any generic pH responsive hydrogel, e.g. acidic, basic or amphiphilic hydrogel. The actual phase transition of the gels occurs in a small range close by the apparent acid dissociation constant pK_a of the hydrogel which is identical but not same with the pK_a of the ionizable group. Approximately at the apparent pK_a of the gel the ionization begins accompanied by a drastic swelling of the hydrogel. If the ionization of the ionizable component is completed the swelling process stops. Further pH increase only increases the ionic strength. Depending on the proposed chemistry the swelling ratio of the hydrogels could be made different by varying the concentration of the monomers during the synthesis of the hydrogel. Apart from this, extent of cross-linking of the hydrogel also plays a crucial role in deciding the swelling ratio of the hydrogels.

Due to its varied properties they have been used in many applications, such advanced drug delivery. In the human body there are distinct regions of low and high pH in the same tract. Example, in the gastro-intestinal tract the pH of the stomach is (<3) and is quite different from the neutral pH maintained in the intestine. This large difference is exploited by polyelectrolyte hydrogel which have minimal swelling properties in neutral pH and is used to release drugs specifically in this region. Another example is the use of pH responsive hydrogel for localized antibiotics for stomach ulcer (Patel and Amiji 1996). Apart from these the pH responsive properties have been used in other applications such as actuators and sensors. One drawback of pH responsive hydrogel is the much reduced

mechanical properties and its slow responsive. The slower responsive could be tackled by higher porosity or increasing additives during the synthesis of the hydrogel which increase its dissociation constant without affecting the pH behavior too much (Gemeinhart et al. 2000, Ju, Kim, and Lee 2001, Zhao and Moore 2001). The kinetics and thermodynamics of pH responsive hydrogels, important factors were first investigated by Ricka and Tanaka by the quantitative consistency of Donnan theory of swelling for weakly charged ionic gels (Ricka and Tanaka 1984). As discussed in a different section later for the case of ionic hydrogel the factor of electrolyte concentration also plays an additional role in the swelling properties. The mutual interaction of the ions ($\Delta\pi_{\text{ion}}$), elastic effect of the network ($\Delta\pi_{\text{elas}}$) and free energy effect of the water molecules ($\Delta\pi_{\text{mix}}$) can be summarized as

$$\Delta\pi = \Delta\pi_{\text{elas}} + \Delta\pi_{\text{mix}} + \Delta\pi_{\text{ion}} = 0$$

Furthermore, pH behavior of such hydrogels is dependent on the two primary quantities- firstly, the amount of ionizable moieties and secondly, the dissociation constant of the ionizable groups. Although the basic mechanism of pendant group ionization is similar to the respective monoacids or monobase, the dissociation of the polyelectrolyte hydrogel is different. The ionization of polyelectrolyte is substantially dependent on the presence of adjacent ionized groups. This factor significantly shifts the apparent dissociation constant of the hydrogel (K_a) from that of the corresponding monoacid or monobase. The second important factor, is the number of ionizable groups. pH-responsive polymeric systems have been extensively studied, both from the theoretical and applied perspectives. Such polymeric systems could be synthesized through free-radical or controlled polymerization techniques.

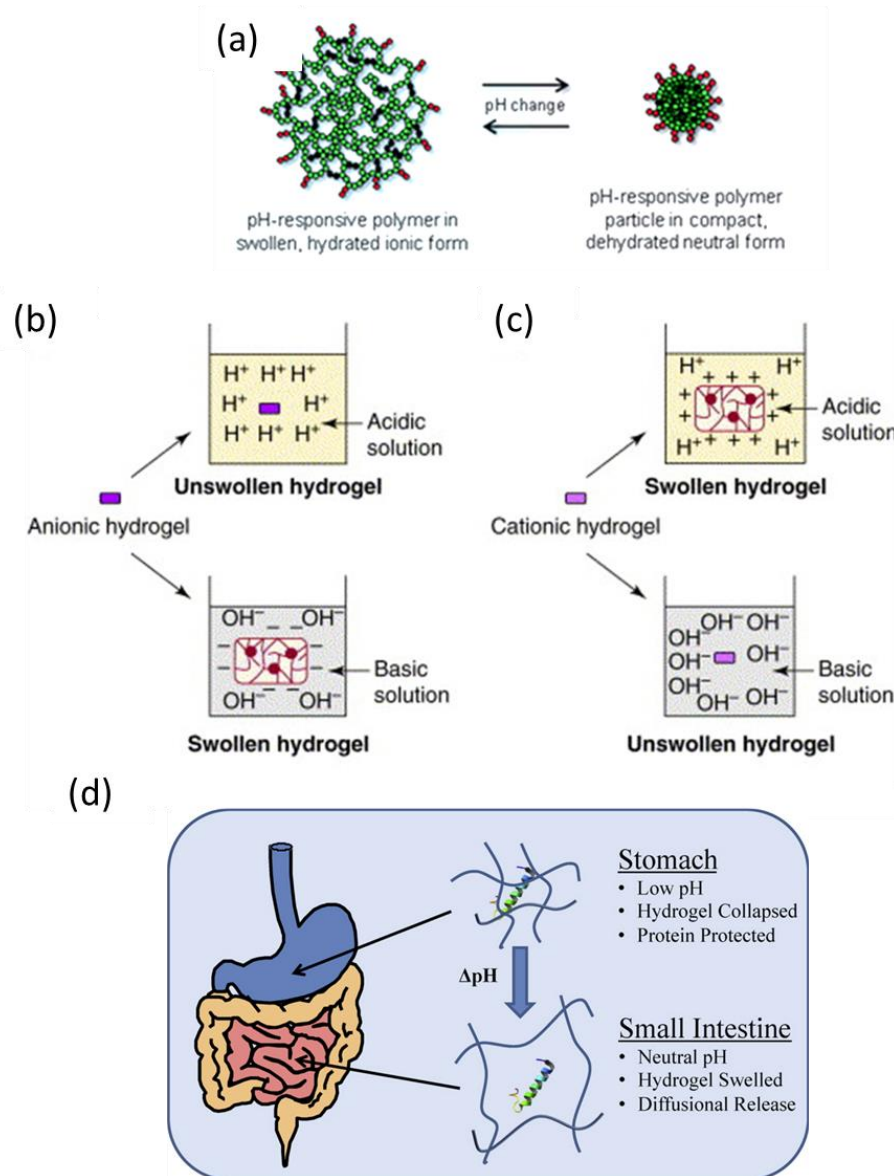


Figure 2.4. Classification and types of pH responsive hydrogel: (a) Schematic representation of the swelling and de-swelling of pH responsive polymers, Compositional reversibility of: (b) anionic and, (c) cationic hydrogels in response to solution pH changes d) pH responsive hydrogel application in drug delivery. Adopted and modified from (Gupta, Vermani, and Garg 2002, Koetting and Peppas 2014).

With the controlled polymerization, well-defined block copolymers resulting in the formation of nanostructured particles or polymeric brushes were produced. In aqueous systems containing homopolymers or microgels, external pH produced phase separation and swelling/deswelling of particles, respectively. For block copolymers, the pH-responsive polymers self-assembled into aggregates of different shapes on application of an external stimulus. In general, pH-responsive polymers contained either polyacid or polybase segments, and when fully neutralized, these polymers were transformed to polyelectrolytes or polyampholytes. They have found wide application in controlled release of drugs, DNA or gene delivery, protein separation, coating thickeners and applications where triggering by external pH is necessary.

Increasing focus is dedicated to the synthesis and applications of these novel materials. The increasing use of these novel materials particularly in the drug delivery applications, demands renewed approach for improving the mechanical and incorporating faster response properties in such polymeric systems. In this respect, majority of the work been pursued are in the field of click chemistry, whereby various types of polymeric segments, or additional ligands could offer better response properties. In addition, the application of biomolecular responsive polymeric systems in novel biosensor devices would be a very exciting opportunity for future activity.

Light Responsive Hydrogels

Light as a stimulus is one of lesser focused subjects in the development of environmentally responsive hydrogels. The most appealing advantage of light responsive hydrogels over other prevalent environmentally responsive hydrogels, such as temperature and pH, is the fact that light can be applied instantaneously to trigger the phase transformation process. This unique characteristic allows for the precise use and control over the environmental response behavior. Light responsive hydrogels have been pretty attractive in the field of actuator design where a quick actuation/output from the material is warranted on account of some stimulus. Previously, Zhang et al. in a previous work exploited this quick turn on and off behavior to design a “gated” membranes controlling the transport of ions or the flow of gases or liquids through micro-channels.(Kameda et al. 2003) Light responsive materials have also potential applications in developing optical switches, display units, and ophthalmic drug delivery devices.

On the basis of response mechanism light responsive hydrogel are divided into two broad categories. First, are those materials which demonstrate light responsive properties due to conversion of the incident light energy to local heating of the hydrogel. Although such hydrogel have been utilized in certain exciting application before, e.g. infra-red or near infra-red drug delivery, they have not been very attractive due to requirement of high intensity of light and its limited response kinetics. Second class of light responsive material, are the compounds which demonstrate direct light responsive properties, e.g. azobenzene, spirobenzopyran, etc.(Sasaki et al. 2010, Soll, Antonietti, and Yuan 2011) These compounds depend on the certain wavelength of light to transform their molecular orientation, e.g. conversion of cis azobenzene to trans azobenzene.

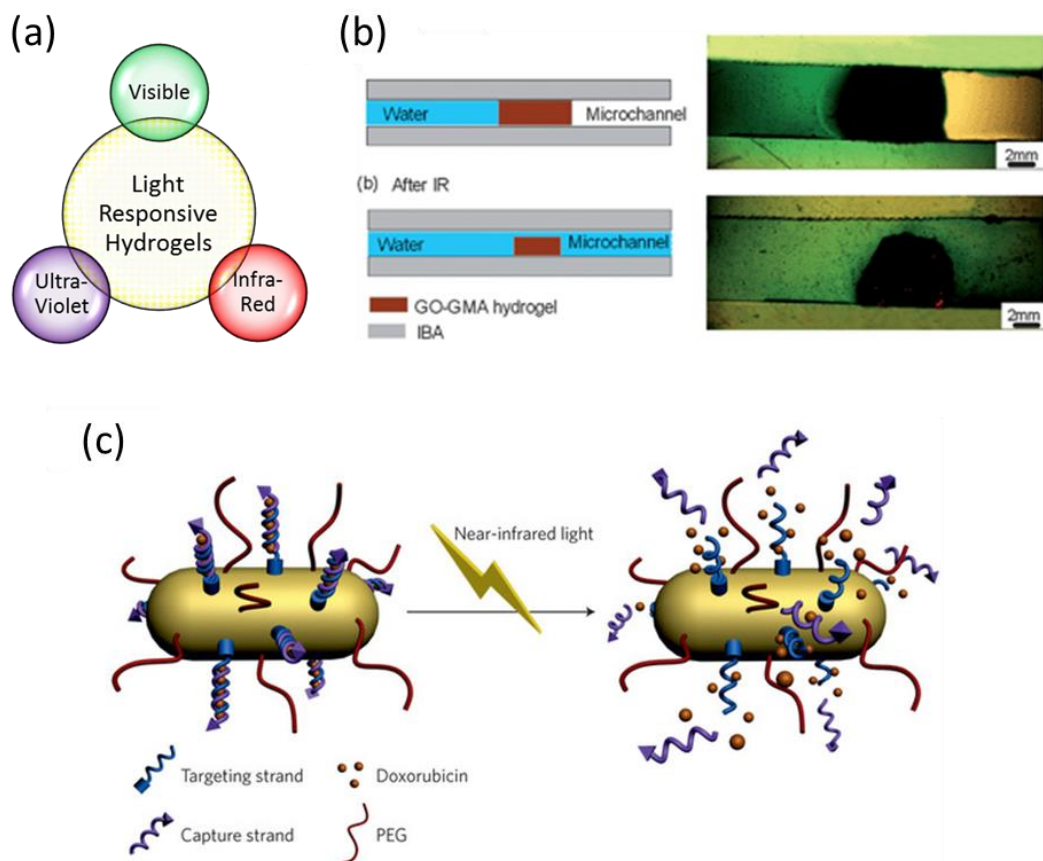


Figure 2.5. Classification and applications of light responsive hydrogels: (a) Light responsive hydrogels classified according to the responsive wavelength, (b) “smart” microchannel based on IR responsive hydrogels,, (c) UV responsive hydrogels utilized in controlled drug delivery application. Adopted from (Mura, Nicolas, and Couvreur 2013, Lo, Zhu, and Jiang 2011).

In such a system the transformation of the molecular orientation affects the hydrophilic properties of the hydrogel immensely as of one of them has a marked better hydrophilic properties than its counterpart. Unfortunately, most of the known direct light responsive materials either respond to ultra-violet or infra-region, which limits its applicability.

Another useful method of classifying light responsive hydrogels is on the basis of the incident light they respond to, e.g. infra-red, ultra-violet, or visible light (Figure 2.5a). An example of UV-sensitive hydrogels is a PNIPAAm network integrated with a leuco derivative molecule, bis(4-dimethylamino)phenylmethyl leucocyanide.(Mamada et al. 1990) The leuco derivative molecule can be ionized upon ultraviolet irradiation. At a fixed temperature, the hydrogels discontinuously swelled in response to UV irradiation but shrank when the UV light was removed. The UV light-induced swelling was due to an increase in osmotic pressure within the gel due to the appearance of cyanide ions formed by UV irradiation and subsequently reduces when the light source is removed. Similarly, visible light-sensitive hydrogels, can be prepared by introducing a light-sensitive chromophore (e.g. trisodium salt of copper chlorophyllin) to poly(N-isopropylacrylamide) hydrogels (Suzuki and Tanaka 1990). When light (e.g. 488 nm) is applied to such a hydrogel, the chromophore absorbs light which is then dissipated locally as heat by radiation less transitions, increasing the 'local' temperature of the hydrogel. The mechanism of infra-red hydrogel on the other hand absorb is similar to visible light responsive hydrogel, example gold based hydrogel are known to be IR sensitive. All of these hydrogel are pretty useful but still hindered by fundamental material limitations, e.g. slower response, limited light sensitivity bandwidth, and importantly limited options of visible light responsive materials. Therefore, there is a need to look at fast light responsive hydrogels.

2.1.2 Swelling Kinetics and Thermodynamics

The strong dependence of thermodynamic factors on the swelling and de-swelling mechanism of hydrogels was first postulated by Flory and Huggins in 1951.(Huggins 1942a, b) Since then, their postulate has been used in various modifications to describe the behavior of many environmentally responsive hydrogels system like temperature,(Yoshida et al. 1994b) pH,(Li et al. 2005) light(Suzuki, Ishii, and Maruyama 1996). Flory and co-workers described the swelling behavior of a non-ionic hydrogel as equilibrium between two opposing free-energy contributions. As briefly discussed previously, the first is the water-polymer interaction which promotes swelling and the second is the elastic forces of the network which resists this change. Although these two are the major factors can be used to describe the swelling mechanism, there are other two thermodynamic interactions which also play a significant role. These are the water-water interaction and the polymer-polymer interaction. Depending on the strength of these factors and the structure of the molecule itself, hydrogels exhibit a change in their swelling properties with change in the temperature, pH, concentration or light. Additionally, if the hydrogel is of ionic or polyelectrolyte in nature, there are significant contribution of the electrostatic interaction between the solvent media and the polymer network. In this view, Baker and co-workers proposed a modified Flory model for describing the thermodynamic contribution of the ions present in a pH responsive hydrogel using the Donnan potential.(Yphantis and Roark 1971, Chu et al. 1995, Molina, Gómez-Antón, and Piérola 2004) According to this theory the electrolyte inside the gel is equal to the product of the activity coefficients outside the gel.(Baker et al. 1992)

Figure 2.6 describes the primary effect on the structure of an environmentally responsive hydrogel due to the interplay amongst these three important thermodynamic factors. At a particular state the environmental responsive hydrogel has an extended nature, due to the dominant polymer-water interaction. At this condition the entropy of the solvent molecules could be stated as minimum due to the strong hydrogen bonding between the water and polymer molecule which decreases the randomness of the system (Figure 2.6 left). Subsequently, due to change in the environment conditions which could be in terms of temperature, light or pH alteration, the molecule shifts its hydrophilic nature to more hydrophobic character due to the dissociation of the polymer and the water molecules (Figure 2.6 right). This sudden change in the molecule configuration is brought about in an intermediate state between the two extreme conditions and termed as region of phase transformation, where the fine balance between the three thermodynamic interactions is completely altered leading to a sudden change in the physical properties of the hydrogel, which could be in term of volume, mass, stiffness and more.

Although, thermodynamics is a useful way of describing the unusual swelling and de-swelling mechanism seen in an environmentally responsive hydrogel, however, in practice the rate at which the swelling takes place or the kinetics of the hydrogel swelling system play an even more important role in choosing a certain hydrogel for a particular application. For example, slower responsive hydrogel have a larger role in biomedical or drug delivery application, where the drug or protein molecules have to be distributed or released over a specified period of time (Nagai et al. 2006, Naskar, Palui, and Banerjee 2009, Zhang et al. 2005). The time frame of such a distribution is crucial as the concentration of the drug in the blood stream is required to be maintained in a specific range over a period of time.

On the other hand, application where actuation or sensing property of the hydrogel is utilized, a faster responsive hydrogel is desired.(Harmon, Tang, and Frank 2003)

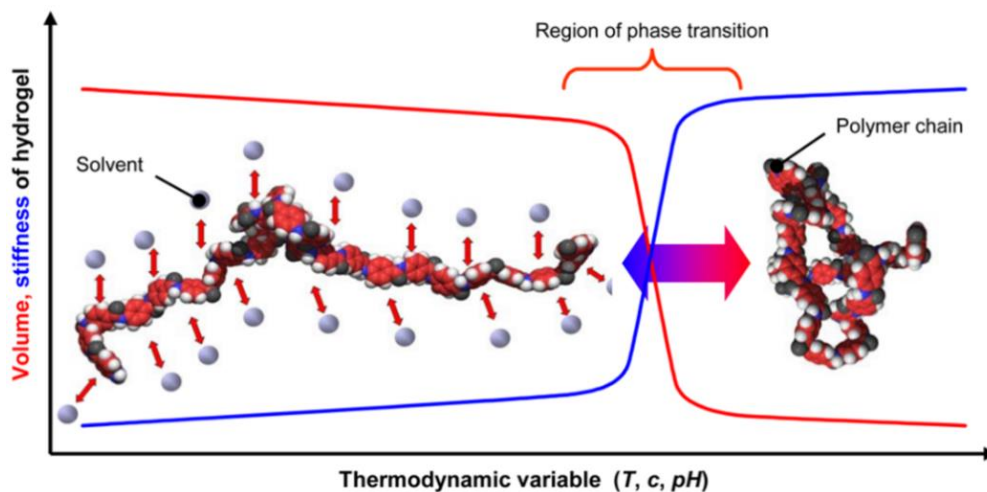


Figure 2.6. Different stage of hydrogel transition: The swollen phase of the gel (left) is dominated by polymer-solvent interactions obtaining the best mixing of the polymer chains and the aqueous solution. The shrunken phase of the hydrogel (right) is determined by polymer-polymer-interactions, which remove solution out of the gel. Adopted from (Richter et al. 2008).

Before swelling, the hydrogel network is glassy and tough due to the dominant polymer-polymer interaction which was described due to the hydrophobic nature (Yoshida et al. 1994a). Subsequently, when the hydrogel is placed in contact with water or solvent media, water driven by chemical potential gradient enters into the hydrogel and depending on the intensity of polymer-solvent interaction as well as the rate at which the solvent enters, determines the hydrogel swelling behavior. Ganji et.al determined explained this chemical potential driven process as a separation of the un-solvated glassy phase from the rubbery hydrogel region with a moving boundary and the meshes of the network in the rubbery phase to be ever expanding, allowing other water molecules to penetrate within

the hydrogel network.(Ganji, Vasheghani-Farahani, and Vasheghani-Farahani 2010) Generally for slow responsive hydrogels, this separation and expansion of the different boundaries, is diffusion dominated with the associated migration of water into pre-existing or dynamically formed spaces among hydrogel chains, while swelling involves a large-scale segmental motion. Thus the final water content of hydrogels depends on both kinetics and thermodynamics parameters.

Figure 2.7 demonstrates the swelling phenomenon in a generic non-ionic hydrogel network as a continuous process of transformation from a glassy, brittle state or partial rubbery state to a turgid, stretched out region of the hydrogel. Swelling in hydrogel is a complicated procedure and does not strictly adhere to the only Fick's law of diffusion and needs considerable modifications to it, especially in the terms of time dependence. Depending on the medium temperature, morphology of the network and hydrogel chemistry the kinetics of the hydrogel may or may not adhere to simple first law of Fick's diffusion. Bajpai et al summarizes the various methodologies proposed to understand hydrogel diffusion and divides them into two distinct types of diffusion process depending on the state of the hydrogel network temperature.(Bajpai et al. 2008) The first case is when the network in which the glass transition is below the medium temperature. Under such circumstances the network elastic behavior is of great prominence as it has higher mobility and therefore allows for easier diffusion of the water or solvent molecules. This case is also referred to as the Fickian diffusion or the state in which diffusion rate (R_{diff}) is less than relaxation rate of the network due to the higher mobility (Figure 2.7a). The second and more observable case is when the glass transition is higher than the medium temperature. This case is also referred to as the non-Fickian diffusion and is highlighted by the restricted passage of water

molecules due to the glassy and brittle nature of the polymer network. The case can be further divided on two subsections on terms of the diffusion rate- case II and anomalous diffusion. In case II diffusion the hydrogel diffusion rate (R_{diff}) is faster than relaxation network (R_{relax}) (Figure 2.7c). The other option is when the relaxation and the diffusion rate are equal, which is termed as the anomalous transport. (Figure 2.7b)(Ganji, Vasheghani-Farahani, and Vasheghani-Farahani 2010)

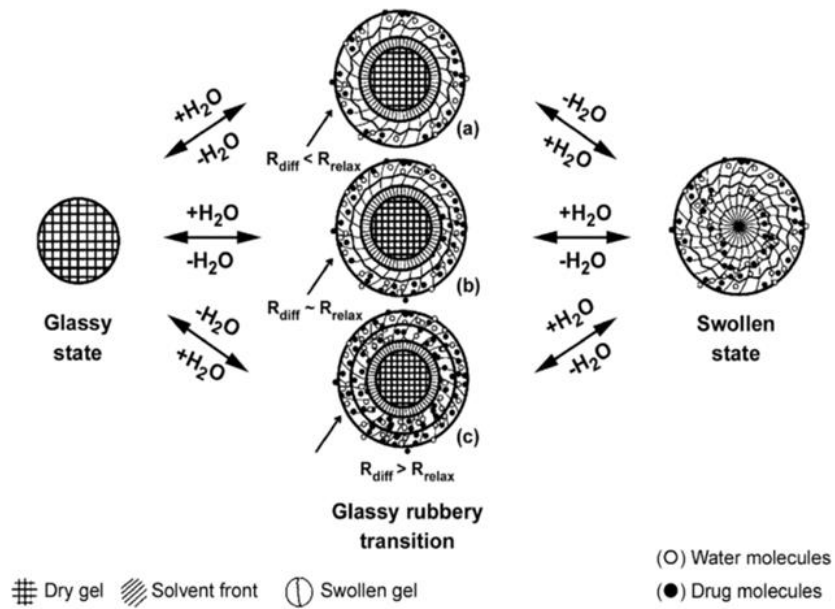


Figure 2.7. Different diffusion processes :(a) Case I diffusion (b) Anomalous Diffusion, (c) Case II diffusion. Adopted from (Rossi and Mazich 1991).

As described above the kinetic behavior of conventional hydrogel swelling is mainly dominated by plain diffusion, which is importantly dependent on the surface area of the hydrogel surface and the diffusion co-efficient, as described by Fick's law of diffusion and the boundary condition. Generally, the diffusion constant is stable for particular solvent media for a moderate temperature range. Thus the area of the hydrogel, is another prime factor determining the overall kinetic behavior of the hydrogel.(Rossi and Mazich

1991) With the ever increasing interest of utilizing hydrogel, for sensor and actuator application, the idea of faster swelling and de-swelling behavior of hydrogel has become very popular. For faster responsive hydrogels the swelling characteristics is dominated by the capillary and convection properties. The capillary action and convection dominated solvent uptake in such hydrogels, is mainly due to the larger pore size of such material.

Ganji et al. in his review paper provided a brief classification of hydrogels based on the pore size and its impact on the swelling property (Chen and Hoffman 1995a). According to this, the porous structure of hydrogels is classified into nonporous, microporous, macroporous and superporous (Ganji, Vasheghani-Farahani, and Vasheghani-Farahani 2010). Furthermore, Lowman definition quantified a nonporous hydrogels with a macromolecular dimension in the range of 10-100 Å (Lowman, Peppas, and Hydrogels 1999). In these hydrogels, the polymer chains are densely packed and provide strictly limited solvent transport via the diffusion through free volumes. Microporous hydrogels usually have pore sizes between 100 and 1000 Å. In these hydrogels, the pores are water filled and the solvent transport occurs due to a combination of molecular diffusion and convection in the water filled pores. Macroporous hydrogels have large pores of dimension 0.1 to 1 µm and the solvent transport is through mechanism dependent on diffusion in the water filled pores. Superporous hydrogels have much larger pore size in the range of several hundred micrometers.

Previously, many different methods for developing greater pore size and faster response characteristics with limited effect on the polymer chemistry have been proposed, such as, incorporation of in-homogeneities,(Schexnailder and Schmidt 2009) low temperature synthesis,(Yokoyama et al. 1986) or incorporation of inorganic particles. Though

each method has its potential advantage, most of such these synthesis techniques are plagued by low mechanical properties, as the basic scaffold becomes weak. The improvement and the control of the response behavior without compromising on the structural property is one part of major focus areas of this work.

2.2 Strategies of Integrating Soft and Hard Materials

Material property investigation is one of the widely studied and fascinating fields in the scientific world. Many valuable properties are exclusive and restricted to a certain group of materials. Material integration could be one of the promising approaches whereby we can exploit complimentary properties of different materials and exploit the synergistic advantages of different materials. In modern world, many applications of integrated materials could be seen, where one material provides structural rigidity and another provides functionality, e.g. car tire, where the tire rim provides for structural integrity while the rubber provides traction. Microscopically too, such type of material integration is common, e.g. pickering emulsion polymerization,(Ma et al. 2010) where nano sized particles stabilize two immiscible phases containing monomers; thereby eliminating the need for surfactant molecules, which otherwise is an essential component for such kind of synthesis technique. A complete review of hard and soft material/structures will be too vast and in this report we only highlight work which is closely related to the main topic of this discussion, which is primarily related to stretchable electronic devices or the processing of such materials.

Recently, integration of materials have been become a topic of great interest explored in electronics industry primarily because of the growing need of conformable and flexible device. Previously, most of the work in the field of advanced electronics focused

either directly or indirectly to improve speed by reducing down the size of semi-conductor devices, e.g. transistors to directly increase the density of circuits in a confined space while still optimizing the efficiency of the circuit in terms of power usage. The surge for demand of alternative forms of electronics mainly came some decades ago from the need of flat panel displays. This led to increasing attention for conformable devices, which can lead to additional functionality. Recently, lot of attention has been given to traditional devices having alternate forms. Examples of such work, are recent interest for origami based devices (Cheng et al. 2013, Song et al. 2014)

For the conformable, the primary factors is shifted to coverage and durability rather than transistor size or speed; a primary focus of conventional semiconductor fabrication research as discussed before. Apart from display technologies, majority of the conformable materials have been utilized or proposed are related to biomedical or sensors applications e.g., electronic paper,(Hayes and Feenstra 2003, Wang et al. 2004) health monitoring systems,(Pantelopoulos and Bourbakis 2010, Schwartz et al. 2013) smart military vest etc. Despite the growing number of application, much more uses can be envisaged which can have far reaching influence in the biomedical industry. One of the main focuses of such conformable electronics is in the area of smart prosthetics, e.g. artificial muscles, smart heart valves, knee –replacement, eye. Similarly, this approach could also have tremendous potential by offering seamless mounting on tissues or other material to provide extraordinary functionality in surgical devices, fabrics or even human interfaces, e.g. onboard health monitoring. Importantly, such application also brings newer challenges to the forefront, such as bendability and stretch ability, which have not been encountered in conventional semi-conductor research.

The concept of stretchable devices has been envisaged by two complimentary techniques. The first method, proposes the use of novel material which have both semi-conducting properties and good mechanical property.(Sekitani and Someya 2010) Although, this method was the most popular initially and has been received considerable attention, they still lag behind conventional semiconductor in terms of cost and performance The alternative method, proposes to use traditional semi-conducting material, e.g. silicon, with stretchable rubber-like substrates, e.g. poly(dimethylsiloxane) (PDMS) to offer good stretchability as well as device performance. This integration leads to the behavior of buckling which has been explained latter. The fundamental concept behind stretchable or curvilinear electronics using this technique is to use the elasticity of PDMS to store elastic energy and to drive the buckling of Si ribbons on PDMS. In fact, the same fundamental foundation leads to wrinkling in soft/hard material systems across a wide spectrum, from wrinkles on fruits and aging human skins(Yin et al. 2008, Cerda and Mahadevan 2003, Mahadevan and Rica 2005) to controlled pattern formation(Bowden et al. 1998, Bowden et al. 1999, Chung, Nolte, and Stafford 2009) and other thin film systems (e.g., semiconductor materials on soft substrates(Hobart et al. 2000, Moon et al. 2007)), among many others(Huang et al. 2007). These commonly observed wrinkling examples are due to the elasticity or viscoelasticity of the soft materials, which drives the wrinkle kinetics and formation.

The fundamental concept behind stretchable or curvilinear electronics using this technique is to use the elasticity of PDMS to store elastic energy and to drive the buckling of Si ribbons on PDMS. In fact, the same fundamental foundation leads to wrinkling in

soft/hard material systems across a wide spectrum, from wrinkles on fruits and aging human skins (Yin et al. 2008, Cerda and Mahadevan 2003, Mahadevan and Rica 2005) to controlled pattern formation (Bowden et al. 1998, Bowden et al. 1999, Chung, Nolte, and Stafford 2009) and other thin film systems (e.g., semiconductor materials on soft substrates (Hobart et al. 2000, Moon et al. 2007), among many others (Huang et al. 2007)). These commonly observed wrinkling examples are due to the elasticity or viscoelasticity of the soft materials, which drives the wrinkle kinetics and formation.

Soft lithography is an excellent example, particularly in the integration of soft and hard materials. Compared to other parallel techniques for printing such as – photolithography, electron-beam lithography, soft lithography can be used for unusual systems, e.g. those in biotechnology, plastic electronics, etc.); structures with nanometer dimensions (i.e. below 50-100 nm); large patterned areas (i.e. larger than a few square centimeters); or nonplanar (i.e. rough or curved) surfaces. This technique is also more advantageous over other established techniques in terms of lower capital and operational costs. Soft lithography uses elastomeric stamps such as poly(dimethylsiloxane) (PDMS) to fabricate or replicate micrometer-sized structures defined by hard materials (Xia and Whitesides 1998a, b). Figure 2.9 describes the various steps of this type of printing technique. Initially, the mold is fabricated with an elastomer such as PDMS, followed by placing contact with the transfer elements. Finally due the transfer elements are brought in contact with the substrate which puts the elements on the material. Following the lead of soft lithography, kinetically controlled transfer printing was recently developed (Meitl et al. 2006) by using the viscosity of PDMS to selectively transfer micro-sized features.

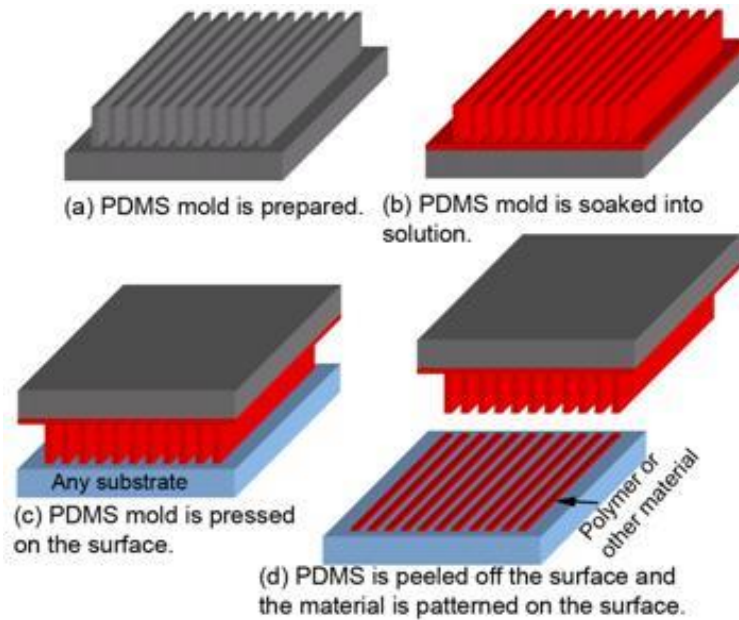


Figure 2.8. Steps in a soft lithography process (a) PDMS mold is prepared, (b) PDMS mold is soaked in a solution (c) PDMS mold is pressed on the desired solution (d) PDMS is peeled off and the pattern is revealed on the surface. Adopted from (Yu et al. 2003).

The popularity of soft lithography also opened possibility for thin film integration for the new and emerging area, namely, stretchable and curvilinear electronics. The means to overcome the intrinsic brittleness of some semiconductor materials in electronics (e.g., silicon (Si)) is to use buckles or wrinkles. The fabrication process is illustrated in Fig. 3: (a) bonding the brittle silicon ribbons with a pre-stretched PDMS slab, and (b) releasing the pre-stretched PDMS slab to form wrinkles of the brittle Si ribbons. This novel approach of thin film integration on soft and conformable substrates is different from the previously studied thin metallic interconnects in stretchable electronics. The buckled brittle Si is superior to this previous technique as it allows for much higher strain rates up to 20% without

fracture. Importantly, such a method has been able to integrate single crystal silicon for stretchable application which was unthinkable before. Single crystal silicon integration opens up possibility for flexible diode with stable performance characteristics, as demonstrated by Roger et al (Ahn et al. 2007). Since then wider and much powerful circuit integration with flexible electronics has been studied, with many fascinating application such as, electronic eye, health monitoring tattoo, and recently a new field altogether, namely, transient electronics.

The examples discussed here have shown many novel uses of integration of hard and soft material. However, few of the work in this field have focused on the development of multifunctional substrate which could enhance the applicability of such integrated system. The present work involves integrating substrates which apart from allowing integration of the silicon elements, would also allow the substrates to impart certain “smart” behavior. One of the best examples of such materials are environmentally responsive hydrogels.

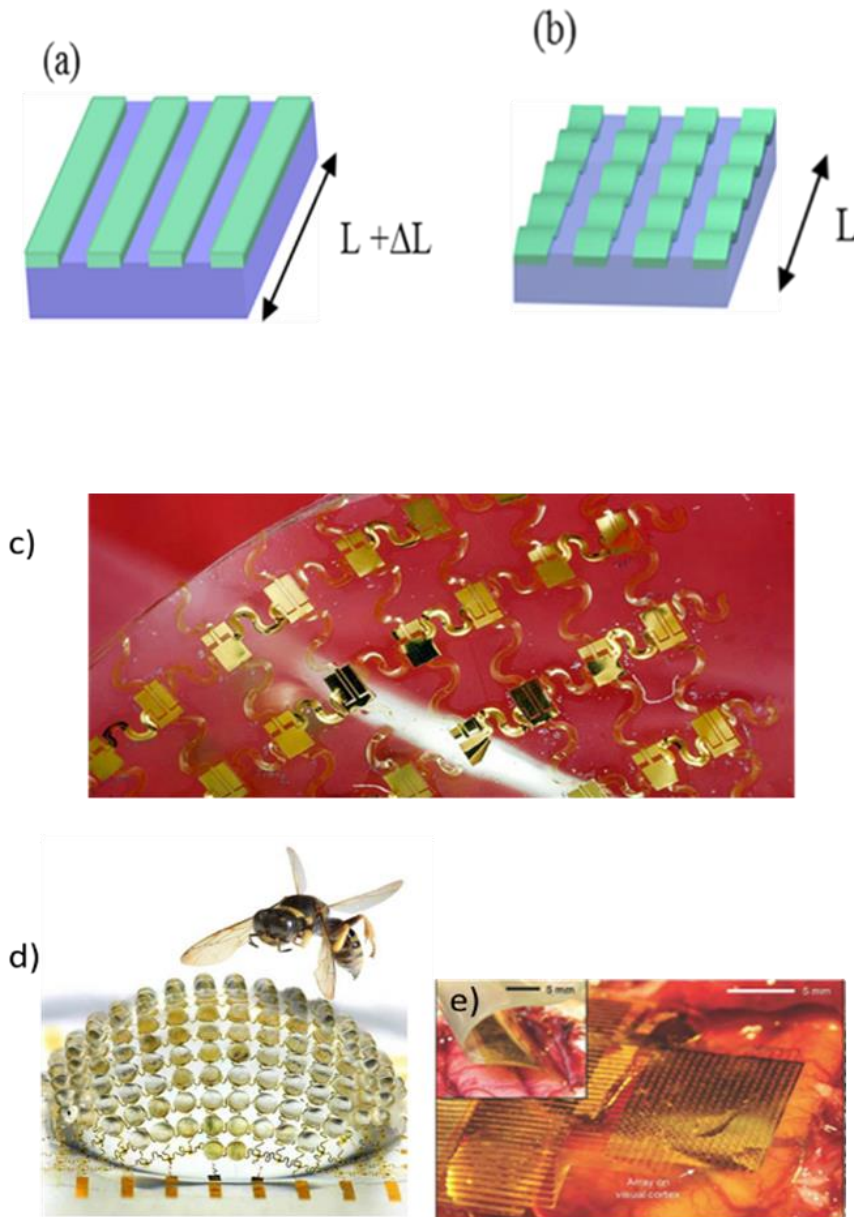


Figure 2.9. Example of soft and hard material integration (a),(b) Wrinkles in Hard/Soft Matter: Buckling pattern developed on ultrathin silicon (hard) due to release of pre-strained PDMS (soft) substrate, (c) health monitoring tattoo (d) hemispherical electronic eye mimicking the eye of bee. Adopted from (Song et al. 2013).

2.3 Motivation of Work

2.3.1 Tuning the Transition Temperature and Mechanical Properties of Poly(N-isopropylacrylamide)

Since Heskins and Guillet first conducted systematic temperature-response studies of poly(N-isopropylacrylamide) (PNIPAAm) in 1968,(Heskins and Guillet 1968) PNIPAAm and other similar co-polymer derivatives have been extensively utilized as environmentally responsive hydrogels in diverse engineering applications as seen previously, such as drug delivery(He, Kim, and Lee 2008b, Pan et al. 2011), actuators(Bassik et al. 2010), sensors (Mueller et al. 2012, Matsuguchi, Harada, and Omori 2014), smart devices, etc. (Schroeder et al. 2013, Chatterjee et al. 2013). The key reason for its wide applicability could be attributed to the existence of remarkable properties of responding to one or more stimuli such as light, temperature or pH. To utilize these materials and integrate them into modern system, we first focus on hydrogels which have fast swelling and de-swelling behavior along with the capacity of controlling the stimuli response, e.g. transition temperature in thermally responsive hydrogels.

Conventional hydrogels however demonstrate slow responsiveness due to the diffusion dominated solvent uptake process, which directly depends on the surface area of the hydrogel. Furthermore, due to the “skin effect”, an outer periphery of the hydrogel shrinks and further retards the de-swelling rate of larger gel pieces (Kim, Bae, and Okano 1992a). Previously, this issue has been tackled by increasing the pore size of the hydrogels by introducing external porogens during the synthesis (Zhang et al. 2001, Kato, Sakai, and Shibata 2003) or by developing structural inhomogeneity inside the hydrogel network. (Ma et al. 2004, Zhang, Yang, and Chung 2002b) . Such approaches have been instrumental in

accelerating the hydrogel swelling and de-swelling characteristics by incorporating capillary effect and convective transport for the solvent absorption instead of conventional diffusion mechanism as discussed above (Kaneko et al. 1998, Zhang, Yang, and Chung 2002a, Zhang and Zhuo 2001) However, the mechanical properties of such porous hydrogels can be significantly lower than the non-porous hydrogels. Thus there are fine balances of improving the mechanical properties of the porous hydrogels versus response rates.

Along with the desire for development of fast responsive hydrogels, the ability for modulation of the transition temperatures is also critical for wider applicability of environmentally responsive hydrogels. Controlling the formation and dissociation of the hydrogen bonds by altering the media quality through addition of an organic co-solvent or surfactant results in a change of the lower critical solution temperature (LCST). Previously, common solvents such as methanol (Winnik, Ringsdorf, and Venzmer 1990b) and tetrahydrofuran (Winnik et al. 1993) have been utilized to alter the LCST of the linear PNIPAAm polymer in dilute solutions. Although independently the solvents act as excellent solvents for PNIPAAm, when mixed with water, they demonstrate interesting effects on the LCST due to presence of dominant solvent-solvent interaction which is termed as co-non-solvency (Winnik, Ringsdorf, and Venzmer 1990a, Zhang and Wu 2001b, Yamauchi and Maeda 2007, Hofmann and Schönhoff 2009). Surfactants, on the other hand, modify the LCST of PNIPAAm polymer by specifically targeting the hydrophobic isopropyl groups on the PNIPAAm chain, thereby stabilizing the coil-globule transition when heated (Walter et al. 1996, Lee and Cabane 1997). These works have been instrumental in understanding the behavior of PNIPAAm molecules, however, most of these pertain to linear PNIPAAm polymer in dilute solutions and do not offer considerable insight on the effect of these additives

on the behavior of cross-linked or fast responsive PNIPAAm based hydrogels. Furthermore, comprehensive characterization methods for examining the response behavior of environmentally responsive hydrogels are also needed. Often such characterizations methods are restricted to time lapse studies of absorption or release of solvent, or involve tedious characterization techniques which do not offer a lot of thermal and mechanical information.

In the present dissertation work, one of the major emphasis has been to develop novel hydrogels which can respond to thermal stimulus faster as well as have good mechanical properties. Specifically, macroporous gels which have been postulated to have faster response characteristics due to larger pore size (greater than 10 μm) are developed by adopting low temperature polymerization with addition of siloxane compounds in the synthesis. These hydrogels were further compared with lower porosity hydrogels termed as microporous hydrogels with a pore size less than 1 μm . The microporous hydrogels were synthesized at room temperature and without the addition of siloxane group in the synthesis. Both the macroporous and microporous hydrogels were characterized using microscopy techniques such as scanning electron microscope (SEM) and confocal microscope. Apart from the morphological analysis, the effect of additives such as co-solvent (methanol) or surfactant (sodium dodecyl sulfate) on the macroporous and microporous hydrogels was studied using a differential scanning calorimetry and rheometer. Such studies offered considerable in-sight of the effect of hydrogel morphology on the thermal and mechanical properties of PNIPAAm based hydrogels. The studies here would enhance the present knowledge of both fast responsive and conventional PNIPAAm hydrogels and promote them to be more extensively utilized in advanced applications.

2.3.2 Incorporation of Visible Light Response in Poly(N-isopropylacrylamide) Hydrogels

Light responsive hydrogels are one of the most fascinating classes of environmental responsive hydrogels. The main advantages of light stimulus over other forms of environmental response are that the stimuli could be easily controlled in terms of dosage and intensity, with instantaneous manner of applying it easily. The development of light responsive hydrogel with tunable properties as proposed here could be very useful for many applications. One such potential application we are focusing here is the development of tactile display to accommodate the demand of visually impaired people to interact with modern electronic devices such as smartphones, tablets, etc. Although, numerous such systems have been developed previously with mechanical and electrical transducers, they are limited in applicability due to cumbersome setup. The proposed tactile display would be a convenient add-on the screen providing seamless integration. Furthermore, such a development would also enhance the current knowledge of light responsive hydrogel for other devices such as visible light responsive sensors and actuators by integrating hard material, such as silicon, thereby enhancing the functionality of such material.

Tactile display devices exploit sensory mechanism of humans, thereby enabling better interaction with the virtual world of modern electronic devices. Tactile display manipulate the display surfaces using actuators which are driven with electric motors (Shinohara, Shimizu, and Mochizuki 1998, Roberts et al. 2000), piezoelectric actuators (Copeland and Finlay 2010, Burch and Pawluk 2009, L\ et al. 2005, Pattanakul et al.) which modify electrical signal to pressure signal for the sensory touch etc. Other mechanisms include the use of pneumatic pressure for the recognition of display pattern and shape memory al-

loys(Yobas et al. 2003, Velazquez et al. 2008). Recently, researchers in MIT have developed tactile sensors and wearable devices which would enable users to read information by tactile method of morse codes. The researchers had sensors strapped to different part of the body to transmit data from electronic mails in form of short vibratory messages (Jones, Lockyer, and Piatieski 2006, Jones 2011). However, most of the research and development are being done with the view of visually challenged people for whom the cutaneous approach might be more useful

Similar to the previous motivation we want to incorporate light responsive characteristics along with improving the response and mechanical properties of such responsive hydrogels. Importantly, such properties, would be found useful in other applications which do not allow for thermal stimuli. Light response hydrogels, as seen earlier could be divided into various categories, depending on which range of light source the hydrogel is responding to. Popular among, is IR source as this wider impact in the therapeutic medicines. However, in the present system we would like to incorporate visible light response. Visible light response has major advantages over other wavelength as it does not require expensive light sources. Tanaka et al. previously demonstrated that light response hydrogels based on PNIPAAm could be synthesized based on established chromophores, such as salt based on chlorophyllin. These salts are known to have a delocalized electrons which can easily migrate to higher energy orbitals when irradiated with light of suitable wavelength. On reversal of the excited electrons, energy is liberated which results in shrinking of the hydrogels. Although, this technique is advantageous it requires high dosage of incident light to allow hydrogels shrink.

To overcome this inherent drawback of slow indirect heating, other molecules could be incorporated which have solid hydrophilic and hydrophobic nature. These molecules are expected to influence the hydrophilic state of PNIPAAm. One of the popular example of such molecules are azobenzene, rhodamine and other molecules. Unfortunately, most of the mentioned molecules respond only to UV or IR wavelength. Among the few molecules known, are spirobenzopyrans are a series of photochromic compounds which can be isomerized by stimuli such as light, temperature changes, and co-existing protons. Such a system of molecule could be found to very appropriate for the above purposes for light responsive hydrogels, especially for applications which demand sensitivity in the visible light region, e.g. tactile display.

One of the major challenges of integrating in the PNIPAAm hydrogels is of the miscibility of spirobenzopyrans with PNIPAAm. Although spirobenzopyrans themselves are generally insoluble in water, conjugation with water-soluble solvent makes their evaluations and applications possible in aqueous polymer systems. In the present work, we utilize tetrahydrofuran a well-known hydrophilic solvent to be useful for such purposes. Apart from the miscibility of such chromophores with PNIPAAm, we would also emphasize on tuning the response properties of such systems, as we have previously seen in thermally responsive PNIPAAm system. By incorporating the acidic groups in the synthesis we aim to increase the response time as well as improve the ring-opening and closing mechanism of spirobenzopyran.

In the particular work, as discussed we propose to use the idea of light responsive hydrogels as tactile display. One of the priorities for such a system to work efficiently is to

have better mechanical properties, which would allow for these materials to undergo various cycles of stress by the human touch. For such purposes we propose to integrate these materials with clay materials which would allow them to be stretchable enough to be used in such devices.

2.3.3 Integration of Environmentally Responsive Hydrogels with Silicon

The integration of hard and soft materials as seen previously has opened new avenues for the development of novel flexible and stretchable devices. The integration of soft elastomeric substrates with conventional semi-conducting material with decreased thickness in the range of few hundred nanometers, e.g. ultra-thin silicon, has allowed it be used in flexible applications without damaging the properties of the material. However, the inherent challenge with elastomeric substrates is that there is always a mechanical force required to drive the desired change. Such limitation can be overcome by the use of “smart” materials, which have a stimulus responsive behavior. In this work, the approach of environmentally responsive hydrogels as substrates is investigated. Specifically, such devices would combine the merits of high quality crystalline semiconductor materials and the mechanical flexibility/stretchability of elastomers, with the additional environmental response.

Yu et al. first proposed such integration and further successfully used this method to make silicon, an otherwise environmentally non-responsive material, to respond to thermal stimulus.(Yu et al. 2011) By integrating the silicon nanoribbons with temperature responsive hydrogels, the silicon nanoribbons demonstrate the ability to change their mechanical configuration as a change in ambient temperature. The potential application of

such a combination with both environmental responsiveness and mechanical flexibility/stretchability is broad and fascinating. A few examples of its potential use could be as electronic eyes with stimuli tunable curvatures that may be applied to the field of medical endoscopy, in the form of flexible, light sensitive endoscopes that can be used to maneuver into and visualize lesions in hard to reach spaces such as the cavernous sinus in the brain and the knee for arthroscopic applications.(Abuzayed et al. 2010, Campbell et al. 2010)

In establishing the viability of such an approach there are two important parameters that are yet to be explored in more detail. The first important requirement is developing an accurate control on the environmental and mechanical properties of the substrate. This is important for using the hydrogel substrate in different conditions or to provide the flexibility of generating different signals from the same substrate for different applications. As most of the studies in this thesis work involve the use of thermo-responsive polymer, the need for the controllability of the thermo-responsive properties is felt necessary. Secondly, the control over the silicon response as in buckling pattern obtained on the ultra-thin ribbon is also necessary. The control over the buckling response is necessary from the viewpoint of putting active sensor or circuitry as part of the silicon ribbon. Both these challenges have been dealt in detail over the course of the work and solutions to problems have discussed separately in different subsections.

Hydrogels, one of the most ubiquitous examples of environmentally responsive material has been used in many applications as discussed in great detail before. In spite of their potential usefulness, the idea of employing hydrogels in modern electronics is still a relatively new field. The main reason has been the lack of electrical properties of these

materials in addition to integrating and packaging issues. One of the new methods of integrating stimuli sensitive hydrogels has been demonstrated by Yu et al. by combining silicon ribbons with a temperature sensitive hydrogel, poly(N-isopropylacrylamide) (PNIPAAm). (Yu et al. 2011) This integrated structure revealed that the silicon ribbons can be made responsive to an external stimulus, such as temperature, and more importantly, such responses are reversible without fracture of the thin film silicon. This work opens up a new approach of combining traditional semiconductor materials with environmentally responsive hydrogels.

Although the work presented by Yu et al. contributed to the integration of soft and hard materials, one challenge that remains to be addressed is to enable integrated materials behave in a controlled manner so that the circuit would have certain active and inactive areas. In the present work this idea has been investigated with silicon ribbons using a photolithographic method. The controlled morphology of the thin film would eventually enable tunable responses, with the active areas corresponding to the sensors or devices and the inactive areas corresponding to the interconnections between them. Furthermore, an environmentally responsive, integrated bi-layer structure with two different types of hydrogel with tunable curvature has been integrated with thin silicon. The varying sensitivity led to a large discrepancy in the swelling ratio in a given solvent, thus resulting in the control of the curvature. Such controlled response, combined with precise silicon bonding to the gel surface, would lead to unique patterned buckling on the thin film when exposed to a given environmental stimulus.

CHAPTER 3

EXPERIMENTAL METHODOLOGY

3.1 Materials

N-isopropylacrylamide (NIPA) and acrylic acid (AA) from Sigma Aldrich Chemicals were used without further purification. N,N' methylenebisacrylamide (MBAAm), ammonium persulfate (APS), N,N,N',N'-tetramethylethylenediamine (TEMED) and tetramethylsilane (TMOS) were purchased from Sigma Chemical and used as supplied. A polydimethylsiloxane (PDMS) preparation kit was purchased from Dow Chemicals. Alexa Flour 488 was purchased from Invitrogen and used for imaging purpose under a confocal microscope.

3.2 Synthesis of Macroporous and Microporous PNIPAAm hydrogels

The macroporous hydrogel synthesis started with mixing 600 mg of NIPA with 12.6 mg MBAAm in 5.354 g of deionized (DI) water, and purged with nitrogen in a water bath maintained at 10 °C. Subsequently, 8.9 mg (23 µL) of TEMED and 104 mg (208 µL) of TMOS was added and mixed well. After 10 minutes of degassing, 1,084 µL of APS solution (1%) was added to the mixture. After waiting for 3 more minutes, the polymeric solution was then cooled down and maintained at -15 °C for 24 hours. The frozen gel samples were subsequently thawed and immersed in DI water to remove any unpolymerized monomers.

For microporous hydrogels, the synthesis started with mixing 600 mg of NIPA with 12.6 mg MBAAm in 5.354 g of deionized (DI) water, and purged with nitrogen in a water bath maintained at 25 °C. After 10 minutes of degassing, 1,084 µL of APS solution (1%)

was added to the mixture. The reaction was allowed to proceed at room temperature for 24 hours.

3.3 Preparation of PNIPAAm/PAA Bilayer Hydrogels

600 mg of NIPA was initially mixed with 12.6 mg MBAA in 5.354 g deionized (DI) water. A vortex mixer was used to mix the above solution for 10 minutes, after which 8.9 mg (23 μ L) of the accelerator TEMED was added and mixed. Following 10 minutes of degassing, 1,084 μ L of 1% APS aqueous solution (initiator) was added in the mixture. An appropriate amount of the polymer solution was added in a cylindrical mold with dimensions of 16 mm diameter and 20 mm height, then following with degassing with nitrogen for 15 minutes so that the polymerization can take place. For the pH sensitive layer, 600 mg NIPA, 375 μ L AA and 12.6 mg MBAA were added to 5.354 g of DI water. The mixture was agitated well in a vortex mixer for 10 minutes, after which nitrogen gas was bubbled through it to degas for 20 minutes. 230 μ L TEMED and 1084 μ L of 1% APS aqueous solution was then added to the above mixture. A specific amount of this mixture solution was added on top of the initial PNIPAAm layer which was partially polymerized. After which, the mold was kept in an oven at 50 °C for 1 hour to allow the polymerization process to complete. Finally, a bilayer gel structure was obtained with a PNIPAAm top layer and poly(NIPA-co-AA) bottom layer.

3.4 Bonding of Silicon to PNIPAAm Hydrogels

After the hydrogel was synthesized and reached equilibrium in fresh water, a mixture of Sylgard 184 Silicone elastomer base and curing agent (with a ratio of 30:1) was spread on the top surface of the swollen hydrogel slab. The uncured PDMS spontaneously

spread out and formed a continuous thin layer with smooth surface in a few minutes due to the flow driven by surface tension. After the PDMS was solidified, the sample was exposed to ultraviolet light with atomic oxygen (UVO) for 150 seconds to generate hydroxyl (–OH) groups on the top surface of the PDMS layer, which is essential for transfer printing Si thin films. The Silicon ribbons were then transferred to the hydrogel/PDMS system.

3.5 Synthesis of Light Responsive Hydrogels

3.5.1 Physical Approach

Briefly, to synthesize the chlorophyllin based PNIPAAm hydrogel, 0.6 gram of the N-isopropylacrylamide monomer will be mixed with 0.3 gram of copper (II) salt of chlorophyllin in certain amount of water. Further, the mixture will be degassed and a solution of tetramethylenediamine (catalyst) and ammonium persulfate (initiator) will be added to start the polymerization process and subsequently allowed to continue for 6 hours at room temperature. The obtained gel will then washed with copious amount of water and dried in

3.5.2 Chemical Approach

Briefly, a solution of 1.47 g (5.0 mmol) of 1',3',3'-trimethyl-6-hydroxyspiro(2*H*-1-benzopyran-2,2'-indoline) and 2.0 mL (14.3 mmol) of triethylamine in dry THF (50 mL) was stirred at 0 °C. A total of 0.57 mL (7.0 mmol) of acryloyl chloride was added to the mixture, and then the mixture was stirred at 25 °C for 15 h. After the solvent was removed in vacuum, ethyl acetate and saturated aqueous sodium hydrogen carbonate were added and the aqueous phase was extracted with ethyl acetate. The combined organic phase was washed with brine, dried over anhydrous magnesium sulfate, and filtered. After evaporation of the solvent, the residue was purified by silica gel column chromatography (1/6 ethyl acetate/*n*-hexane as the eluent) to give the acrylated spirobenzopyran monomer (1.14 g,

3.29 mmol, 65 w/w%). Subsequently, NIPAAm monomer (84.0 mg, 0.7425 mmol), acrylated spirobenzopyran co-monomer (2.60 mg, 0.0075 mmol) and the BAAM (5.8 mg, 0.0375 mmol) cross-linker were dissolved in the THF/water mixture (1.0 mL; volume ratio was 70/30). Next, TEMED (1 μ l) and finally the aqueous solution of APS (1 mg) in H₂O (20 μ L) were added. Further, to incorporation of acrylic acid was done to enhance the re-swelling ratio of the hydrogels. Specifically, 1 ,2.5,5 wt% of acrylic acid compared to PNIPAAm wt in the hydrogel was used.

3.6 Materials Characterization

Scanning Electron Microscopy

The surface morphology of the hydrogels was studied using a scanning electron microscope (XL Series-30, Philips). Specimens were initially freeze-dried and then glued to the brass holders followed with gold sputtering for 100 s using a sputter machine (JFC-1200 Fine coater) prior to the SEM examination.

Confocal Microscopy

The structure of the hydrogels was investigated using a Leica SP5-X Confocal Microscope. Alexa Fluor 488 fluorescent dyes were absorbed by the hydrogels to differentiate between the polymeric network and intermittent pores. An Argon laser (488 nm) was used to image these materials.

Instron

The compressive stress-strain curves of both macroporous and microporous hydrogels were obtained by conducting tests on a MTS servo hydraulic test system with a load

cell of 500 grams. Tests were run in displacement control in longitudinal direction at a loading rate of 1 mm/min.

Rheometry

A TA rheometer (TA Instruments AR-G2) was employed to perform a temperature sweep on both the macroporous and microporous PNIPAAm hydrogels. The temperature responsive hydrogel samples were first equilibrated in water or the appropriate media and then subjected to a ramp rate of 0.25 °C/min and frequency of 1 rad/s. The upper and lower temperatures for the temperature sweep tests were decided depending on the media.

Dynamic Mechanical Analysis

The dry films of hydrogels were tested for their glass transition temperature using a TA dynamic mechanical analyzer (TA Instruments Q 800). The films were attached to tensile testing grips and subjected to a temperature ramp condition of 3 °C /min from 25 °C to 220 °C at a frequency of 1 Hz.

Differential Scanning Calorimetry

A TA Differential Scanning Calorimeter (TA Instruments Q-20) was used to characterize the transition temperature of the thermoresponsive hydrogels. First, the dry gels were equilibrated with HPLC water or the appropriate media and then analyzed with respect to same solvent as reference. The upper and lower temperatures for the DSC experiments were decided depending on the media with a heating rate of 3 °C/min.

Re-swelling and swelling Ratio Measurements

The swelling ratios of the hydrogels were measured gravimetrically after wiping off the excess water on the surface. The hydrogel was incubated in a particular media for 24 hours at room temperature. The re-swelling ratio measurements were calculated as $S_r =$

W_t/W_D where W_t is the net weight of the equilibrated hydrogel after the solvent is re-absorbed and W_D is the dry weight of the hydrogel. Similarly, the swelling ratio was calculated as $S_D = W_t/W_o$, where W_t is the weight of equilibrated hydrogel after is solvent absorbed by the hydrogel and W_o is the weight of dry hydrogel.

CHAPTER 4

RESULTS AND DISCUSSIONS

4.1 Tuning the Swelling Kinetics of PNIPAAm

4.1.1 Dependence of Synthesis Technique on Morphology and Swelling Kinetics

Figure 4.1 shows the significant difference in morphology of poly (N-isopropylacrylamide) hydrogels synthesized using different procedures. For the hydrogels demonstrated in Figure 4.1a, 4.1b the reaction temperature of the monomeric mixture was maintained below the freezing point of water which results in the formation of large ice crystals in the system and provides framework for the formation of macroporous PNIPAAm hydrogels. Additionally to ensure uniform growth of the ice crystals, the synthesis process was divided into two stages. In the first stage monomeric solution was initially mixed at a temperature of approximately 10 °C in an inert environment for a few minutes. Following this, the mixture was again placed under the same condition (10 °C) for few more minutes before finally placing it in a freezer maintained at -18 °C. The initial step of low temperature equilibration facilitated in uniform nucleation and growth of ice crystals in the system. Previously Zhang et al. (Zhang and Zhuo 1999) and Strachotova et al., (Strachotova, Strachota, Uchman, Šlouf, et al. 2007) have highlighted the importance of such a two-step temperature reduction process. Importantly, a temperature regime of lower than -20 °C in the final stage is not conducive for formation of macroporous hydrogel as smaller and numerous solvent crystals are formed and result in smaller pore sizes. (Lozinsky et al. 1984, Srivastava, Jain, and Kumar 2007) After the reaction was completed the hydrogels were thawed, which allowed the ice crystals in the hydrogel to melt, thereby creating a three dimensional interconnected porous network, as depicted in both the SEM (Figure 4.1a)

and confocal images of the macroporous hydrogels (Figure 4.1b). In contrast, the microporous hydrogels shown in figure 4.1c and 4.1d, were synthesized at room temperature without any change in monomeric or initiator composition except the omission of TMOS. A visual comparison from the micrographs clearly revealed the efficacy of such a low temperature methodology in creating a uniform three-dimensional and inter-connected porous network. Furthermore, such a technique was proven to have faster re-swelling rate due to solvent absorption by capillary action and convective flow of fluid media into the porous network as opposed to the slower and surface area dependent diffusion process in the microporous hydrogel (Figure 4.2a).

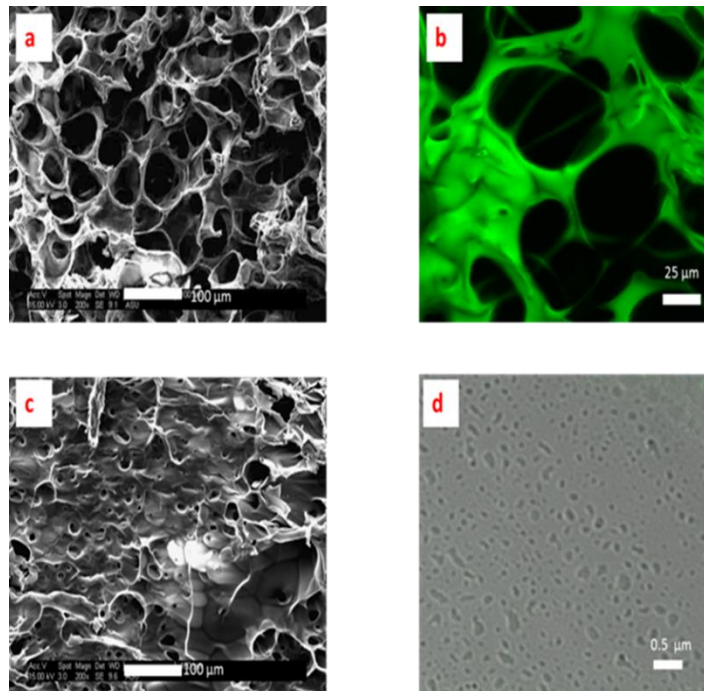


Figure 4.1. SEM and Confocal microscopy for morphology studies of PNIPAAm hydrogel: (a), (b) macroporous hydrogel with average pore length of $\sim 50\mu\text{m}$; (c), (d) microporous hydrogel with average pore length $\sim 1\ \mu\text{m}$.

4.1.2 Dependence of Synthesis Conditions on Mechanical Properties

Although low temperature synthesis successfully assists in the formation of a desired three dimensional large porous polymeric hydrogel system, it results in lowering of the mechanical properties and structural integrity which is an adverse effect of such synthesis (Zhang et al. 2001). One of the facile ways of achieving faster responsive PNIPAAm hydrogels with better mechanical properties is by copolymerizing NIPAM with tri-methylsiloxane(TMOS) or other siloxane compounds to create porous network with better mechanical properties (Strachotova, Strachota, Uchman, Šlouf, et al. 2007, Zhang and Zhuo 2001). In the macroporous hydrogel synthesis, an in-situ silicate network was incorporated by a hydrolysis reaction of TMOS with water. The silica network provides an additional backbone for the PNIPAAm hydrogel by stabilizing the pores and channels, thereby delivering improved re-swelling rates over conventional microporous hydrogel as previously discussed in Figure 4.2a and also form a mechanically strong network.

The postulated improved swelling and de-swelling response rate and better mechanical properties of the fast responsive macroporous hydrogel were further accurately quantified and compared by a viscoelastic-temperature study on both the hydrogels (macroporous, microporous) with the help of a rheometer. The gap change information acquired from such temperature sweep studies revealed that the macroporous hydrogels had a steeper slope, suggesting a quicker de-swelling behavior when compared to microporous hydrogels (Figure 4.2b). The rheological data also demonstrated that the storage modulus and the loss modulus of the macroporous gels were much higher than the microporous gels (Figure 4.2c). A separate compressive stress analysis on the saturated hydrogels using an Instron instrument revealed that the macroporous gels were 1.33 times

tougher than the microporous gels (Figure 4.2d). Both the rheometer and Instron results validated the important idea that the silicate network played a decisive role in strengthening the framework of the gels. As such this method is more simpler and efficient than the other previously reported techniques such as (1) the incorporation of surfactants during the hydrogel preparation, (Antonietti et al. 1999, Gemeinhart et al. 2000) (2) hydrogel preparation during the LCST (Kabra, Gehrke, and Spontak 1998, Zhang and Zhuo 2000, Baek et al. 2001) or (3) hydrogel preparation just by a freeze dry and hydration process (Kato and Takahashi 1997).

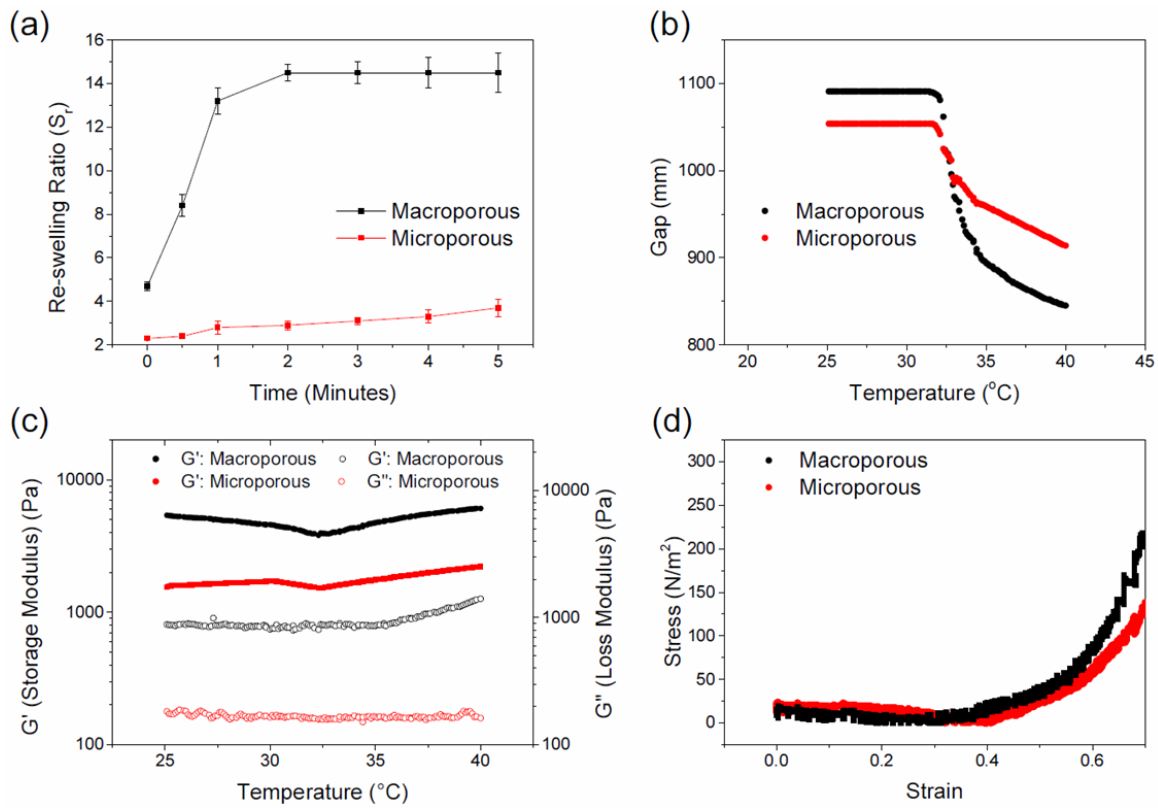


Figure 4.2. Mechanical Properties of Macroporous and Microporous Hydrogel: (a) Comparison of Re-swelling rate of the hydrogels; (b) Gap change in Rheometer for macroporous and microporous hydrogels; (c) Rheometer analysis of macroporous and microporous hydrogels; d) Instron compressive analysis of water saturated hydrogels.

Figure 4.3a, 4.3b demonstrates the DMA data to analyze the glass transition temperatures (T_g) of the macroporous and microporous hydrogels respectively by utilizing $\tan\delta$ which is a ratio of the loss modulus (G'') to the storage modulus (G'). Interestingly, the glass transition temperatures of the dry macroporous hydrogel ($T_g = 181.7\text{ }^\circ\text{C}$) is significantly higher than the microporous hydrogel ($T_g = 149.7\text{ }^\circ\text{C}$). As we already know, the glass transition corresponds to the temperature at which there is substantial mobility of the polymeric chains. If the interactions among polymer chains are strong, a higher temperature would be needed to promote this chain mobility. In the case of macroporous hydrogels due to addition of the silicate network there might be slowing down of chain mobility which subsequently results in a higher T_g . These results are interesting, as such an increase in glass transition has not been seen by other reported techniques to synthesize fast responsive macroporous hydrogels (Antonietti et al. 1999, Gemeinhart et al. 2000, Kato and Takahashi 1997).

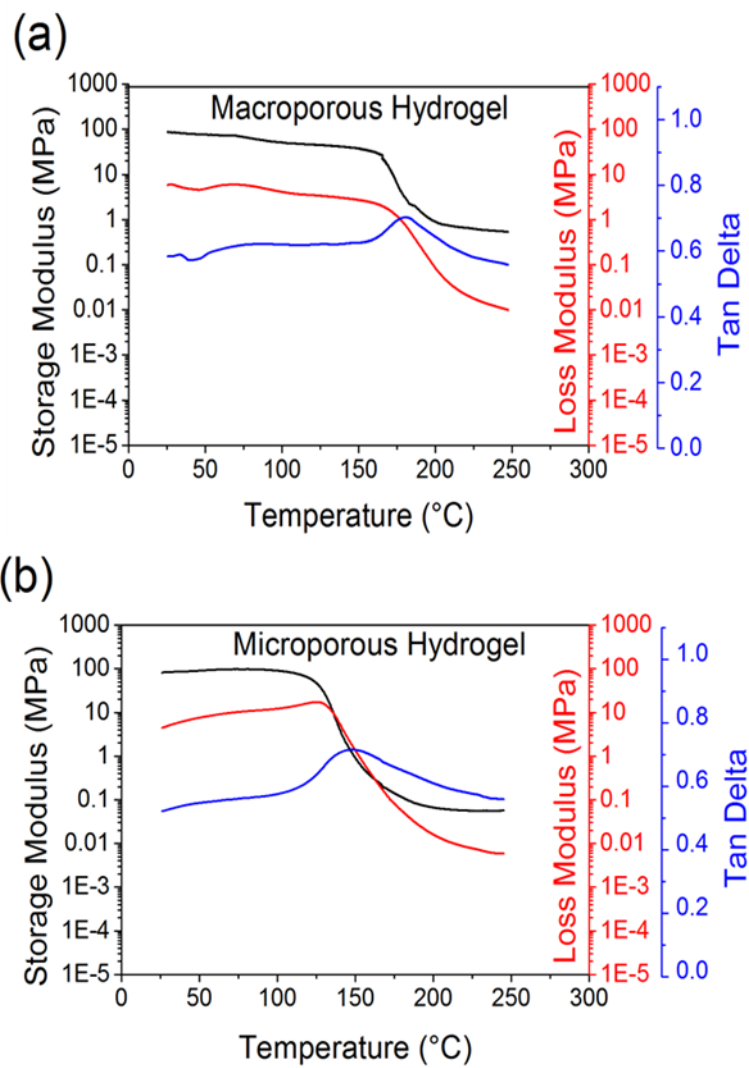


Figure 4.3. DMA analysis of dry hydrogel: (a) Macroporous PNIPAAm hydrogel; (b) Microporous PNIPAAm hydrogel.

4.2 Tuning the Transition Behavior of Poly(N-isopropylacrylamide)

4.2.1 Effect of Co-Solvent

Figures 4.4a and 4.4b demonstrates the DSC thermograms depicting the transition temperature of macroporous and microporous PNIPAAm based hydrogels respectively due to the addition of an organic solvent (methanol) in the media. Conventionally, the transition temperature is referred to the endothermic peak in the DSC thermogram (Zhang and Zhuo 1999). Both the macroporous and microporous hydrogels demonstrate a significant shift in the transition temperature as the concentration of the methanol is varied (Figure 4.4c). This observation is in good agreement with experiments done initially by Winnik et al. to study the effect of methanol as a co-solvent for linear PNIPAAm polymer in dilute aqueous solutions. (Winnik, Ringsdorf, and Venzmer 1990b) This rare and interesting occurrence of cononsolvency is quite different from cosolvency in which a mixture of two or more solvents acts as a solvent for a particular compound, such as a polymer, when independently both the solvents are inept in solubilizing the third component. (Wolf and Blaum 1975) In this case PNIPAAm demonstrates cononsolvency, as both methanol and water are excellent solvents for it, however when mixed together the LCST of the PNIPAAm molecule shifts, suggesting marked decrease in the solubility. The present case is different from the linear PNIPAAm polymer chains as both the macroporous and microporous hydrogels discussed here are cross-linked.

In the past, there have been competing explanations for the presence of cononsolvency. The first one suggests the complexation between water and methanol induced by the presence of the PNIPAAm network. (Amiya et al. 1987, Hirotsu 1988) But such an

argument had difficulty in explaining the re-entrant swelling behavior in an extremely dilute solution with linear PNIPAAm polymer. (Schild, Muthukumar, and Tirrell 1991, Yang, Li, and Wu 2004, Zhang and Wu 2001a) The second theory postulates, the presence of ‘competitive’ absorption between PNIPAAm-water and PNIPAAm-methanol. (Tanaka, Koga, and Winnik 2008, Tanaka et al. 2009) But such an argument also does not hold ground based on its initial hypothesis that the solvent-solvent interaction is insignificant, which has been subsequently contested by other work. (Dixit et al. 2002, Guo et al. 2003) The last theory initially proposed by Zhang and Wu, (Zhang and Wu 2001c, b) explains quite well the peculiar behavior of both linear PNIPAAm polymer and cross-linked PNIPAAm based hydrogels in the presence of methanol. It predicts the formation of stoichiometric compounds between the solvent molecules which are poor solvents for PNIPAAm hydrogels.

Figure 4.4d depicts the change in the enthalpy value during the phase transition of macroporous and microporous hydrogel by integrating the peaks obtained from the DSC thermograms. For the macroporous hydrogel the enthalpy value (only water) is higher than the microporous hydrogel, suggesting that for a given temperature increase above the transition temperature, the amount of water released is higher. This is because the freed water within the heterogeneous macroporous hydrogel is able to diffuse outward more easily than from the microporous hydrogel. Such an analysis is also in accordance with the faster re-swelling and de-swelling rate of macroporous hydrogel discussed in the previous section (Figure 4.2a, 4.2b) and also with earlier reported results on other macroporous hydrogel synthesized using a different technique (Zhang, Yang, and Chung 2002a)

The rise in the methanol percentage in the media induced a sharp decrease in the enthalpy change during the phase transition as evident from Figure 4.4d. Such a decrease highlights the limited affinity of such a media for both the macroporous and microporous hydrogel. This depression in enthalpy content and transition temperature is followed by an abrupt increase of both these values as the media became more methanol rich and therefore more suitable for hydrogen bonding with the hydrogels as deduced earlier by Winnik et al. (Winnik, Ringsdorf, and Venzmer 1990b) Intriguingly the effect of higher concentrations of methanol on the macroporous hydrogel could not be perceived by the DSC resulting in a disappearance of endothermic peak for methanol concentration at 60% by volume. Such an observation probably implies that the better interconnected porous network of macroporous hydrogel leads to enhanced solvent entry and substantial hydrogen bonding.

Moreover, although there is a similarity in variation of the transition temperature as a function of methanol concentration for both macroporous and microporous hydrogels, the enthalpy value during the phase transition is different along with a variation in the transition temperature itself. The lower transition temperature of macroporous hydrogel over microporous hydrogel for the same methanol concentration in the media could be explained with the faster mechanism of solvent absorption and release by the macroporous hydrogels as discussed earlier to explain similar alteration in transition temperature and enthalpy values for pure water as media. Thus faster outward solvent movement leads to the suppression of the transition temperature for the same concentration of the methanol. Interestingly, Figure 4.4c also indicates that the drop in enthalpy values of macroporous hydrogel in methanol environment is significantly sharper than microporous hydrogels. Such observations have not been reported before and probably indicate different affinity

for methanol by macroporous hydrogel in comparison to microporous hydrogel. Also this could imply stronger hydrogen bonds which are not susceptible to breaking and re-formation through temperature changes. Overall, these findings highlight the variance in the thermal effects of cononsolvency in PNIPAAm based hydrogel as function of porosity.

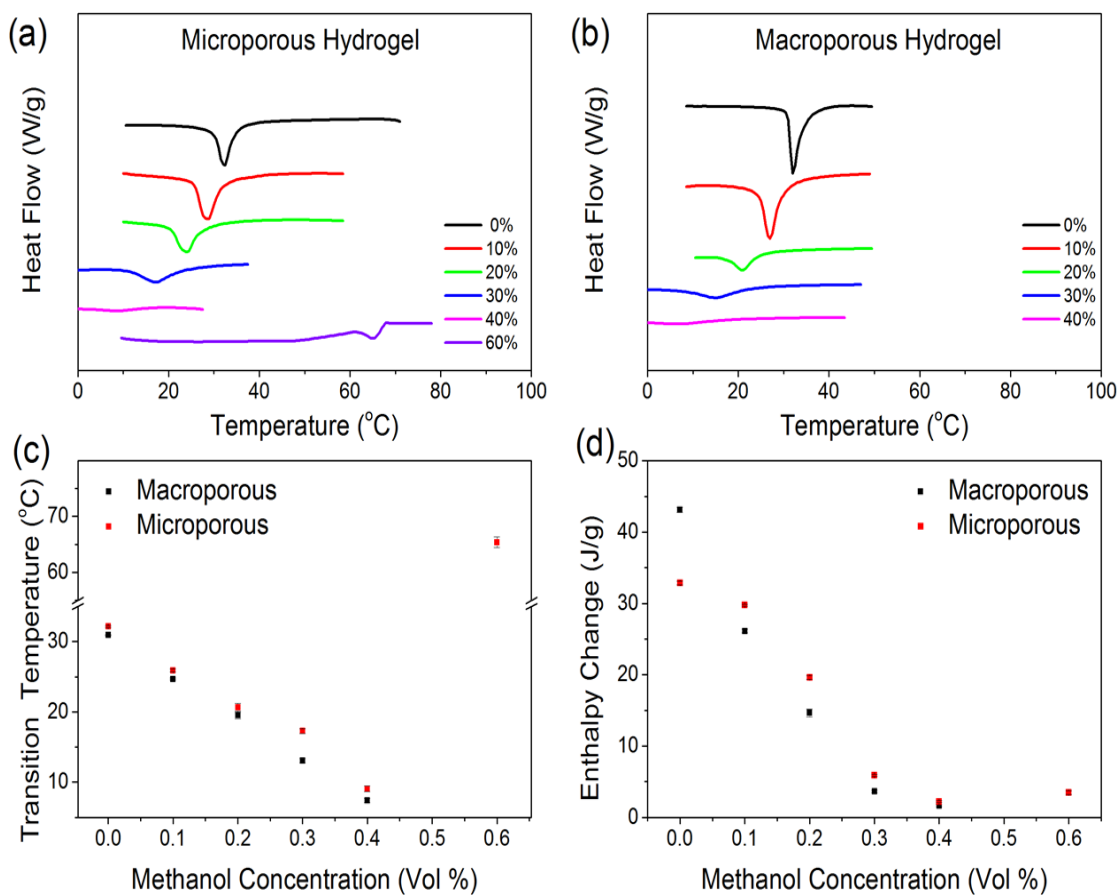


Figure 4.4. Transition temperature and enthalpy change during transition of PNIPAAm hydrogel with variation of methanol percentage: (a) DSC thermograms of macroporous hydrogel; (b) DSC thermograms of microporous hydrogel; (c) Comparison of LCST with change in porosity and change of solvent; (d) Comparison of heat of fusion with change in porosity and change of solvent.

Both the macroporous and microporous hydrogels demonstrated a decrease in swelling ratio at concentrations of methanol when the transition temperature had decreased, and increased again as the methanol concentration rises over certain percentages (Figure 4.5a). The decrease in the swelling ratio suggests the limited absorption of methanol-water mixture by both macroporous and microporous hydrogels which as discussed before decreases the enthalpy change during phase transition as well as the transition temperature. However as the methanol percentage is increased over 50% the swelling ratio recovers suggesting suitable media for hydrogen bond formation and lower water-methanol interaction. Interestingly, the phenomenon is heightened in the case of microporous gels in which the swelling ratio has been affected to much larger extent. The larger pore size of macroporous hydrogels thus circumvents the abrupt swelling ratio by allowing more solvent molecules to penetrate into the hydrogel.

Apart from the differences in swelling ratio there is also effect on the mechanical properties due to the presence of methanol in the media. At 20% methanol concentration by volume in the media the macroporous hydrogel demonstrated a slight increase in the storage modulus (G') and loss modulus (G'') when compared to similar experiment results in the previous section using a rheometer and pure water media (Figure 4.2c, 4.5b). The increase of the mechanical properties could be deduced to the lower solvent uptake and the shrunken nature of the macroporous hydrogel in presence of methanol. Along with the increase of the mechanical properties the increase of the G' at approximately 20 °C suggests the transition temperature and validates the DSC results signifying the depression of the transition temperature due to the presence of methanol in the media.

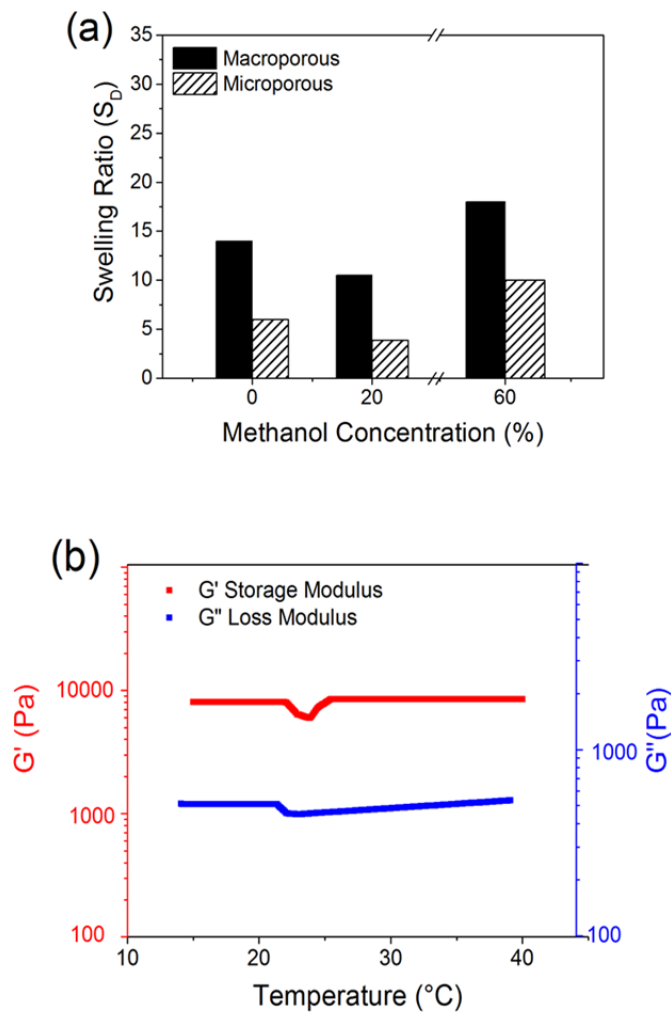


Figure 4.5. Effect of methanol concentration on the swelling ratio and rheological properties (a) Comparison of swelling ratio between macroporous and microporous hydrogel under different methanol concentration (b) Rheometer analysis of macroporous hydrogel equilibrated with 20 % methanol concentration.

4.2.2 Effect of Surfactant

Figures 4.6a, 4.6b depict the effect on the transition temperature of microporous and macroporous hydrogel respectively as a function of increase in the concentration of anionic surfactant, sodium dodecyl sulfate (SDS). SDS has been chosen as it has been previously established that anionic surfactants interact more strongly with non-ionic polymers like PNIPAAm when compared to cationic surfactants. (Anthony and Zana 1994, Loh, Teixeira, and Lee 2004) The results are also in good agreement with the first observed effects of surfactants on the coil-globule transition of linear PNIPAAm polymers (Meewes et al. 1991) and later, on cross-linked PNIPAAm hydrogel. (Kokufuta et al. 1993)

The effect of surfactant on the transition temperature of PNIPAAm has been attributed to alterations in the hydrophobic interactions of PNIPAAm with water due to presence of charged moieties in the media. Various earlier works have deduced that the hydrophobic part of surfactant binds locally with the isopropyl group of PNIPAAm hydrogel. (Kokufuta, Suzuki, and Sakamoto 1997, Dhara and Chatterji 2000, Borsos and Gilányi 2011) This converts the intrinsically non-ionic nature of the PNIPAAm polymeric network to polyelectrolyte type. Thus these additional acquired charges on the PNIPAAm polymer network directly influences the transition temperature of the PNIPAAm hydrogels by balancing the hydrophobic forces brought about by the disruption of the hydrogen bond with water or other media when the temperature is raised. This explanation is also similar to the observed increase of the transition temperature of ionic hydrogels and microgels. For example, poly(N-isopropylacrylamide-co-acrylic acid) hydrogel has a higher transition temperature than simple PNIPAAm hydrogel due to ionized carboxylic acid group (-COOH) presence on the polymeric chain, (Kratz, Hellweg, and Eimer 2000) which subsequently

increases the hydrophilic nature of the polymeric network and counters the hydrophobic nature of PNIPAAm molecule above a certain temperature.

The compiled effect of the transition temperature as a function of porosity is represented in Figure 4.6c. These results when compared to the earlier section, i.e. effect of methanol on the transition temperature due to co-nonsolvency seems different (Figure 4.4c), as the alterations due to surfactant on the transition temperature could be ascertained as of increasing nature only, unlike methanol, where both increase and decrease of transition temperature occurs depending on the methanol percentage in the media. The effect of presence of the surfactant molecules in the media can be better analyzed through changes in the enthalpy value during transition (Figure 4.6d). The macroporous and microporous hydrogel both demonstrated an increase in the enthalpy change during transition with increasing surfactant concentrations. This occurrence is explained through higher stability of the PNIPAAm due to local binding of surfactant molecules on the PNIPAAm chain as discussed earlier, thereby suggesting that the transition process here is more thermal energy intensive owing to the stronger surfactant interaction with the polymeric network. Also interestingly the microporous hydrogels produced much higher enthalpy changes during phase transition and higher transition temperature when compared to macroporous hydrogel. These results suggests that due to the lower pore size in the microporous hydrogel the proximity of the polymeric chains is far greater which subsequently increase the effect of the surfactant molecules and lead to higher interactions between the electrolytic charges of the surfactant molecules locally bound on the polymer network. The higher interaction of the electrolytic could cause greater charge repulsion and expansion of polymer network and results in increase of polymer network stabilization with respect to temperature.

The additional ions on the network also increase the osmotic pressure and results in increase of the overall swelling ratio as seen in Figure 4.7a. These results were in good agreement with the work done earlier by Kokufuta et.al on conventional cross-linked hydrogels (Kokufuta et al. 1993, Kokufuta, Suzuki, and Sakamoto 1997). The microporous hydrogel demonstrated greater than six fold increase in the swelling ratio when the surfactant concentration in the media was 10mM or higher, while the macroporous hydrogels showed a maximum increase of approximately 1.6 times increase in the swelling ratio. Such results probably imply that the microporous hydrogels have a higher local osmotic pressure or higher charge interaction of the surfactant molecules or both when compared to macroporous hydrogels on account of considerable differences in porosity. Further the effect on mechanical properties due to presence of surfactant in the media was studied with the help of rheometer. The decrease of the storage modulus (G') and loss modulus (G'') when compared to pure water media indicates the increase in the swelling ratio in such an environment (Figure 4.2c, 4.7b). Moreover the comparison between the effect of methanol (Figure 4.5b) and surfactant could be drawn from such experiments. As seen before methanol causes increase in the G' and G'' at low concentrations due to limited swelling ratio while the presence of anionic surfactant in the media decreases both the moduli considerably due to a much higher swelling ratio. The rheometer results also validate the increase of transition temperature as analyzed by DSC due to the presence of surfactant in the media. Here at a temperature of approximately 62 °C an increase in the G' and G'' is noticed suggesting a volume transition of the macroporous hydrogel in such a media.

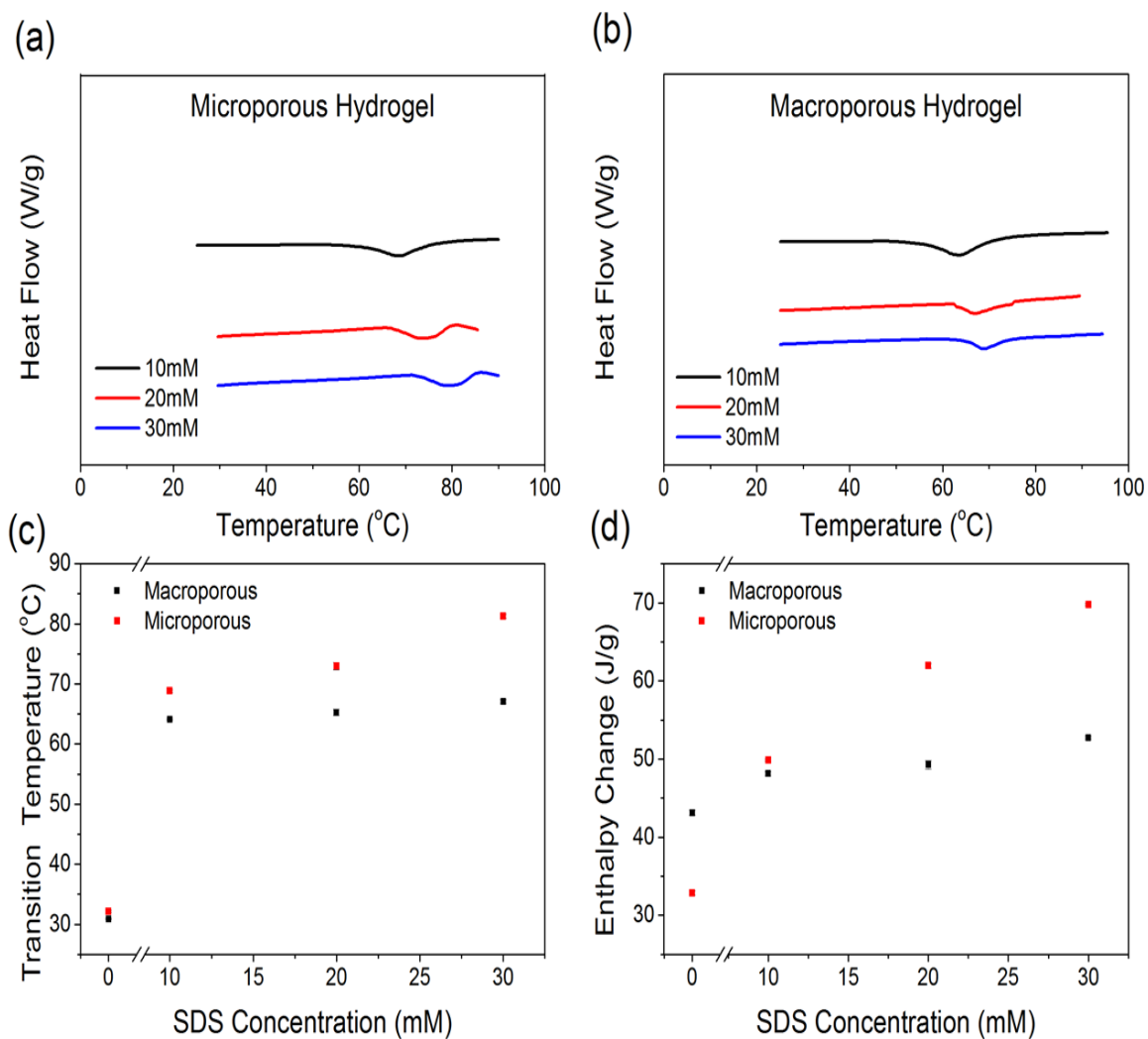


Figure 4.6. Transition temperature and enthalpy change during transition of PNIPAAm hydrogel with variation of surfactant concentration: (a) DSC thermograms of macroporous hydrogel; (b) DSC thermograms of microporous hydrogel; (c) Comparison of transition temperature with change in porosity and change of surfactant concentration; (d) Comparison of heat of fusion with change in porosity and change of surfactant concentration.

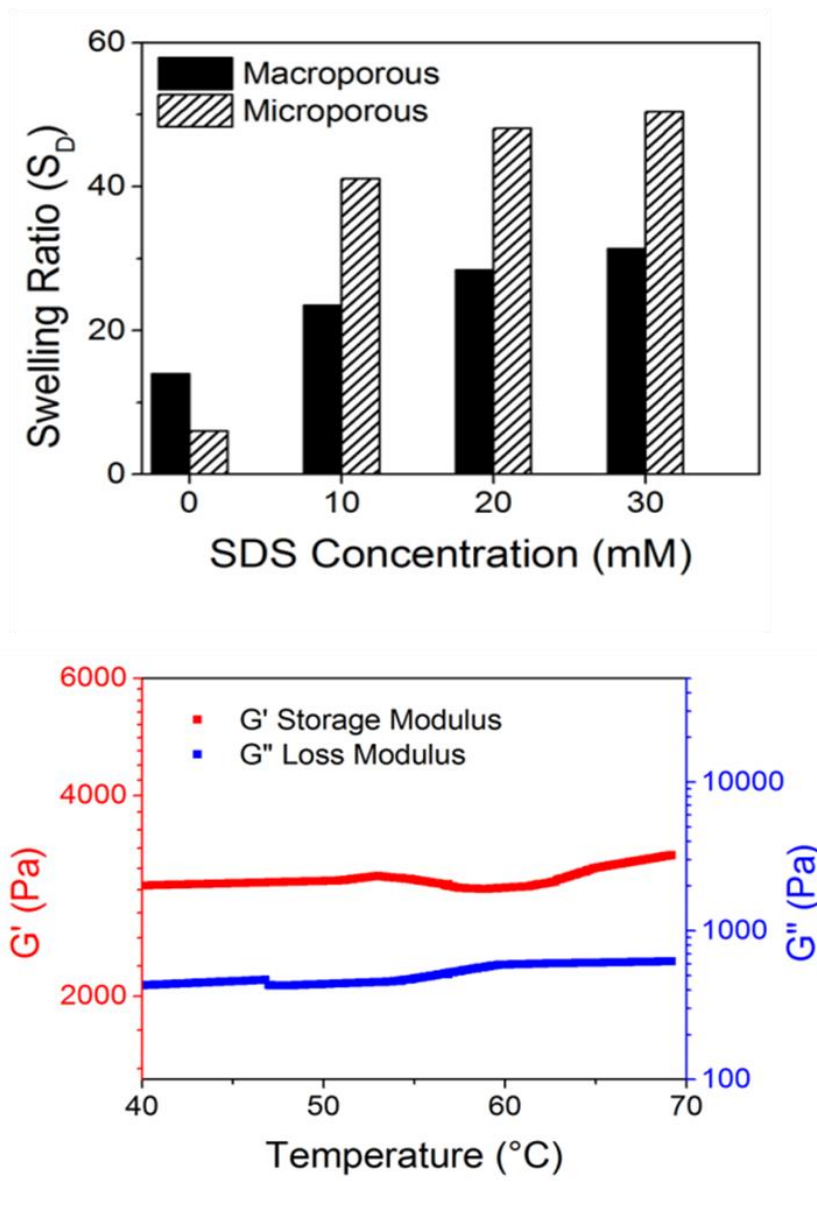


Figure 4.7. Effect of surfactant on the mechanical properties and swelling ratio (a) Rheometer analysis of macroporous gel equilibrated with 10 mM; (b) Swelling ratio under different SDS concentration.

4.3 Integration of Poly(N-isopropylacrylamide) Hydrogels with Silicon

4.3.1 Development of Adhesion Mechanism between Hydrogels and Silicon

Figure 4.8 is the illustration of the proposed integration of hydrogels with the hard materials, such as silicon. Previously it has successfully demonstrated that when silicon is made thin enough, in range of 500 nm or less allows for the reversible buckling of silicon (Sun and Rogers 2007). In the present work, we focus on making these buckling pattern responsive to environmental stimulus by integrating the thin film silicon with soft environmentally responsive hydrogels, functioning as “smart” substrate.

One of the major challenges in integration of such soft and hard material in a single system has been the lack of adhesion properties between these two diverse materials. Furthermore, as the hydrogel in its equilibrated state majorly consists of water, it becomes a major challenge to have consistent bonding between the hydrogel surface and silicon thin film. One of the unique methods of solving this problem could be by the use of an intermediate layer which would help to alleviate the problem of adhesion of silicon and hydrogels. Here, an elastomeric material which is hydrophobic in nature and is proposed to have the ability to bond with silicon and allow for complex transfer printing techniques. One example of such a material is poly(dimethylsiloxane) or PDMS. Previously, PDMS has been utilized for transfer of silicon due to excellent adhesion between silicon and the PDMS elastomer. Another major advantage of PDMS, particularly here, is the fact that PDMS is highly hydrophobic in nature, which resist the penetration of water from the hydrogel system to interact with the silicon entities.

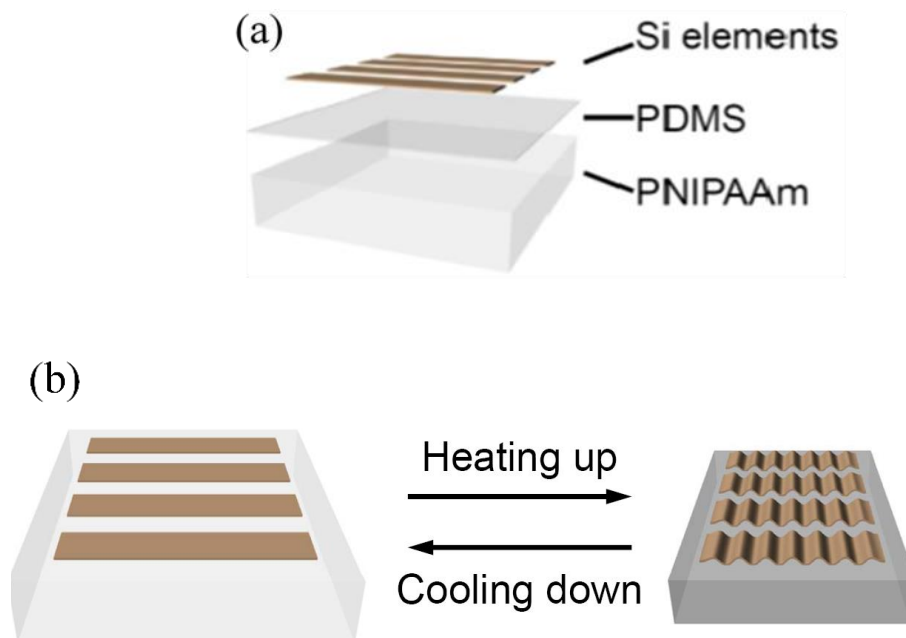


Figure 4.8. (a) Layer-assembled structure of the PNIPAAm/PDMS integrated with Silicon nanoribbons. (b) Schematics of the hydrogel swelling/shrinking drivable Silicon thin ribbons.

However, PDMS due to hydrophobic nature does not share any adhesion with water based system such as hydrogels. Previously, we have successfully demonstrated that the porosity of the hydrogels as well as the mechanical properties could be had been increased by incorporation of silicate compound, tetramethyl orthosilicate, which formed a silicate network inside the hydrogel network. For the purposes of adhesion also, the renewed chemistry of the macroporous hydrogel is leveraged. XPS spectra demonstrates how the PNIPAAm hydrogel undergo condensation reaction with the hydrogel surface (Figure 4.9 b)

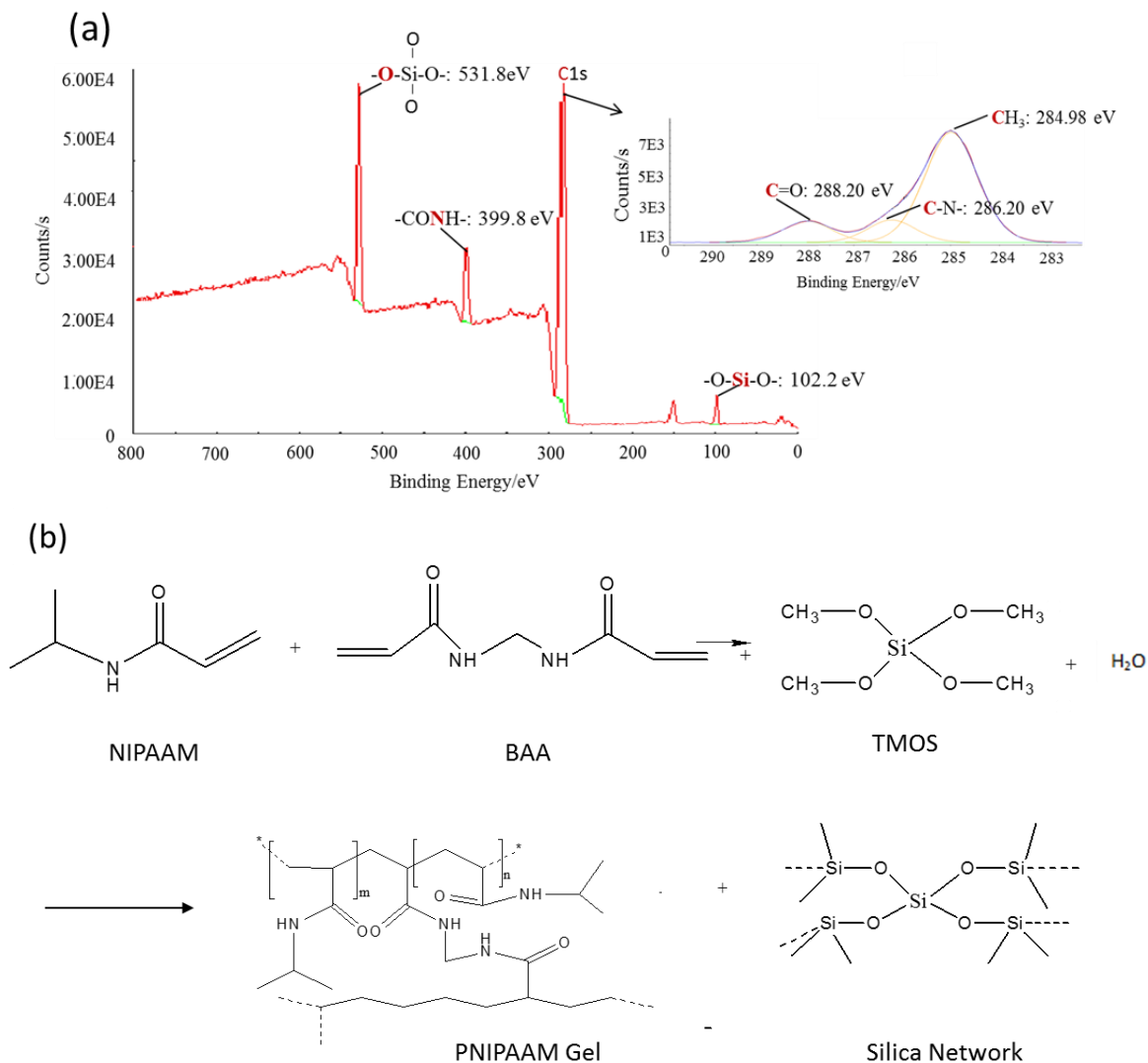


Figure 4.9. (a) XPS spectra of the PNIPAAm-based hydrogel. The exact value of binding energies and their chemical state of the corresponding elements at each peak are labelled. The inset is core-level spectrum of the C in (a) (Blue line is from the raw data); (b) Formation of PNIPAAm-based gel integrated with TMOS (Adopted and modified from Y Pan et al., 2012).

From the XPS spectra, the characteristic peaks and their corresponding binding energies can be identified and characterized. The binding energy located at 151 eV is characteristic of Si2s line, normally XPS artifacts, and is not used for further analysis. The carbon (C1s) spectrum can be curve-fitted with three peak components (see the inset image in Figure 4.9 (a)): with binding energy at 284.99 eV for CH₃ species, at 287.96 eV for C=O species and at 286.22 eV for the C-N species (Beamson and Briggs 1992). The peak position of N1s at 399.8 eV, matches very well with -CONH- species (Khang et al. 2006, Sun et al. 2006a). These peaks demonstrated the presence of amide group of the PNIPAAm molecule. The binding energy of 102.2 eV corresponds to Silicon bound to two oxygens, -O-Si-O-, which is considered to be photoemission from SiO₂ (Brookes et al. 2001, Chiba and Takenaka 2008, Sellmer, Prins, and Kruse 1997). Most importantly, the O1s spectrum in the sample is at 531.8 eV which is nearly identical to that in silicate, 531.9 eV (Wang, Nabatame, and Shimogaki 2005), especially considering that the acceptable error of the technique is ± 0.7 eV. Thus, we can now suggest that the state of both Si and O is similar to silica, which is in agreement with the reaction mechanism (shown in Figure 4.9 (b)) (Strachotova, Strachota, Uchman, Slouf, et al. 2007). Thus during the hydrogel formation, the silica network was dispersed in PNIPAAm network as well at the interface there was substantial silicate network formed by the hydrolysis reaction of TMOS followed by self-condensation reaction. Therefore, these we can now propose PDMS adhesion with hydrogels through condensation reaction. Specifically, exposure to UVO, the residual methyl from the PDMS would be changed into hydroxy groups which can be bonded with Si by condensation reaction (similarly as the reaction between hydrolysis-TMOS and PDMS).

4.3.2 Response Properties of Silicon Integrated with Hydrogels

4.3.2.1 *Buckling Behavior of Non-Patterned Silicon Thin film on Hydrogels*

As previously discussed thin film semiconductors have shown excellent potential for the development of flexible and stretchable electronics when they are integrated with elastomers such as poly(dimethylsiloxane) PDMS. Using the same technology, Yu et al. first reported an interesting approach of making thermoresponsive ultra-thin silicon nanostructures, in which several hundred nanometers thick silicon nanoribbons are integrated with thermo-responsive hydrogels and are able to change their mechanical configurations rapidly upon altering the ambient temperature.(Yu et al. 2011) Ultra-thin silicon ribbons become adaptive and can be reversibly driven to be flat and ‘wavy’ according to the cyclic change of the temperature.

Figure 4.10 schematically shows the cyclic behavior of the silicon nanoribbons on thermally sensitive hydrogels from Yu et al previous studies.(Yu et al. 2011) The macroporous poly(N-isopropylacrylamide) hydrogel described earlier was chosen and the overall integrated structure demonstrated excellent thermal response in terms of both speed and volume shrinkage. The improved mechanical properties of the macroporous hydrogel are of great significance as the hydrogel is constantly exposed to stress during fabrication. The earlier section explained how the combination of low temperature synthesis and presence of siloxane linkages in the monomeric mixture resulted in improvement of both the mechanical and the response properties. Additionally, it is important to mention that the present integration require sharp and large change in linear direction for the silicon nanoribbons to be effectively buckled.

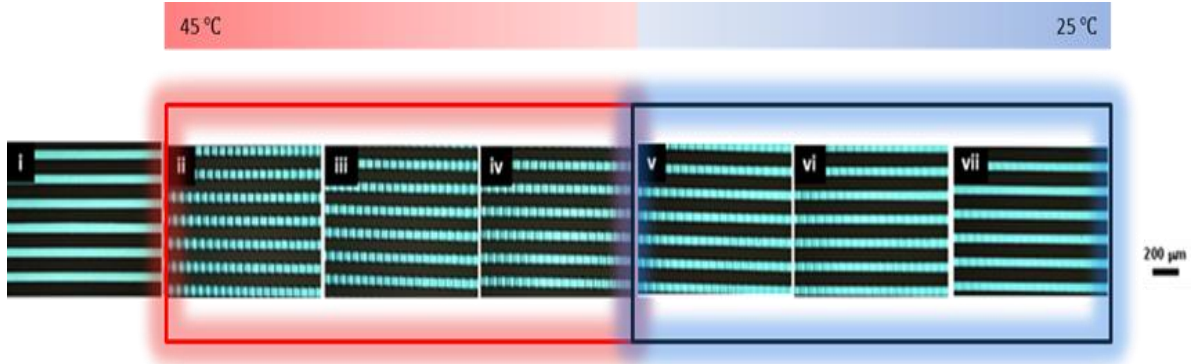


Figure 4.10. Buckling pattern on silicon ribbons integrated with thermoresponsive PNIPAAm hydrogels: i) After transfer printing, ii) 2 min after immersion into hot water (45 °C), iii) 4 min, iv) 6 min, v) 8 min, vi) 10 min, and vii) 12 min.

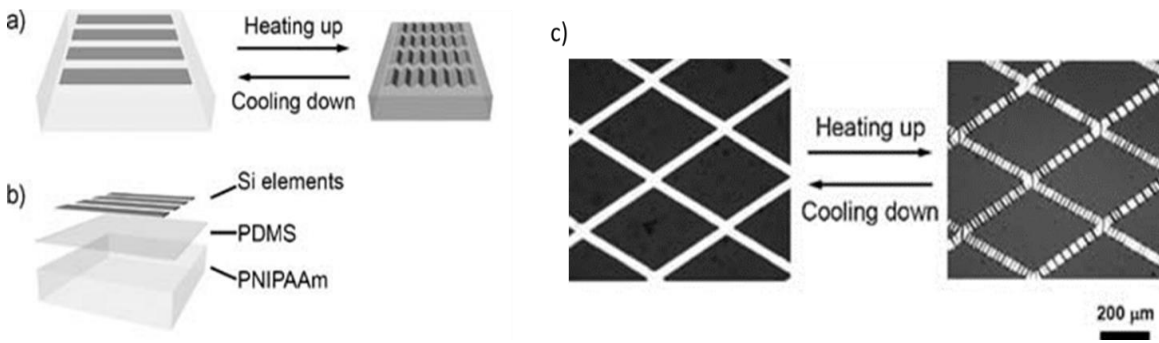


Figure 4.11. Hydrogel and Silicon thin film Integration: a) Schematic of the hydrogel swelling/shrinking drivable silicon thin ribbons, b) Layer-assembled structure c) Demonstration of the thin Si diamond network structure becoming buckled when the hydrogel substrate shrinks. Adopted from (Yu et al. 2011)

Figures 4.11a, 4.11b demonstrates the various steps in integrating a thermo-responsive substrate with ultra-thin silicon ribbon. The system consisted of three components, a macroporous PNIPAAm gel, a PDMS layer (which was vital for the latter high-yield transfer steps), and Si nanoribbons. Interestingly, the siloxane group described earlier for improvement in mechanical properties also promoted the bonding between the PNIPAAm gel and the PDMS layer. Specifically, the silica network produced by hydrolyzed TMOS and N-isopropylacrylamide (NIPAAm) monomer during gel synthesis had residual Si–OH groups. The residual Si–OH groups attached to the silica network distributed inside the PNIPAAm gel network from TMOS, bonded with the hydroxy-terminated PDMS through a condensation reaction. Such integration was done with both one-dimensional and two dimensional silicon ribbon pattern (Figure 4.11 c). The results revealed that the when the transition temperature of ~ 32 °C is reached, the PNIPAAm hydrogel shrinks along with flat ribbon placed on top via an intermediate PDMS layer. The out of plane buckling of the silicon results from the compression load on the stiff/soft materials, where soft materials can undergo shrinking while stiff materials have to buckle to release the compressive strain as postulated earlier. (Bowden et al. 1998, Efimenko et al. 2005, Genzer and Groenewold 2006, Jiang, Khang, et al. 2007) The image analysis of the buckled structured demonstrated in Figure 4.11 demonstrate that the linear change of approximately 15 % in the hydrogel produced wavelength of 30-35 microns with the evolution of time.

4.3.2.2 Buckling Behavior of Patterned Silicon Thin Film Integrated on Planar Hydrogels

The method described Yu et al. represents a new class of combination between soft and hard materials, and opens ways for exciting future environmentally sensitive electronics. However, the control over the pattern of their response and buckling had not been explored and also the wavelength of the silicon is small. For implementation of circuit level design, the buckling pattern needs to have a larger wavelength so as to have active areas and inactive areas. In order to implement such a control, a photolithography method was employed; such method had previously shown exciting results using flat elastomeric substrates such as PDMS.(Childs et al. 2005, Sun et al. 2006b) In order to incorporate the aforementioned methodology, the gels had to be further processed with an intermediate PDMS layer. The PDMS and PNIPAAm bulk gel were bonded using TMOS via a condensation reaction which has been earlier reported. (Yu et al. 2011, Strachotova, Strachota, Uchman, Šlouf, et al. 2007) The PDMS served two important purposes. First, it offers a smoother surface for the silicon layer transfer and second, it provides a waterproof boundary which is essential for the silicon transferring. Subsequently, to generate patterned active and inactive bonding areas, a mask was used and exposed to an UV environment. Upon contact with silicon, the exposed sites would form strong siloxane linkages between silicon and PDMS, while the rest of the parts would only have weak van der Waals interactions.(Sun et al. 2006b) Thus the silicon ribbon would then have intermittent bonding and weak bonding areas with the PDMS surface. Figure 4.12 describes the process of integrating silicon on hydrogels.

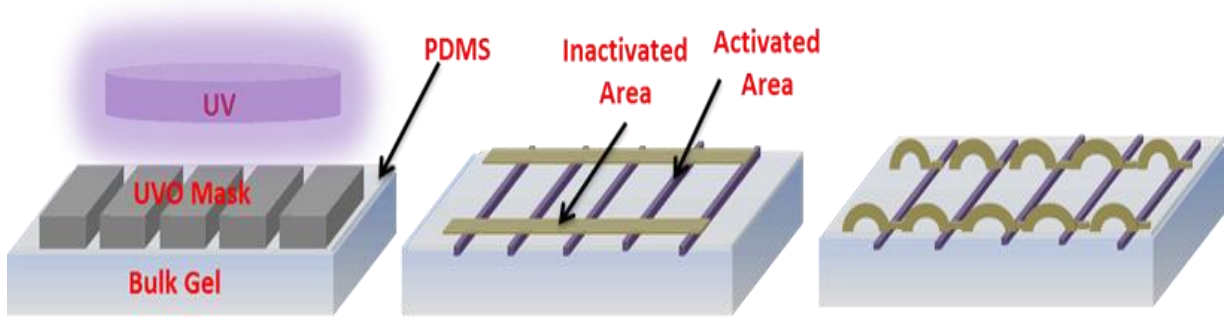


Figure 4.12. Schematic showing of the process of integrating thin silicon ribbon (300 nm thick) with PNIPAAm gel: a UVO mask was used to control the buckling pattern.

The integrated soft and hard material was then studied under an optical microscope followed by an environmental scanning electron microscope (ESEM). In order to facilitate ESEM imaging the materials had to be quenched at low temperature using liquid nitrogen after the sample was heated above the lower critical solution temperature (LCST). This was done to maintain the integrity of the silicon pattern formed due to the shrinkage of the gel. The images depicted that under an influence of a thermal stimulus, the integrated material can be used to generate different patterns of buckled response. The images were then analyzed using ImageJ, an image analysis software, for measuring the wavelength of the silicon wave like patterns (Figure 4.13 a-c). Such analysis suggested that the wavelength of the silicon buckles agrees with the equation developed previously in pre-strained elastomeric substrates integrated with silicon ribbons, where $Wavelength = \frac{W_{inactive}}{1+\epsilon}$. (Jiang, Sun, et al. 2007) Here $W_{inactive}$ is the width of inactive region of the mask or the part of the silicon not strongly bonded to the PDMS. The ϵ is calculated using $\frac{\Delta L}{L}$, where L is the original one dimensional length of the hydrogel and ΔL is the linear dimension change resulting from the volume shrinkage under the influence of thermal stimulus. The strain

generated was 0.29, which theoretically produced a wavelength of 69.8 μm for the 90 μm inactive mask; this matched very well with the measured mean wavelength of 68.5 μm . Similar results were also obtained for the mask with 190 μm as the inactive region. Thus the silicon buckling wavelength can be finely tuned by changing different UV masks with different active and inactive regions. This degree of control is desired for effective strain mitigation due to the hydrogel shrinkage without comprising the active sites.

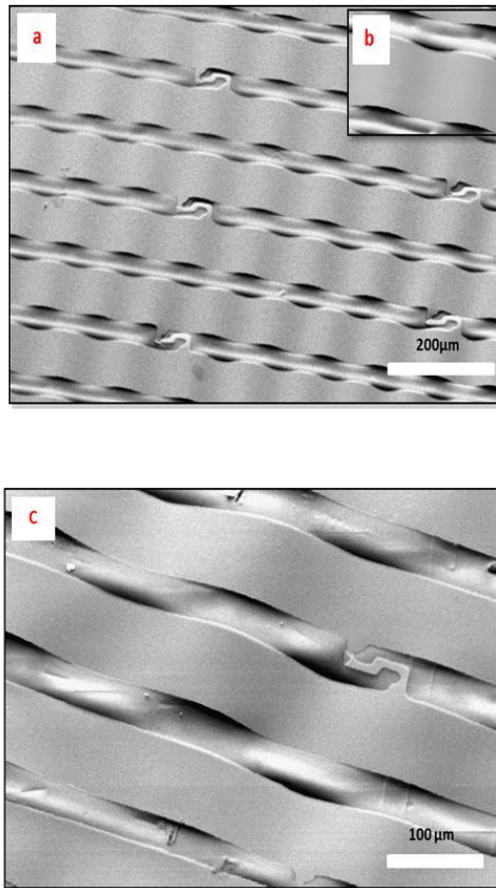


Figure 4.13. Environmental scanning electron microscopy images of controlled buckling pattern of the integrated silicon on PNIPAAm hydrogel: (a) (Mask: 30 μm active – 90 μm inactive) wavelength $68.5 \pm 6.3 \mu\text{m}$; (b) Close-up image of the pop-up structure; (c) (Mask: 30 μm active – 190 μm inactive) wavelength $142.6 \pm 6.8 \mu\text{m}$.

The fast LCST-volume change phenomenon of the macroporous hydrogel described earlier has been leveraged in the present case; as the dimension changed dramatically during LCST, it resulted in a great amount of strain in the system, which was then successfully utilized to drive the onboard silicon ribbons to form distinct patterns. The macroporous PNIPAAm generated strain sufficiently large for the silicon to respond and also have a quick reversible nature. When introduced to stimuli, the response time and volume shrinkage of the PNIPAAm gels are largely dependent on the mechanism of uptake and release of solvents by these gels. As previously estimated and discussed in the earlier section, the gels with larger pore size than 1 μm pore size would have a faster capillary action dominated solvent uptake and release mechanism. The gels having pore size below this value would have generally a slower uptake mechanism. (Peppas and Khare 1993, Baker, Blanch, and Prausnitz 1995) In the present case, the thermal response of integrated structure is hypothesized as a function of pore size because this would most likely dictate the rate of uptake and release of water.

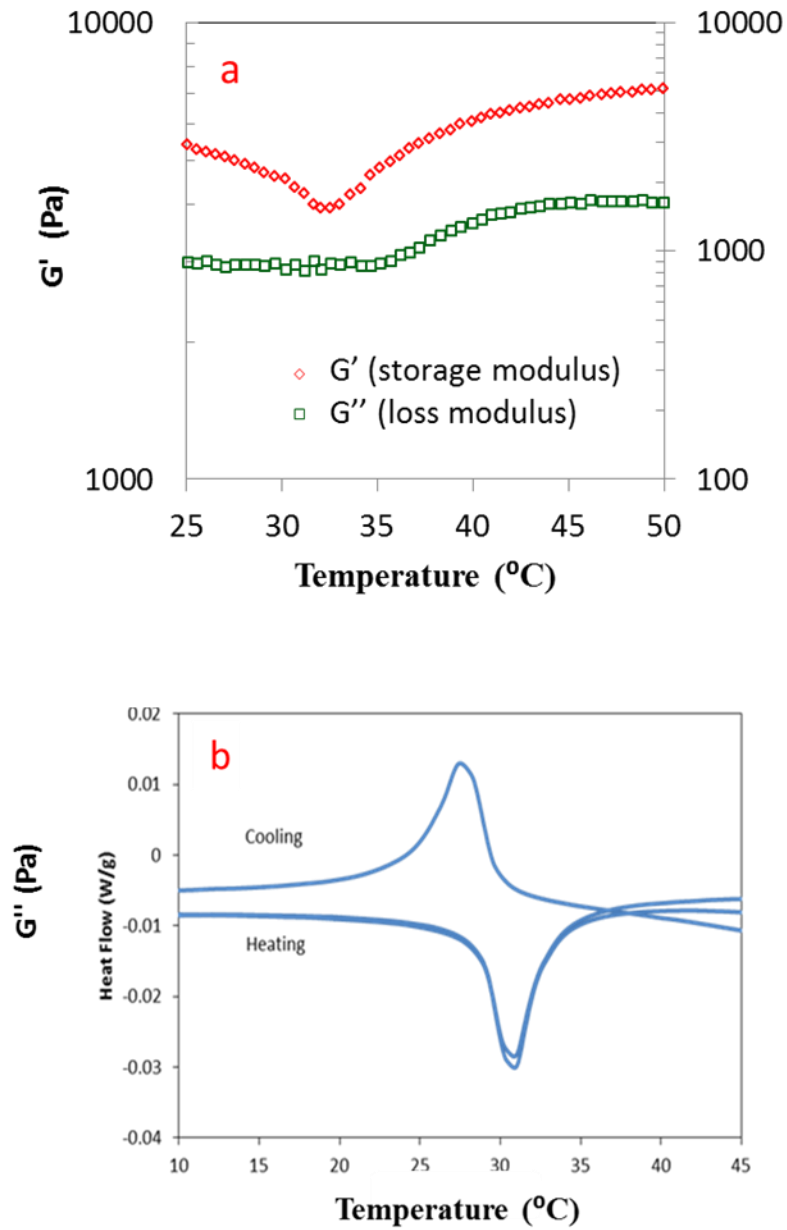


Figure 4.14. Material characterization of PNIPAAm hydrogel: (a) Rheological testing of the hydrogel; (b) DSC capturing LCST behavior of gels and quantifying heat absorption during transition.

The mechanical properties were tested with a rheometer suggesting that the storage modulus G' is much greater than loss modulus G'' , suggesting the hydrogel behaves solid like (Figure 4.14a). The thermal response of the hydrogels was again quantified using a differential scanning calorimeter (DSC). The DSC results suggested the LCST of the gel to be around 32°C (Figure 4.14 b). The DSC curves also revealed the reversible nature of the LCST phenomenon and quantified the energy required during transition as before. An endothermic peak was observed when the PNIPAAm was heated and an exothermic peak occurred during the cooling cycle. The endothermic peak here corresponds to the amount of energy required for the dissociation of the phases, while the release of energy corresponds to the bond formation during the cooling cycle. Table 1 shows that the macroporous PNIPAAm gel has nearly identical energy during the heating and cooling cycle and confirms the completely reversibility. The glass transition temperature of the dried gel was also measured to be $143.7 \pm 2.1^{\circ}\text{C}$ by the DSC, which revealed that these materials can be used at high temperature with minimal structural deformation.

4.3.2.3 Buckling Behavior of Silicon Thin Film on a Curved Bilayer Hydrogels with Tunable Curvature

One of our focuses is to create controlled response of thin film silicon; here we adopt two different hydrogels with distinct properties, for example, with dissimilar swelling ratios and stimulus sensitivity, to design a three-dimensional curved structure. The gels were then integrated with thin silicon ribbons with the assistance of a PDMS intermediate film as discussed in the previous section. However due to the complexity of the substrate shape, intermediate bonding and non-bonding regions with silicon was not attempted, only simple bonding with silicon was performed as reported previously.(Yu et al. 2011)

In the present work, a co-polymer of NIPA and acrylic acid was chosen for the bottom layer and a thermo-sensitive PNIPAAm was chosen for the top layer. The diverse swelling ratio is attributed to the higher hydrophilic nature of acrylic acid, which results in a more drastic swelling ratio in water. In addition, unlike the PNIPAAm hydrogel discussed previously, the PNIPAAm hydrogel here was less sensitive to thermal stimulus and de-swelled considerably much less with temperature increase (~ 11 %) compared to thermo-responsive gels in the previous section (~ 29%). This was done intentionally to prevent delamination of such an integrated bilayer structure due to the high amount of strain created at the gel interface. More importantly, the functionality of the top layer was to provide an appropriate constraint on the higher swelling bottom layer to create a three-dimensional curved structure (Figure 4.15 a-b). Figure 4.15 b is an Abaqus finite element model describing the curvature change of the bilayer substrates in swelled and de-swelled states. The model was especially useful for adjusting proportions of layer thickness in order to obtain the desired overall curvature.

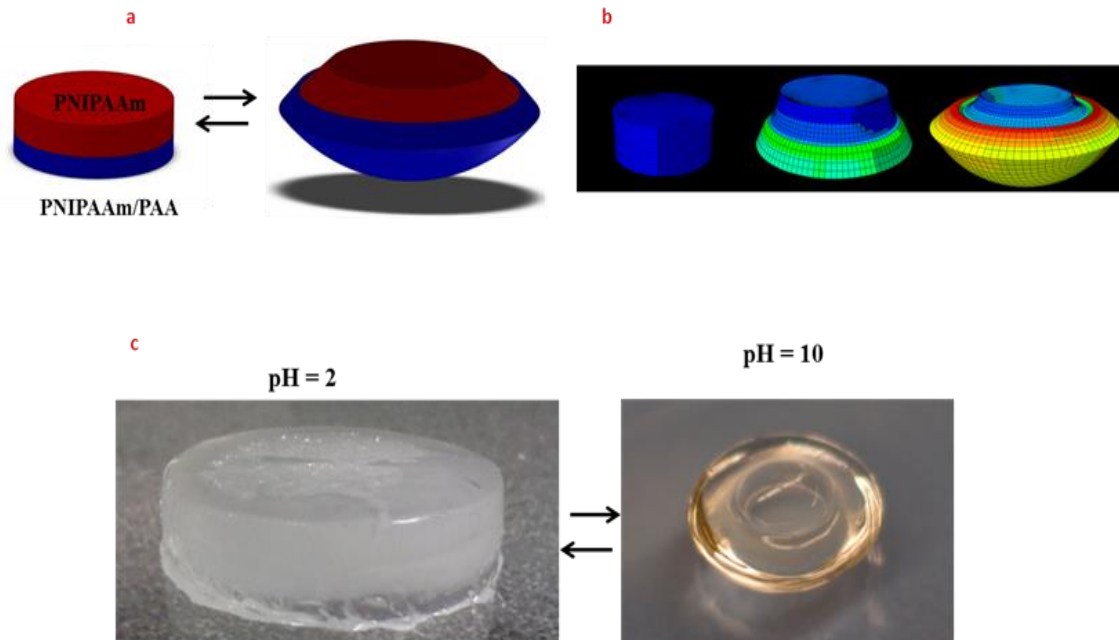


Figure 4.15. Bilayer hydrogels with tunable curvature: (a) Pictorial representation of a bilayer hydrogel; (b) Finite element modeling of bilayer gels depicting the various stages of swelling; (c) pH responsiveness of the bilayer hydrogel, top layer is the PNIPAAm hydrogel (temperature sensitive) and bottom layer is co-polymer of acrylic acid and PNIPAAm hydrogel (pH sensitive).

The bottom layer behaves as a pH-sensitive hydrogel due to the presence of acrylic acid and can essentially accept and/or donate protons in response to a pH change (Nge et al. 2004). At a low pH, the poly acrylic acid-co-NIPA hydrogels are relatively un-swollen since the acidic groups (-COOH) on the gel are protonated and hence neutralized. When the environmental pH is above the pKa of the ionizable moiety, the pendant acidic groups are deprotonated. As ionization increases, fixed charges are developed on the polymer net-

work and there is a resultant increase in electrostatic repulsions between the ionized polymer chains, further increasing the swelling. Other than electrostatic repulsions, a large osmotic swelling force from the presence of ions also increases the uptake of solvent in the network.(Ranjha, Mudassir, and Majeed 2011)

The important factor in such an integrated system is that the shrinkage of the bottom layer in acidic pH and the non-responsiveness of the top layer produce a curved integrated structure to become a function of external stimulus, acidity or basicity. As the bottom layer shrinks, there is a release of strain, which makes the bilayer structure flatten out (Figure 4.15 c). The above behavior is reversed when the basicity of the surrounding media is increased. Also the thermo-responsive characteristics of the top layer make the structure responsive to the temperature as well. Interestingly, the bottom layer, a co-polymer of PNIPAAm does not demonstrate any significant thermal responsive behavior. This is because the ionized acrylic acid components convey sufficient solubility to offset the aggregation of the hydrophobic temperature sensitive components above a specific concentration of acrylic acid.(Chen and Hoffman 1995a) This fact ensures that the stimulus response of both the top and the bottom layer remains mutually exclusive and thus a multifunctional material is obtained.

These responses generated interesting pattern, include heterogeneity, with a thin film of silicon integrated on the top of the bilayer hydrogel. As demonstrated in Figure 4.13(a), such integration would lead to buckled features on the thin film. The temperature and the pH both would cause the silicon to buckle on account of the strain developed, the independent response of both the above stimuli on the integrated structure was studied using an optical microscope. The study revealed that regions at the center of the ribbon did

not buckle in presence of basic pH because of the low strain in these regions (Figure 4.16 b-c), however, in response to temperature there was more buckled regions due to the upper layer contracting, this increases the strain on the silicon ribbon and causes more buckled features (Figure 4.16 d-e).

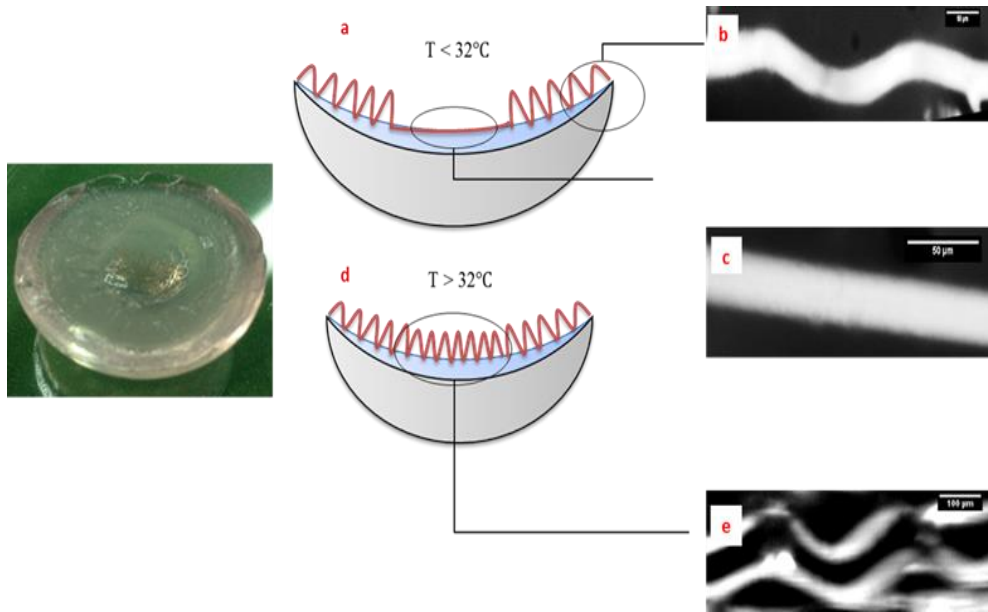


Figure 4.16. Responsiveness of silicon thin film integrated with bilayer hydrogel: (a) effect of pH (pH= 10); (b) buckling of silicon ribbons at the edges (scale bar $50\mu\text{m}$); (c) flat silicon at the center (scale bar $50\mu\text{m}$); (d) pictorial representation of buckling under influence of temperature; (e) horizontal view of buckling under influence of temperature $> 32^{\circ}\text{C}$ and pH= 10 (scale bar $100\mu\text{m}$).

For such integrated structures to respond effectively to an environmental stimulus, we need to understand the material characteristics in detail, especially the thermal and the rheological characteristics. The rheological studies revealed that, under an acidic environment, pH sensitive gels had a relatively higher storage modulus (G'); the G' decreased with

increasing pH while the viscous modulus (G'') increased with increasing pH (data not shown). Figure 4.17 demonstrates the complex modulus G^* ($\sqrt{G'^2 + G''^2}$) decreased with increasing pH over the entire strain range, suggesting that the storage modulus (G') is the more dominant factor in the hydrogel which implies a more solid like behavior of these gels. The above results are in agreement with the visual observations which suggest that the gels shrink (high complex modulus) in acidic environment and expand (low complex modulus) in a basic environment. Additionally, the G^* revealed the linear viscoelastic region followed by a shear thinning like-behavior at higher strain.

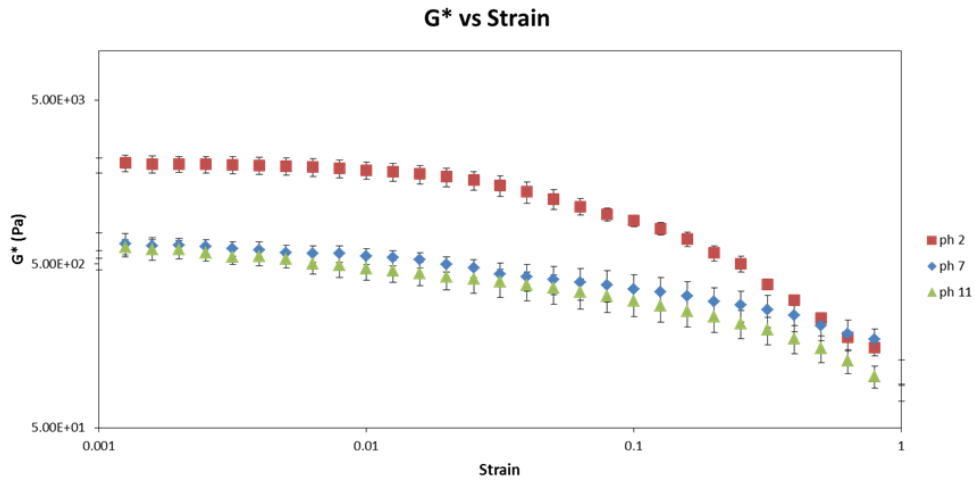


Figure 4.17. Rheological characterization of bottom layer (pH sensitive): G^* as a function of strain at constant frequency of 1 Hz under different pH conditions.

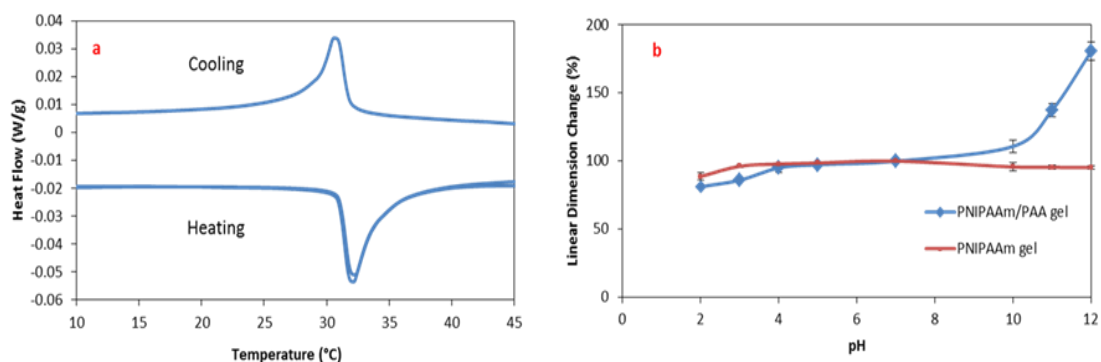


Figure 4.18. Environmental response of the bilayer hydrogel: (a) DSC capturing LCST behavior of top layer and measuring heat absorption during transition; (b) Linear dimension change of bottom and top layer of gels with pH.

As mentioned before the thermal characterization was performed using a DSC to validate and quantify the transition energy requirement. The PNIPAAm gel here (refer to as microporous gel) demonstrated a similar LCST transition point (Figure 4.18) as before; however, the heat flow curve of the gel when compared to the previous section was quite different. The macroporous PNIPAAm gels in the first section exhibited much lower heat absorption at the LCST in comparison to the present PNIPAAm gels (Table 1). This may be attributed due to an easier passage of water from the polymeric network gel due to the larger pore size. However, the pore size in the present top layer of PNIPAAm is consciously made low, to avoid large swelling ratio at the top which might lead to delamination between the bilayer hydrogels. Glass transition temperatures of the top and bottom layer were measured as 59.8 ± 1.7 °C and 91.4 ± 0.9 °C respectively. The glass transition analysis proved that the gels could be used at moderately high temperatures above room temperature, which would be the desired operating temperature for such materials.

Table 1. Comparison of LCST and heat absorption of the macroporous and microporous thermos-responsive PNIPAAm gels during heating and cooling cycles

Macroporous PNIPAAm			Microporous PNIPAAm		
LCST	Heat absorbed (Heating cycle)	Heat released (Cooling cycle)	LCST	Heat absorbed (Heating cycle)	Heat released (Cooling Cycle)
31.4 ± 0.42 °C	1.38 ± 0.29 J/g	1.32 ± 0.32 J/g	31.7 ± 0.21 °C	2.29 ± 0.12 J/g	2.19 ± 0.42 J/g

4.4 Incorporation of Visible Light Response in Poly(N-isopropylacrylamide)

4.4.1 Comparison of Physical and Chemical Approaches

Previously, we have discussed that direct heating of simple cross-linked PNIPAAm hydrogels, result in their shrinkage along with expulsion of water molecules which were entrapped in the polymer network. This is explained due to the presence of a property known as the lower critical solution temperature (LCST) in PNIPAAm. This peculiar property allows the PNIPAAm polymer network to change from a hydrophilic nature to a hydrophobic one, when heated above this crucial value. In the present section, we try to incorporate light response properties into PNIPAAm hydrogels with the help of certain additives; which have been integrated either physically or chemically. The validation of the light response properties of these hydrogels was done by using light directed from a laser source through a confocal microscope with a specific wavelength of 488 nm. The confocal microscopy also helps to understand the morphology change and response properties of the polymer network on account of incident light.

Initially, we irradiate simple PNIPAAm hydrogels by a laser light which depicts no shrinkage and thereby prove that these gels can function as an effective control experiment for study of light response properties (Figure 4.19a). This observation also suggests that laser intensity required for such a change would be too high as the light response of simple PNIPAAm would rely on the heating prowess of the laser source to demonstrate any LCST property. Specifically, in the present set of experiments, the simple hydrogels were exposed up to 100mW of laser intensity without any observable effect on the polymeric network.

The same observation was also made when the PNIPAAm hydrogels of macroporous nature were irradiated with a laser light. This observation evidently proves that pore size increase has no effect on light response properties in simple PNIPAAm.

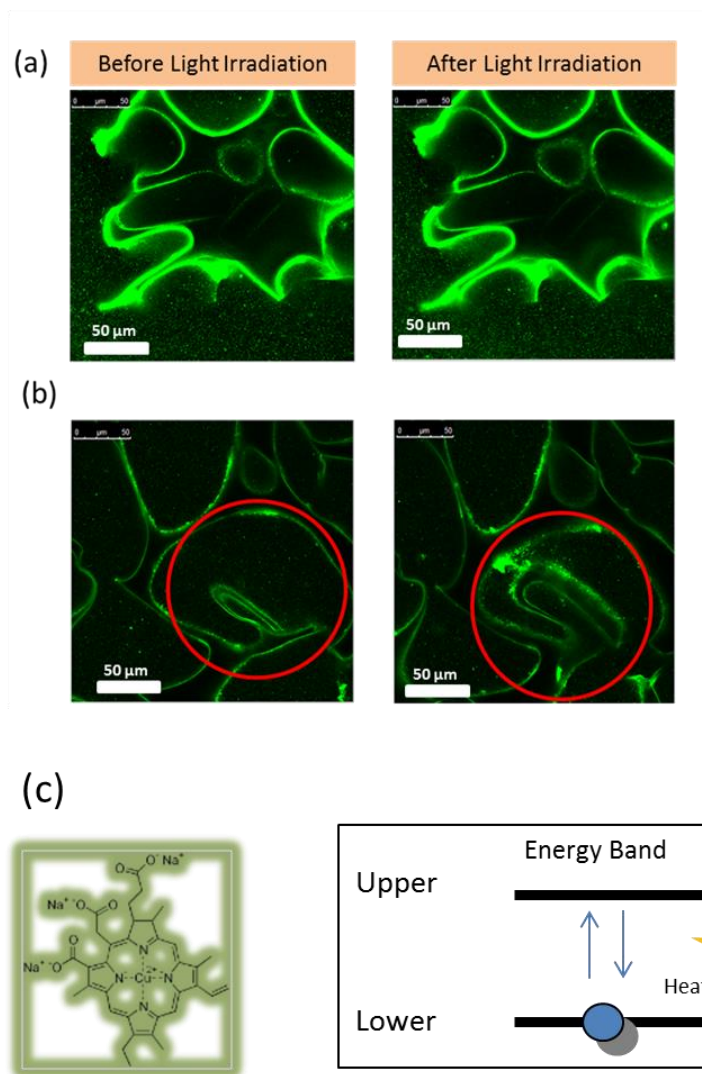


Figure 4.19. Effect of laser light (488 nm) on different hydrogels as function of time (2 minutes) (a) cross-linked PNIPAAm with no chromophore and (b) PNIPAAm with a 2% chlorophyllin (c) illustration depicting the effect of light on the electrons of chlorophyllin and there imminent release of heat energy.

One of the popular methods of incorporating light response properties into PNIPAAm based hydrogels is through addition of some additives which can convert light energy into heat, thereby indirectly improving the thermal response properties of PNIPAAm. Popular among these materials are gold nanoparticles. Gold nanoparticles exhibit the interesting phenomenon of surface plasmon absorption by virtue of which these nanoparticles when dispersed within a thermally sensitive polymer network, e.g. PNIPAAm can thermally activate and result in shrinkage of the entire network (Kim and Lee 2004). Gold nano-rods thus function as effective photo-thermal converters, permitting near-infrared (NIR) light to be transmitted deep into polymer network. Such behavior is particularly helpful for development novel drug delivery mechanism, for targeting particular organs or tissue by non-invasive therapeutic techniques (Kawano et al. 2009). Although, previously some studies have claimed that such hydrogels sometimes respond to some near visible light wavelength as well, during course of the initial investigation for this project we discovered the response times in such hydrogel is extremely slow and requires light of high intensity to observe any substantial change in swelling of the hydrogel (Sershen et al. 2000).

Compared to gold nanoparticles the chosen physical additive here, sodium copper salt of chlorophyllin, demonstrated a better response property. Figure 4.19b, demonstrates that when sodium copper salt of chlorophyllin is incorporated into the PNIPAAm system, the hydrogels starts responding to the same laser with a wavelength of 488nm at an intensity of 100mW. Tanaka et al. described this observation on the basis of chromophoric ability of the chlorophyllin salt and to the indirect heating of the PNIPAAm hydrogel (Suzuki and Tanaka 1990). Figure 4.19 c, shows an illustration to explain the mechanism of indirect

heating of PNIPAAm gel network with the incorporation of chlorophyllin salt. Thus, chromophores such as sodium copper chlorophyllin, absorb the light of particular wavelength which leads to excitation of electrons from their normal ground state to a higher energy orbitals. On reversal of the electron to the normal ground state the extra energy (in the form of heat) triggers the volume transition of the temperature sensitive gels.

However, there are three major drawbacks of such a system. First, as such shrinkage of polymer network is caused by the indirect heating of polymer network (heat produced by movement of electrons inside chlorophyllin salt) such observations are only restricted to thermally responsive hydrogels, such as poly(N-isopropylacrylamide) (Suzuki and Tanaka 1990). Secondly, on account of the fact that main cause of such an observation is the excitation and de-excitation of electrons and release of heat energy in the chlorophyllin molecule, the process becomes inherently slow when compared to thermal responsive hydrogels, e.g. simple cross-linked PNIPAAm hydrogels. Third and most importantly, confocal microscope studies reveal that light response properties is highly localized and overall the hydrogels demonstrated high in-homogeneity in shrinkage of hydrogel network, when exposed to low intensity visible light (Figure 4.19b). Such observations could be attributed to the low thermal conductivity of the PNIPAAm hydrogels and the inability of the chlorophyllin salt to increase the thermal conductivity (Jiang, Kelch, and Lendlein 2006). Therefore, an alternate mechanism of incorporating light responsive characteristics is needed which could circumvent the drawbacks of the present system by approaching the concept of demonstrating light responsiveness in a more efficient manner.

One possible method to overcome these drawbacks could be chemical cross-linking of some molecules into the PNIPAAm polymer network which could exhibit the ability to

influence the hydrophilic character of the hydrogels' through change in their molecular orientations.; e.g. conversion of cis or trans upon light irradiation with each configuration having distinct hydrophilic character. Among molecules exhibiting such a phenomenon, azobenzene and spirobenzopyran are the best known candidates and are known to demonstrate reversibility when exposed to light irradiation. In this particular study, spirobenzopyran has been chosen over azobenzene, as the latter is known to only respond to deep UV wavelength (Zhao et al. 2009). Importantly, when compared to previously discussed chlorophyllin salts, the spirobenzopyran molecules do not produce any heat energy when exposed to light. The basic mechanism of spirobenzopyran has been illustrated in Figure 4.20a and is inherently different from chlorophyllin salts. Here, the ionic and hydrophilic phase of the spirobenzopyran, is termed as merocyanine. The ionic form has a high degree of hydrophilicity and also provides a characteristic deep yellow coloration. The hydrophilic character is converted to a hydrophobic one when the compound is exposed to visible light of certain wavelength; this form is termed as the spiro form and is highly hydrophobic in nature.

Spirobenzopyran in its original form was found to ineffective in effecting any change in terms of light response of the PNIPAAm hydrogels (Sato et al. 2011). To incorporate the light response properties and chemically bind the molecule with the PNIPAAm polymer network, the spirobenzopyran molecule so synthesized was first acrylated with acryloyl chloride. The acrylated compound thus is expected to have vinyl backbone and spiro group as the bend group. The vinyl part of the NIPAAm molecule bond with the acrylated spirobenzopyran along with the characteristic spiro group to impart the

light responsive properties into the system. The so synthesized molecule was further purified using column chromatography. The acrylated spiro and merocyanine configuration of the molecule is further characterized by distinctive absorption wavelengths with the help of UV spectrometer.

The spectroscopy technique also demonstrated the capability of such a compound to re-orient itself as function of light wavelength (Figure 4.20 b). The hydrophilic form of the spiropyran compound clearly demonstrated its light responsive characteristics even at a low concentration of 1% (w/v), with characteristic wavelength (λ_{max}) of 420 nm in a mildly acidic media (pH 4.5). Previously, such observation has been well-documented and explained by the fact that the pH of the media plays a crucial role in deciding the characteristic wavelength (Sumaru et al. 2006). This is due to the ionization of spirobenzopyran to higher order which allows a sharper and different peak. Subsequently, the same solution when exposed to a low intensity white light (5mW) for just 30 seconds allowed for the spirobenzopyran reversion to spiro form (close ring structure). The irradiation of white light resulted in exhibition of a different uv spectra, thereby suggesting that the compound has reverted to another spiro form. As a control experiment and accurately confirm the conversion and presence of the non-ionic form (spiro) on account of light; same concentration of acrylated spirobenzopyran was dissolved in tetrahydrofuran, a non-ionic organic solvent. The non-ionic solvent is required to prevent the alteration of the spiro form to the merocyanine form. The UV spectra from such an experiment proved that there is spontaneous conversion of merocyanine to spiro form on account on light illumination.

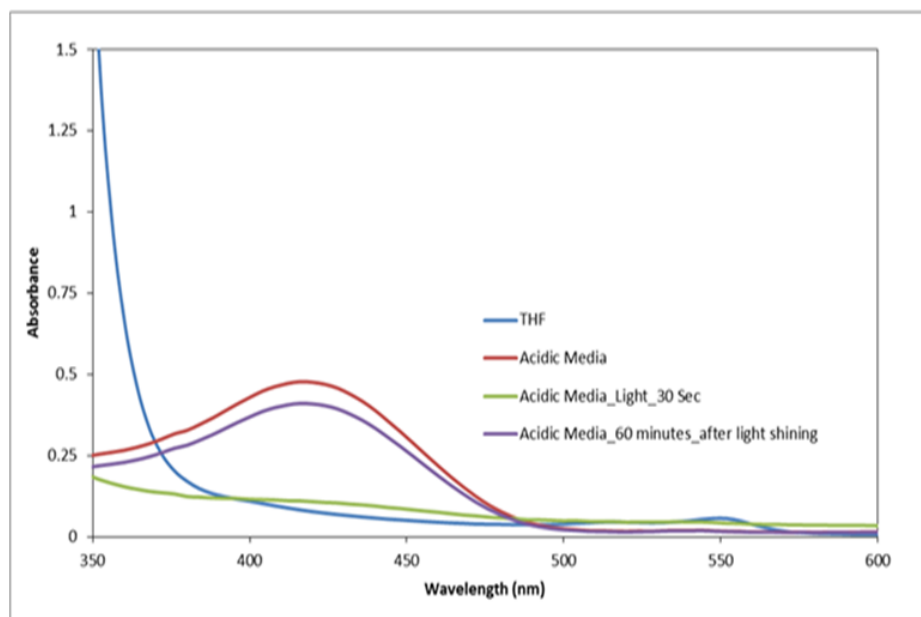
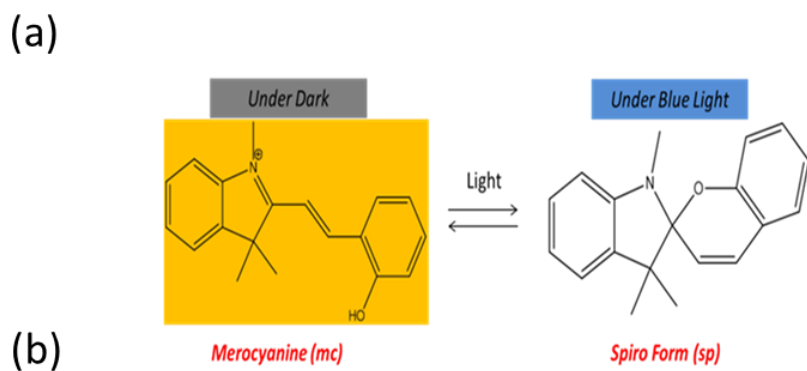


Figure 4.20. Chemical Structure of spirobenzopyran and light responsive behavior: (a) chemical structures and isomerization of spirobenzopyrans due to light irradiation, (b) UV spectroscopy of spirobenzopyran under different conditions.

Subsequently, the as synthesized spiropyrans compound were integrated with the PNIPAAm hydrogel using free radical polymerization process. To initiate a faster response from the hydrogels and to obtain a continuous/homogenous response from the hydrogels, a low temperature polymerization process was adopted. Similarly, acrylic acid was added as a co-polymer for these hydrogels. The significance and properties improvement of the spiropyrans-PNIPAAm hydrogels will be explained in the subsequent sections.

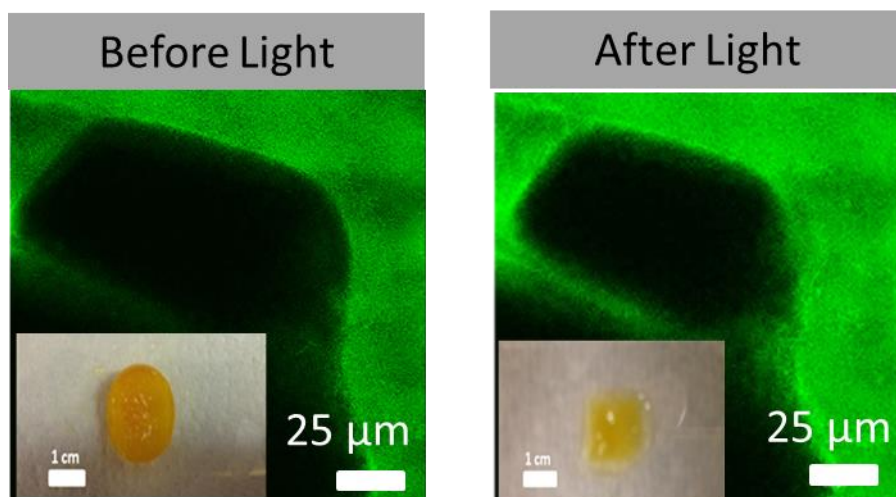


Figure 4.21. Effect of light on spiropyrans-PNIPAAm hydrogels as function of time: Confocal image and effect of 488 nm laser on hydrogels' morphology; (left) shows initial pore size of the hydrogel network and (right) shows decrease of pore size after laser light is irradiated for 10 seconds (linear change $\sim 15\%$), (Inset) bulk co(spiropyrans-PNIPAAm) hydrogel demonstrating de-swelling on account of white light irradiated on it for 30 seconds.

Furthermore, the light responsive characteristics of spirobenzopyran based hydrogels were tested using same laser light of same wavelength as before with the help of a confocal microscope (Figure 4.21 a, 4.21 b). Compared to the chlorophyllin-PNIPAAm hydrogels the present hydrogels based on spirobenzopyran-PNIPAAm were highly sensitive and the observed shrinkage on account of incident light was much more uniform in nature. The average time for contraction of the hydrogels was below 15 seconds. Interestingly, the hydrogels demonstrated clear homogenous shrinking with approximately 20 % contraction. Interestingly, the poly(spirobenzopyran-co-N-isopropylacrylamide) co-polymer hydrogel (Fig. 4.21 inset) demonstrates a significant volume change (~70%) and color change (from deep yellow to pale yellow) before and after light exposure.

Compared to the chlorophyllin based PNIPAAm the time scale of the response properties was substantially improved due to the spirobenzopyran molecule. Figure 4.22 a reveals that chlorophyllin hydrogels with weight percentages concentration even over 10% resulted in a change of 10% in linear dimension when exposed to 5 minutes of high intensity white light. The spirobenzopyran demonstrated much faster response than their chlorophyllin counterparts (Figure 4.22 b). Interestingly, when the spirobenzopyran concentration is increased over 5 wt % the hydrogels demonstrate retardation in the light response characteristics. This fact was also seen and explained by the diminishing hydrophilic character of the hydrogels due to the presence of increase of the spirobenzopyran concentration (Ziolkowski et al. 2013). Furthermore, the spirobenzopyran hydrogels revealed that the UV spectra of the hydrogels would be shifted more towards the deeper visible spectra, a fact which would be useful for development of tactile display based on these hydrogels (Figure 4.22c).

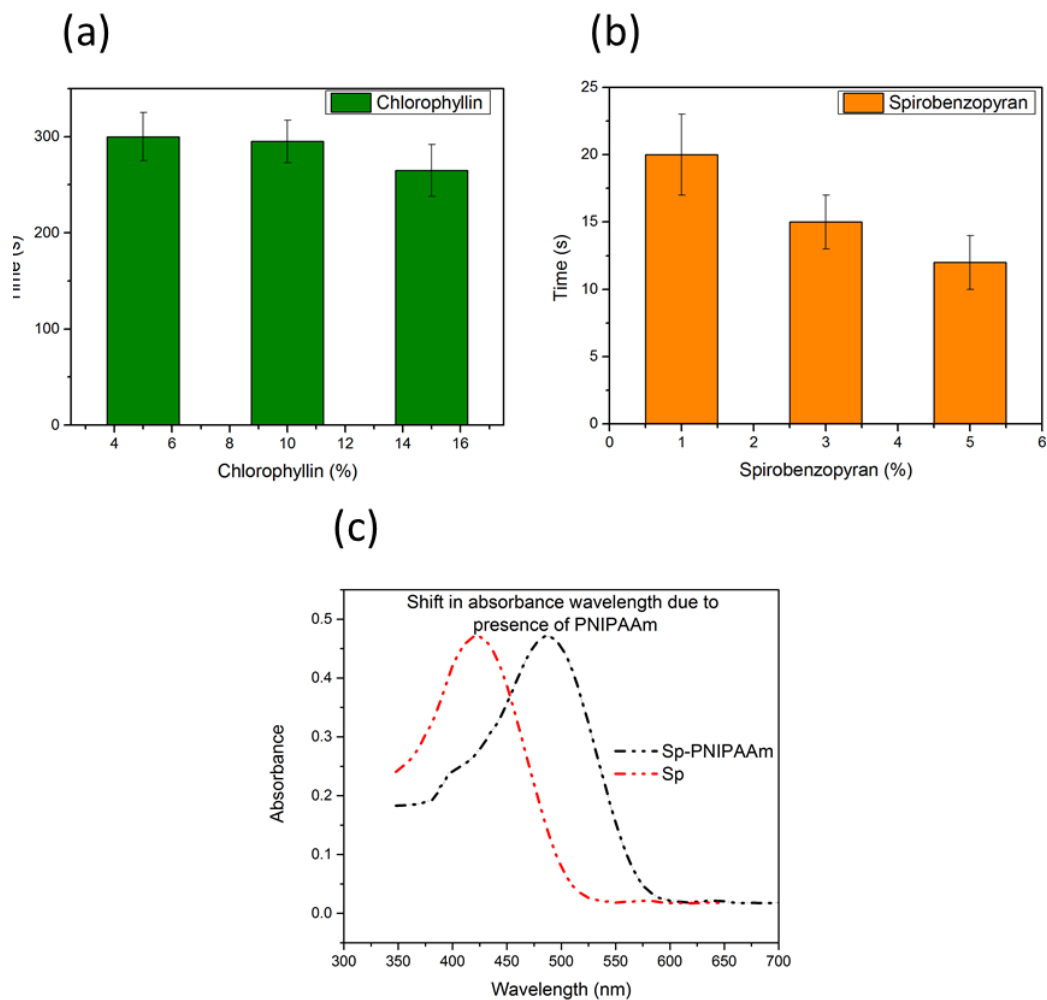


Figure 4.22 (a),(b) Effect of chromophore content on the visible light response of PNIPAAm, (c) UV spectra of spirobenzopyran molecule and hydrogel integrated with spirobenzopyran

4.4.2 Increasing the Response and Mechanical Properties of Spirobenzopyran-PNIPAAm Hydrogels

Effect of Pore Size

Although the light response properties of spirobenzopyran based PNIPAAm hydrogels are considerably better than their chlorophyllin based light responsive hydrogels, they lack the fast response properties of thermally responsive hydrogels which were discussed in the previous sections. The apparent lack of response properties could be attributed to two independent properties of spirobenzopyran based hydrogels, first is the chemistry of the spirobenzopyran favors the closed structure which resembles the cis configuration and is supposed to have less steric hindrance compared to their trans counterparts (Satoh et al. 2011). Secondly, the synthesis conditions previously followed by various groups allow for low porosity hydrogel due to the ambient or above room temperature synthesis conditions.

Satoh et al. previously tried to solve the first drawback by purifying various components of spirobenzopyran and functionalizing the spirobenzopyran ring by electron-withdrawing groups such as $-\text{OCH}_3$. The incorporation of electron-withdrawing groups increases the response properties considerably by almost 6 folds. They explained this substantial increase in response time and de-swelling kinetics to preferential ring closing phenomenon of spirobenzopyran due to lack of the electron-cloud which resist the steric effects of the spiro form (ring closed form). Although Satoh et al. work demonstrated promising results it still cannot be compared to the previous synthesized macroporous thermally responsive hydrogels.

Previously, we discussed the effectiveness of utilizing a low temperature synthesis condition to increase the response properties of microporous thermally responsive hydrogel. Similar to the pervious synthesis technique we adopt mechanism low temperature polymerization process for development of faster responsive light responsive hydrogels and also larger pore size. Also like other conventional hydrogels light responsive hydrogels also demonstrate slow response primarily due to the diffusion dominated solvent uptake process, which directly depends on the surface area of the hydrogel. Furthermore, due to the “skin effect”, an outer periphery of the hydrogel shrinks and further retards the deswelling rate of larger gel pieces (Kim, Bae, and Okano 1992b). On account of the low temperature polymerization process the hydrogels developed in above section demonstrated capillary dominated solvent absorption and release process rather than the conventional diffusion dominated process(Chatterjee et al. 2015). The larger pore size is expected to improve the response time by the help of capillary process.

Figure 4.23 a,b demonstrates that such a method works better than the hydrogels developed previously (Sumaru et al. 2006) or recently the method recently suggested by Satoh et al. in which the addition of electron withdrawing group largely affects the swelling ratio of the spirobenzopyran based hydrogels (Satoh et al. 2011). The present large porous hydrogels demonstrated complete equilibration under 3 minutes and was reversible for many cycles. The studies revealed that the swelling ratio can be considerably improved by the adoption of such a procedure (Figure .4.23 c). Although substantial, it is worth mentioning that as compared to the thermally responsive hydrogels synthesized previously, however the present hydrogels do not show as much improvements as before. This is pos-

sibly, due to lower freezing point of the monomer solution caused by presence of tetrahydrofuran. Adoption of low temperature synthesis resulted in increase of swelling ratio. However, the major problem of thermodynamic stability of the ring closed form and slower reversal of hydrophobic state to hydrophilic state of the hydrogel cannot be overcome by just the increase of the pore size of the network. To facilitate such a possibility energy requirement has to considerably decreased or the more possible creating a localized environment which would favor the ring open form.

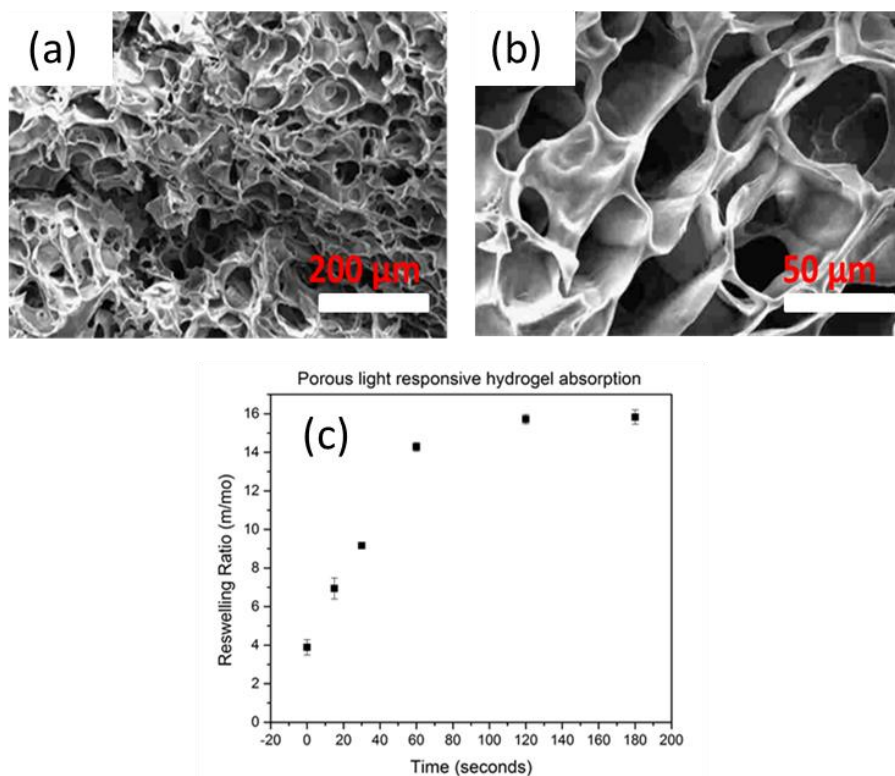


Figure 4.23. Effect of low temperature synthesis on pore size and swelling ratio: (a),(b) SEM microscopy for morphology studies of spirobenzopyran -PNIPAAm hydrogel with average pore length of $\sim 30\mu\text{m}$; (c) Re-swelling ratio of spirobenzopyran based PNIPAAm hydrogels synthesized through low temperature polymerization process.

Incorporation of acrylic acid

The adoption of the low temperature polymerization process yielded good results in terms of increase in response time especially in terms of de-swelling ratio. However, as most of work suggested before light responsive hydrogel based on spirobenzopyran require an acidic media for regaining the light response properties. This is because the thermodynamically favored spiro form(close ring) requires the high activation energy to protonate by itself in neutral media. Generally, as mentioned in the methodology section this is done by incorporation of strongly acidic media of around pH 3 to expedite the ring opening process and conversion to the merocyanine configuration. Although, the acidic media enables regaining the light response properties, for the purposes of the intended usage- tactile display, this fact remains an inherent challenge from the packaging point of view. These constraints are also important as without solving them, the light responsive hydrogels so developed could be termed as single directional and would be disposable system. In the present section, the alternative to such a system is proposed by incorporation of an acidic group in the synthesis conditions. Previously, the incorporation of such a group has enabled faster response time by acidic group functioning as an internalized proton donor/acceptor (Ziolkowski et al. 2013).

Figure 4.24 demonstrates such an improvement by incorporation of acrylic acid in the system. By incorporating an acidic chain in the polymeric system the hydrogels has a faster response time, compared to simple PNIPAAm-SP system. This is mainly due to the difference of de-protonation of the hydrogel network and is deduced to be proximity of acidic environment which reduces the diffusion time of the proton within the network.

Thus the acid media limitation is overcome here by the presence of self-protonating network.. Furthermore, we see the presence of acrylic acid in hydrogel network alters the re-swelling properties and results in much faster response characteristics by inducing a protonating monomer, example acrylic acid. The presence of acrylic acid is also hypothesized to increase the swelling behavior due to the higher hydrophilic character of the PNIPAAm network. Figure 4.24 also compares the re-swelling ratio of various hydrogels synthesized. The black line suggests that the macroporous PNIPAAm hydrogels have the best re-swelling behavior, followed by the acrylic acid spirobenzopyran-co-PNIPAAm hydrogels. More importantly, the hydrogels which do not contain the acrylic acid are found to have a worse re-swelling ratio.

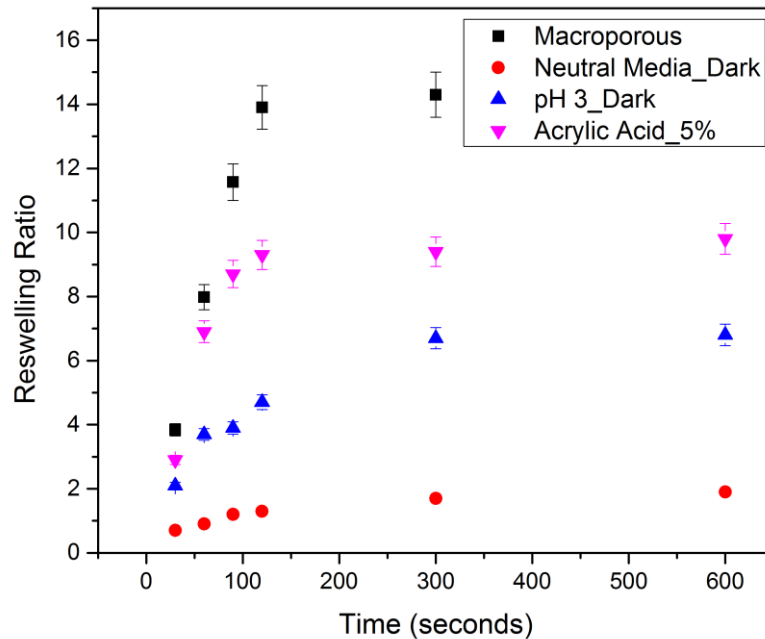


Figure 4.24. Effect of acrylic acid on the re-swelling behavior of spirobenzopyran hydrogels

Increase of mechanical properties of light responsive hydrogels

Along with the response properties, an important facet of hydrogel characteristics are their mechanical properties. Particularly in the present work the mechanical properties gain additional interest as we propose to utilize these hydrogels as tactile display alternatives. Previously, in the thermally responsive hydrogels we had incorporated in-situ silicate network as the method of improving the mechanical properties along with their response properties. In the present work, the silica method was not followed for two important reasons. First, the in-situ network generated by the tetramethyl-orthosilicate (TMOS) relies on a dominant aqueous media, which is lacking here due to presence of the THF. Second, and most importantly the incorporation of such a network does not improve the toughness of the hydrogel, an important attribute required for the hydrogel to be used as a viable alternative for the tactile displays.

Figure 4.25 describes an alternative strategy to develop tough hydrogel has been done by using silicate network dispersed. The DMA compression data reveals that the incorporation of the silicate network resulted in high increase of the toughness as well as the stretchability. These properties could be very useful in the present case of light responsive hydrogel. Previously, also the addition of hydroxyapatite and other clay particle have demonstrated remarkable mechanical and unexpected stretchability (Gaharwar et al. 2011, Wu et al. 2011). The mechanical properties such composite material could be compared to even elastomers due to presence of silicate nanoparticles usually acting as covalently bound and multifunctional cross-linkers to the polymer, which leads to mechanical toughness,

high tensile moduli, and rapid de-swelling in response to stimulus changes. Both the presence of such clay particles as well as the different synthesis technique is expected to improve the properties of the hydrogel discussed here.

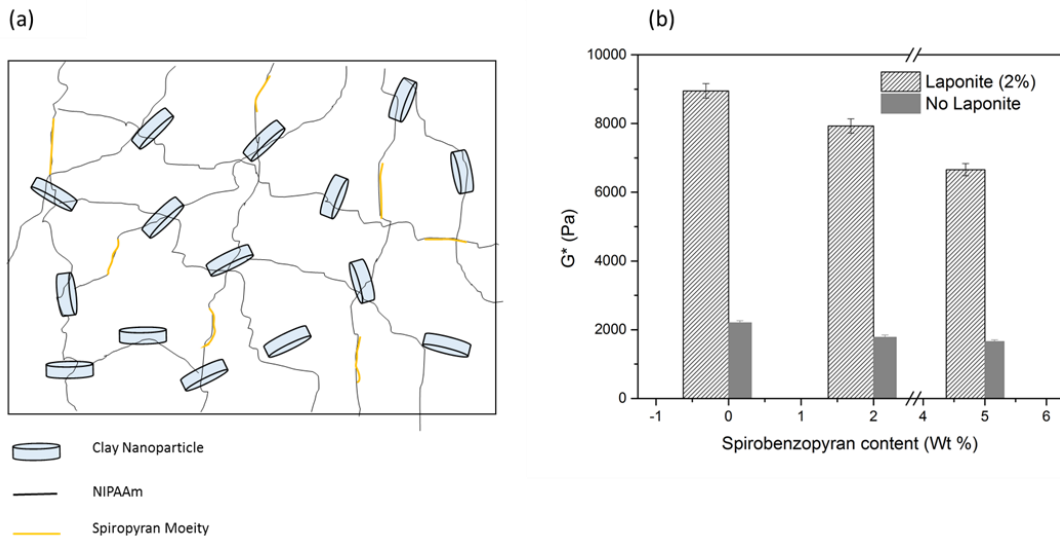


Figure 4.25. Effect of laponite concentration on the mechanical properties of spirobenzopyran-co-PNIPAAm hydrogels (a) Illustration of laponite dispersed in a chemically cross-linked PNIPAAm network (b), (c) comparison of complex moduli due to incorporation of clay particles.

4.4.3 Application of light responsive hydrogels in tactile devices

The hydrogels studied here could be an excellent potential candidate for the development of tactile based surfaces. In this section we review some of the preliminary work done in this field by exploiting the light responsive hydrogel. Figure 4.26a describes the basic mechanism of developing a stereolithographic setup, which is attached to a projector that relays the pattern designed on the computer. The light used here is of white color, an important criterion for this project. The light responsive behavior of the hydrogel was tested by project specific pattern i.e., “ASU” on the hydrogel surface. The experiment successfully verified the light responsive characteristic of the hydrogel (Figure 4.27 b).

Apart from a simple film of hydrogel acting as the tactile display, another possibility of using this hydrogel is through the integration of hard and soft material as seen previously. The proposed mechanism is to have the materials inside narrow copper channels which allow light to be beamed in directly through these. A schematic illustration of such a mechanism is shown in Figure 4.27 a, where light is projected from top to bring about a change in morphology of the top surface of the hydrogel film. Preliminary studies have been conducted with this idea which proves such an idea. We propose that the a development of fast responsive hydrogel would facilitate the development of tactile surface which could easily added-on top of consumer devices, for better human interaction .

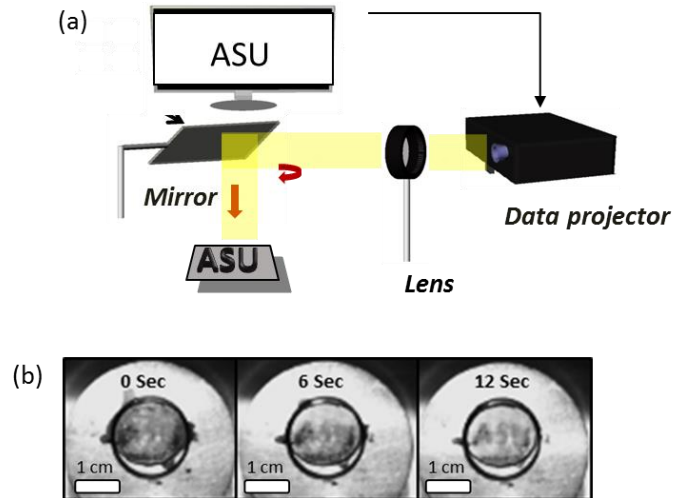


Figure 4.26. Light responsive hydrogel as tactile displays, (a) Schematic illustration of the photolithographic setup used in the test, (b) Time lapse of the pattern developed on the hydrogel

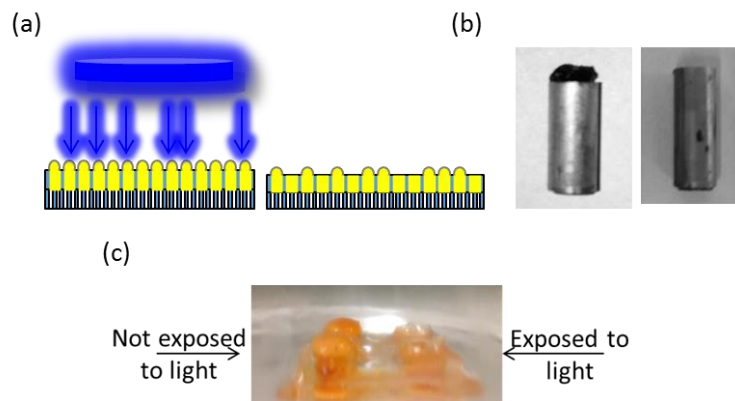


Figure 4.27. Light responsive hydrogel as potential candidate for pixelated tactile device, (a) Schematic of light responsive hydrogel in fixed channels, (b) preliminary light responsive hydrogels demonstrating shrinkage of the hydrogel in the z-direction, (c) hydrogel synthesized in a mold and exposed to light in different sections.

CHAPTER 5

SUMMMARY AND FUTURE WORK

5.1 Summary

In summary, two types of poly(*n*-isopropylacrylamide) (PNIPAAm) based thermally responsive hydrogels, namely macroporous and microporous, were prepared by adopting different synthesis techniques. The structure-property relationship studies of these hydrogels were performed through various characterization techniques such as DSC and rheometer. These studies offered important insight into the difference of the mechanical and thermal properties of PNIPAAm hydrogels as a function of pore size. Importantly, the employment of additives such as a co-solvent (methanol) and an ionic surfactant (SDS) in the media to alter the transition temperature was studied here. These studies were useful in demonstrating the hydrogels response can be tuned as function of media molecules, thereby opening possibility of new applications for these popular “smart” material. Interestingly, these studies also revealed that based on the hydrogel porosity, the response of the hydrogels were different; thereby suggesting a structure property relationship between hydrogels and the media molecules.

Furthermore, using the macroporous hydrogel as a substrate it was demonstrated that environmentally sensitive hydrogels can be successfully integrated with thin-film silicon by using transfer-printing methods, both patterned and non-patterned silicon elements. The integration provided a means of controlled mechanical buckling of the thin silicon film due to changes in environmental stimuli such as temperature. An approach to create substrates with tunable curvatures was also developed. The bowl-like shape was obtained from a bilayer structure comprising of PNIPAAm hydrogel and a copolymer hydrogel made

from (N-isopropylacrylamide) (NIPA) and acrylic acid (AA). Such substrates were integrated with thin film silicon and their buckling phenomenon was studied, thereby revealing the reversible nature of the substrate as well as the integrated silicon.

Also the effect the additives on the light response properties of PNIPAAm was explored. Both physical (chlorophyllin) and chemical (spirobenzopyran) approaches were discussed as a method of incorporating visible light response properties in PNIPAAm. To develop faster response time for such hydrogels, a low temperature polymerization process was adopted along with an acidic co-polymer. As the main motivation of the work was to develop a tactile display for the digital devices, a method of incorporating silicate network into the hydrogels synthesis and making them tougher was also explored. Such incorporations resulted in increase of the mechanical properties along with a limited decrease of the light response properties. Such methods of developing faster responsive hydrogels along with multi-stimuli response could be effective for future development and use of diverse environmentally responsive substrates. Moreover, these “smart” materials could offer broader impacts on numerous applications, especially in the field of adaptable electronics (e.g., flexible sensors, high-performance bio-inspired systems, etc.). Finally, the comprehensive studies would enhance the present knowledge of both fast responsive PNIPAAm and conventional hydrogels and probably help it to be a more attractive for such integration with other hard semiconducting materials.

5.2 Future Work

Influence of Ionic Liquid on Transition Temperature of PNIPAAm

In this work, we successfully demonstrated the effect of media molecules, such as co-solvent and surfactant on the transition temperature of LCST exhibiting polymers like PNIPAAm. Such an observation was explained on the basis of influence of such molecules and diverse interaction pattern with the polymeric chains. Particularly, we see the phenomenon of co-solvency being exhibited when hydrophilic solvent, such as methanol is mixed with water and PNIPAAm; which results in the decrease of transition temperature of PNIPAAm. On the other hand, surfactants has a stabilizing effect which resists the hydrogen bond collapse and thus increases the transition temperature. On the similar lines, another class of molecules, namely ionic liquids could potentially exert the both these effects on the transition temperature of PNIPAAm.

Ionic liquids are interesting class of solvents which have long organic chains along with inorganic anionic groups. Ionic solvents have since been proposed to be used in many applications as green solvents due to low volatility and non-flammability. Ionic liquids could potentially have the ability to be used as co-solvent with water or in its pure state to also control the transition temperature of PNIPAAm. One of the most attractive feature of ionic liquids is that its end group be easily replaced by displacement reaction, this results in alteration of the hydrophilic character of the compound. This feature potentially could give extended ability to influence the transition temperature depending on the end group effect on the transition temperature of PNIPAAm. As part of the future work, we propose such a system of ionic liquids to modulate the transition temperature.

Previously, Ueki et al. (Ueki and Watanabe 2006) demonstrated that the 1-ethyl-3-methylimidazolium bis(trifluoromethane sulfone)imide (EMIM-TFSi) could be used to increase the transition temperature of low density linear PNIPAAm polymer beyond 100 °C. For general co-solvents such a wide increase in the transition temperature is not seen and such a phenomenon is also not well-explained. Therefore, we also propose to use molecular dynamic simulation on understanding the reason behind such observations. Moreover, because such initial observations have only been reported using transmittance mode in simple spectrometer, future studies warrants closer a closer inspection of such a phenomenon on bulk hydrogels using thermal characterization methods such a DSC, similar to what we have used before. Therefore, as part of the future we propose to undertake a two –fold strategy in which we propose to influence the transition temperature of PNIPAAm by the presence of different classes of ionic liquids in the media. Furthermore, we want to undertake molecular dynamic simulations to explain the mechanism followed by ionic liquids on such hyporthesized influence on the LCST behavior along with thermal characterization technique to understand such observation in more detail.

Improvement of Response and Mechanical Properties of Spirobenzopyran-PNIPAAm Hydrogels

Tactile display was one the main emphasis of developing visible light responsive hydrogels which we discussed in the previous section. However, for this technology to be completely integrated with modern electronic devices, we need fast reversible light response characteristics as well good mechanical properties. Although the fast responsive characteristics was developed here with help of low temperature polymerization process,

the mechanical property is still a critical challenge. The mechanical property assumes greater significance in this particular application of tactile display as the hydrogels so developed is proposed to be used as the interface between the human touch and digital screen.

Integration of clay materials had larger impact on the mechanical properties, but it also negatively impacted the light responsive properties. One major reason for this drawback is limited solubility of spirobenzopyran in clay dominated aqueous solution and non-solubility of clay nanoparticles in the organic solvents such as tetrahydrofuran. This fundamental limitation leads us to propose a twofold synthesis technique, e.g. double network or grafting of the light responsive spirobenzopyran molecule on the PNIPAAm hydrogel network. Previously, some research has successfully demonstrated the technique of grafting of hydrophobic polymer chains on PNIPAAm polymer network, such as polyethylene by adopting plasma assisted grafting or UV assisted grafting techniques (Akiyama et al. 2004, Virtanen, Baron, and Tenhu 2000). We propose to use the same technique on PNIPAAm based hydrogels. Furthermore, due to the diversity of the spirobenzopyran as a mechanophore, the above proposed hydrogels could also be stress-sensitive. Such a class of environmentally responsive hydrogels, with multi-responsive properties could thus open new avenues for use of such interesting soft materials. Lastly, the adoption of the hydrogels with traditional display devices would require novel packaging solutions to be developed and should be prime focus for bringing such technologies for everyday use.

REFERENCES

- Abuzayed, Bashar, Necmettin Tanriover, Nurperi Gazioglu, and Ziya Akar. 2010. "Extended endoscopic endonasal approach to the clival region." *Journal of Craniofacial Surgery* no. 21 (1):245-251.
- Ahn, Jong-Hyun, Hoon-Sik Kim, Etienne Menard, Keon Jae Lee, Zhengtao Zhu, Dae-Hyeong Kim, Ralph G Nuzzo, John A Rogers, Islamshah Amlani, and Vadim Kushner. 2007. "Bendable integrated circuits on plastic substrates by use of printed ribbons of single-crystalline silicon." *Applied Physics Letters* no. 90 (21):213501-213501-3.
- Akiyama, Yoshikatsu, Akihiko Kikuchi, Masayuki Yamato, and Teruo Okano. 2004. "Ultrathin Poly(N-isopropylacrylamide) Grafted Layer on Polystyrene Surfaces for Cell Adhesion/Detachment Control." *Langmuir* no. 20 (13):5506-5511.
- Amiya, Takayuki, Yoshitsugu Hirokawa, Yoshiharu Hirose, Yong Li, and Toyochi Tanaka. 1987. "Reentrant phase transition of N-isopropylacrylamide gels in mixed solvents." *The Journal of chemical physics* no. 86:2375.
- Anthony, Olivier, and Raoul Zana. 1994. "Effect of Temperature on the Interactions between Neutral Polymers and a Cationic and a Nonionic Surfactant in Aqueous Solutions." *Langmuir* no. 10 (11):4048-4052.
- Antonietti, Markus, Rachel A. Caruso, Christine G. Göltner, and Markus C. Weissenberger. 1999. "Morphology Variation of Porous Polymer Gels by Polymerization in Lyotropic Surfactant Phases." *Macromolecules* no. 32 (5):1383-1389.
- Atta, Ayman M., Rasha A. M. El-Ghazawy, Reem K. Farag, and Abdel-Azim A. Abdel-Azim. 2006. "Crosslinked reactive macromonomers based on polyisobutylene and octadecyl acrylate copolymers as crude oil sorbers." *Reactive and Functional Polymers* no. 66 (9):931-943.
- Baek, Namjin, Kinam Park, Jae Hyung Park, and You Han Bae. 2001. "Control of the swelling rate of superporous hydrogels." *Journal of bioactive and compatible polymers* no. 16 (1):47-57.
- Bajpai, AK, Sandeep K Shukla, Smitha Bhanu, and Sanjana Kankane. 2008. "Responsive polymers in controlled drug delivery." *Progress in Polymer Science* no. 33 (11):1088-1118.
- Baker, John P, Harvey W Blanch, and John M Prausnitz. 1995. "Swelling properties of acrylamide-based ampholytic hydrogels: comparison of experiment with theory." *Polymer* no. 36 (5):1061-1069.

- Baker, John P, David R Stephens, Harvey W Blanch, and John M Prausnitz. 1992. "Swelling equilibria for acrylamide-based polyampholyte hydrogels." *Macromolecules* no. 25 (7):1955-1958.
- Balakrishnan, Biji, M Mohanty, PR Umashankar, and A Jayakrishnan. 2005. "Evaluation of an in situ forming hydrogel wound dressing based on oxidized alginate and gelatin." *Biomaterials* no. 26 (32):6335-6342.
- Bassik, Noy, Beza T. Abebe, Kate E. Laflin, and David H. Gracias. 2010. "Photolithographically patterned smart hydrogel based bilayer actuators." *Polymer* no. 51 (26):6093-6098.
- Beamson, Graham, and David Briggs. 1992. *High Resolution XPS of organic polymers , The Scienta ESCA 300 database John Wiley & Sons*. Vol. 15. NY: The Science Esca300 Database.
- Bikiaris, D., A. Vassiliou, K. Chrissafis, K. M. Paraskevopoulos, A. Jannakoudakis, and A. Docoslis. 2008. "Effect of acid treated multi-walled carbon nanotubes on the mechanical, permeability, thermal properties and thermo-oxidative stability of isotactic polypropylene." *Polymer Degradation and Stability* no. 93 (5):952-967.
- Borsos, Attila, and Tibor Gilányi. 2011. "Interaction of cetyl-trimethylammonium bromide with swollen and collapsed poly (N-isopropylacrylamide) nanogel particles." *Langmuir* no. 27 (7):3461-3467.
- Bowden, N., S. Brittain, A. G. Evans, J. W. Hutchinson, and G. M. Whitesides. 1998. "Spontaneous formation of ordered structures in thin films of metals supported on an elastomeric polymer." *Nature* no. 393 (6681):146-149.
- Bowden, N., W. T. S. Huck, K. E. Paul, and G. M. Whitesides. 1999. "The controlled formation of ordered, sinusoidal structures by plasma oxidation of an elastomeric polymer." *Applied Physics Letters* no. 75 (17):2557-2559.
- Brookes, Pat N., Stuart Fraser, Robert D. Short, Luke Hanley, Erick Fuoco, Adam Roberts, and Simon Hutton. 2001. "The effect of ion energy on the chemistry of air-aged polymer films grown from the hyperthermal polyatomic ion Si₂OMe₅⁺." *Journal of Electron Spectroscopy and Related Phenomena* no. 121 (1-3):281-297.
- Burch, David S., and Dianne T.V. Pawluk. 2009. A cheap, portable haptic device for a method to relay 2-D texture-enriched graphical information to individuals who are visually impaired. In *Proceedings of the 11th international ACM SIGACCESS conference on Computers and accessibility*. Pittsburgh, Pennsylvania, USA: ACM.
- Campbell, Peter G, Erin Kenning, David W Andrews, Sanjay Yadla, Marc Rosen, and James J Evans. 2010. "Outcomes after a purely endoscopic transsphenoidal

- resection of growth hormone-secreting pituitary adenomas." *Neurosurgical focus* no. 29 (4):E5.
- Cerda, E., and L. Mahadevan. 2003. "Geometry and physics of wrinkling." *Physical Review Letters* no. 90 (7):4.
- Chatterjee, Prithwish, Annie Dai, Hongyu Yu, Hanqing Jiang, and Lenore L. Dai. 2015. "Thermal and mechanical properties of poly(N-isopropylacrylamide)-based hydrogels as a function of porosity and medium change." *Journal of Applied Polymer Science* no. 132 (45): 42776.
- Chatterjee, Prithwish, Yuping Pan, Eric C Stevens, Teng Ma, Hanqing Jiang, and Lenore L Dai. 2013. "Controlled Morphology of Thin Film Silicon Integrated with Environmentally Responsive Hydrogels." *Langmuir* no. 29 (21):6495-6501.
- Chen, Guohua, and Allan S. Hoffman. 1995a. "Graft copolymers that exhibit temperature-induced phase transitions over a wide range of pH." *Nature* no. 373 (6509):49-52.
- Chen, Guohua, and Allan S. Hoffman. 1995b. "Temperature-induced phase transition behaviors of random vs. graft copolymers of N-isopropylacrylamide and acrylic acid." *Macromolecular Rapid Communications* no. 16 (3):175-182.
- Cheng, Qian, Zeming Song, Teng Ma, Bethany B Smith, Rui Tang, Hongyu Yu, Hanqing Jiang, and Candace K Chan. 2013. "Folding paper-based lithium-ion batteries for higher areal energy densities." *Nano letters* no. 13 (10):4969-4974.
- Chiappe, Cinzia, and Daniela Pieraccini. 2005. "Ionic liquids: solvent properties and organic reactivity." *Journal of Physical Organic Chemistry* no. 18 (4):275-297.
- Chiba, Kiyoshi, and Yoshihito Takenaka. 2008. "Embedded structure of silicon monoxide in SiO₂ films." *Applied Surface Science* no. 254 (8):2534-2539.
- Childs, William R, Michael J Motala, Keon Jae Lee, and Ralph G Nuzzo. 2005. "Masterless soft lithography: patterning UV/Ozone-induced adhesion on poly(dimethylsiloxane) surfaces." *Langmuir* no. 21 (22):10096-10105.
- Chu, Y, PP Varanasi, MJ McGlade, and S Varanasi. 1995. "pH-induced swelling kinetics of polyelectrolyte hydrogels." *Journal of applied polymer science* no. 58 (12):2161-2176.
- Chung, J. Y., A. J. Nolte, and C. M. Stafford. 2009. "Diffusion-Controlled, Self-Organized Growth of Symmetric Wrinkling Patterns." *Advanced Materials* no. 21 (13):1358-1362.

- Copeland, Damian, and Janet Finlay. 2010. "Identification of the optimum resolution specification for a haptic graphic display." *Interacting with Computers* no. 22 (2):98-106.
- Das, Anup, Mohit Mehndiratta, Parthaprasad Chattopadhyay, and Alok R Ray. 2010. "Prolonged zero-order BSA release from pH-sensitive hydrogels of poly (AAc-co-DMAPMA) having rich nano through micro scale morphology." *Journal of applied polymer science* no. 115 (1):393-403.
- Dehaen, Wim, and Alfred Hassner. 1991. "Cycloadditions. 45. Annulation of heterocycles via intramolecular nitrile oxide-heterocycle cycloaddition reaction." *The Journal of Organic Chemistry* no. 56 (2):896-900.
- Dhara, Dibakar, and Prabha R Chatterji. 2000. "Phase transition in linear and cross-linked poly (N-isopropylacrylamide) in water: effect of various types of additives." *Journal of Macromolecular Science, Part C: Polymer Reviews* no. 40 (1):51-68.
- Di Crescenzo, Antonello, Davide Demurtas, Andrea Renzetti, Gabriella Siani, Paolo De Maria, Moreno Meneghetti, Maurizio Prato, and Antonella Fontana. 2009. "Disaggregation of single-walled carbon nanotubes (SWNTs) promoted by the ionic liquid-based surfactant 1-hexadecyl-3-vinyl-imidazolium bromide in aqueous solution." *Soft Matter* no. 5 (1):62-66.
- Dixit, S, J Crain, WCK Poon, JL Finney, and AK Soper. 2002. "Molecular segregation observed in a concentrated alcohol–water solution." *Nature* no. 416 (6883):829-832.
- Dong, Bin, Yijin Su, Yonghui Liu, Jie Yuan, Jingkun Xu, and Liqiang Zheng. 2011. "Dispersion of carbon nanotubes by carbazole-tailed amphiphilic imidazolium ionic liquids in aqueous solutions." *Journal of Colloid and Interface Science* no. 356 (1):190-195.
- Efimenko, Kirill, Mindaugas Rackaitis, Evangelos Manias, Ashkan Vaziri, L Mahadevan, and Jan Genzer. 2005. "Nested self-similar wrinkling patterns in skins." *Nature materials* no. 4 (4):293-297.
- Fukushima, Takanori, Atsuko Kosaka, Yoji Ishimura, Takashi Yamamoto, Toshikazu Takigawa, Noriyuki Ishii, and Takuzo Aida. 2003. "Molecular Ordering of Organic Molten Salts Triggered by Single-Walled Carbon Nanotubes." *Science* no. 300 (5628):2072-2074.
- Gaharwar, Akhilesh K, Sandhya A Dammu, Jamie M Canter, Chia-Jung Wu, and Gudrun Schmidt. 2011. "Highly extensible, tough, and elastomeric nanocomposite hydrogels from poly (ethylene glycol) and hydroxyapatite nanoparticles." *Biomacromolecules* no. 12 (5):1641-1650.

- Ganji, Fariba, Samira Vasheghani-Farahani, and Ebrahim Vasheghani-Farahani. 2010. "Theoretical description of hydrogel swelling: a review." *Iran Polym J* no. 19 (5):375-398.
- Gao, Lili, Huayi Yin, and Dihua Wang. 2010. "Ionic liquids assisted formation of an oil/water emulsion stabilised by a carbon nanotube/ionic liquid composite layer." *Physical Chemistry Chemical Physics* no. 12 (11):2535-2540.
- Gemeinhart, Richard A, Jun Chen, Haesun Park, and Kinam Park. 2000. "pH-sensitivity of fast responsive superporous hydrogels." *Journal of Biomaterials Science, Polymer Edition* no. 11 (12):1371-1380.
- Genzer, Jan, and Jan Groenewold. 2006. "Soft matter with hard skin: From skin wrinkles to templating and material characterization." *Soft Matter* no. 2 (4):310-323.
- Gerlach, Gerald, Margarita Guenther, Joerg Sorber, Gunnar Suchaneck, Karl-Friedrich Arndt, and Andreas Richter. 2005. "Chemical and pH sensors based on the swelling behavior of hydrogels." *Sensors and Actuators B: Chemical* no. 111–112:555-561.
- Guenther, M, D Kuckling, C Corten, G Gerlach, J Sorber, G Suchaneck, and K-F Arndt. 2007. "Chemical sensors based on multiresponsive block copolymer hydrogels." *Sensors and Actuators B: Chemical* no. 126 (1):97-106.
- Guo, J-H, Yi Luo, Andreas Augustsson, Stepan Kashtanov, J-E Rubensson, David K Shuh, Hans Ågren, and Joseph Nordgren. 2003. "Molecular structure of alcohol-water mixtures." *Physical review letters* no. 91 (15):157401.
- Gupta, Piyush, Kavita Vermani, and Sanjay Garg. 2002. "Hydrogels: from controlled release to pH-responsive drug delivery." *Drug Discovery Today* no. 7 (10):569-579.
- Harmon, Marianne E, Mary Tang, and Curtis W Frank. 2003. "A microfluidic actuator based on thermoresponsive hydrogels." *Polymer* no. 44 (16):4547-4556.
- Hart, JP, and AK Abass. 1997. "A disposable amperometric gas sensor for sulphur-containing compounds based on a chemically modified screen printed carbon electrode coated with a hydrogel." *Analytica chimica acta* no. 342 (2):199-206.
- Hayes, Robert A, and BJ Feenstra. 2003. "Video-speed electronic paper based on electrowetting." *Nature* no. 425 (6956):383-385.
- He, Chaoliang, Sung Wan Kim, and Doo Sung Lee. 2008a. "In situ gelling stimuli-sensitive block copolymer hydrogels for drug delivery." *Journal of controlled release* no. 127 (3):189-207.

- He, Chaoliang, Sung Wan Kim, and Doo Sung Lee. 2008b. "In situ gelling stimuli-sensitive block copolymer hydrogels for drug delivery." *Journal of Controlled Release* no. 127 (3):189-207.
- Hermant, Marie Claire, Bert Klumperman, and Cor E Koning. 2009. "Conductive Pickering-poly (high internal phase emulsion) composite foams prepared with low loadings of single-walled carbon nanotubes." *Chemical Communications* (19):2738-2740.
- Heskins, M., and J. E. Guillet. 1968. "Solution Properties of Poly(N-isopropylacrylamide)." *Journal of Macromolecular Science: Part A - Chemistry* no. 2 (8):1441-1455.
- Hirotsu, Shunsuke. 1988. "Critical points of the volume phase transition in N-isopropylacrylamide gels." *The Journal of Chemical Physics* no. 88 (1):427-431.
- Hobart, K. D., F. J. Kub, M. Fatemi, M. E. Twigg, P. E. Thompson, T. S. Kuan, and C. K. Inoki. 2000. Compliant substrates: A comparative study of the relaxation mechanisms of strained films bonded to high and low viscosity oxides.
- Hoffman, Allan S. 2002. "Hydrogels for biomedical applications." *Advanced drug delivery reviews* no. 54 (1):3-12.
- Höfft, O., S. Bahr, and V. Kempter. 2008. "Investigations with Infrared Spectroscopy on Films of the Ionic Liquid [EMIM]Tf₂N." *Langmuir* no. 24 (20):11562-11566.
- Hofmann, Christian, and Monika Schönhoff. 2009. "Do additives shift the LCST of poly (N-isopropylacrylamide) by solvent quality changes or by direct interactions?" *Colloid and Polymer Science* no. 287 (12):1369-1376.
- Huang, J., M. Juskiewicz, W. H. de Jeu, E. Cerda, T. Emrick, N. Menon, and T. P. Russell. 2007. "Capillary wrinkling of floating thin polymer films." *Science* no. 317 (5838):650-653.
- Huggins, Maurice L. 1942a. "Some Properties of Solutions of Long-chain Compounds." *The Journal of Physical Chemistry* no. 46 (1):151-158.
- Huggins, Maurice L. 1942b. "Thermodynamic Properties Of Solutions Of Long-Chain Compounds." *Annals of the New York Academy of Sciences* no. 43 (1):1-32.
- Jiang, H. Y, S. Kelch, and A. Lendlein. 2006. "Polymers Move in Response to Light." *Advanced Materials* no. 18 (11):1471-1475.
- Jiang, Hanqing, Dahl-Young Khang, Jizhou Song, Yugang Sun, Yonggang Huang, and John A Rogers. 2007. "Finite deformation mechanics in buckled thin films on compliant supports." *Proceedings of the National Academy of Sciences* no. 104 (40):15607-15612.

- Jiang, Hanqing, Yugang Sun, John A Rogers, and Yonggang Huang. 2007. "Mechanics of precisely controlled thin film buckling on elastomeric substrate." *Applied physics letters* no. 90 (13):133119.
- Jones, Lynette A. 2011. "Tactile communication systems optimizing the display of information." *Progress in brain research* no. 192:113.
- Jones, Lynette A, Brett Lockyer, and Erin Piatetski. 2006. "Tactile display and vibrotactile pattern recognition on the torso." *Advanced Robotics* no. 20 (12):1359-1374.
- Ju, Hee Kyung, So Yeon Kim, and Young Moo Lee. 2001. "pH/temperature-responsive behaviors of semi-IPN and comb-type graft hydrogels composed of alginate and poly (N-isopropylacrylamide)." *Polymer* no. 42 (16):6851-6857.
- Kabra, Bhagwati G, Stevin H Gehrke, and Richard J Spontak. 1998. "Microporous, responsive hydroxypropyl cellulose gels. 1. Synthesis and microstructure." *Macromolecules* no. 31 (7):2166-2173.
- Kameda, Mitsuyoshi, Kimio Sumaru, Toshiyuki Kanamori, and Toshio Shinbo. 2003. "Photoresponse gas permeability of azobenzene-functionalized glassy polymer films." *Journal of applied polymer science* no. 88 (8):2068-2072.
- Kane, Ravi S., Shuichi Takayama, Emanuele Ostuni, Donald E. Ingber, and George M. Whitesides. 1999. "Patterning proteins and cells using soft lithography." *Biomaterials* no. 20 (23–24):2363-2376.
- Kaneko, Yuzo, Satoki Nakamura, Kiyotaka Sakai, Takao Aoyagi, Akihiko Kikuchi, Yasuhisa Sakurai, and Teruo Okano. 1998. "Rapid deswelling response of poly (N-isopropylacrylamide) hydrogels by the formation of water release channels using poly (ethylene oxide) graft chains." *Macromolecules* no. 31 (18):6099-6105.
- Kang, Do Hyun, Sang Moon Kim, Byungjun Lee, Hyunsik Yoon, and Kahp-Yang Suh. 2013. "Stimuli-responsive hydrogel patterns for smart microfluidics and microarrays." *Analyst* no. 138 (21):6230-6242.
- Kato, Norihiro, Yasuzo Sakai, and Shihoko Shibata. 2003. "Wide-Range Control of Deswelling Time for Thermosensitive Poly(N-isopropylacrylamide) Gel Treated by Freeze-Drying." *Macromolecules* no. 36 (4):961-963.
- Kato, Norihiro, and Fujio Takahashi. 1997. "Acceleration of Deswelling of Poly (N-isopropylacrylamide) Hydrogel by the Treatment of a Freeze-Dry and Hydration Process." *Bulletin of the Chemical Society of Japan* no. 70 (6):1289-1295.
- Katono, Hiroki, Atsushi Maruyama, Kohei Sanui, Naoya Ogata, Teruo Okano, and Yasuhisa Sakurai. 1991. "Thermo-responsive swelling and drug release switching of interpenetrating polymer networks composed of poly (acrylamide-co-butyl

- methacrylate) and poly (acrylic acid)." *Journal of Controlled Release* no. 16 (1):215-227.
- Kawano, Takahito, Yasuro Niidome, Takeshi Mori, Yoshiki Katayama, and Takuro Niidome. 2009. "PNIPAM Gel-Coated Gold Nanorods for Targeted Delivery Responding to a Near-Infrared Laser." *Bioconjugate Chemistry* no. 20 (2):209-212.
- Keerl, Martina, and Walter Richtering. 2007. "Synergistic depression of volume phase transition temperature in copolymer microgels." *Colloid and Polymer Science* no. 285 (4):471-474.
- Khang, D. Y., H. Q. Jiang, Y. Huang, and J. A. Rogers. 2006. "A stretchable form of single-crystal silicon for high-performance electronics on rubber substrates." *Science* no. 311 (5758):208-212.
- Khang, Dahl-Young, John A. Rogers, and Hong H. Lee. 2009. "Mechanical Buckling: Mechanics, Metrology, and Stretchable Electronics." *Advanced Functional Materials* no. 19 (10):1526-1536..
- Kim, Dae-Hyeong, Jong-Hyun Ahn, Won Mook Choi, Hoon-Sik Kim, Tae-Ho Kim, Jizhou Song, Yonggang Y. Huang, Zhuangjian Liu, Chun Lu, and John A. Rogers. 2008. "Stretchable and Foldable Silicon Integrated Circuits." *Science* no. 320 (5875):507-511.
- Kim, Jin-Chul, Soo Kyoung Bae, and Jong-Duk Kim. 1997. "Temperature-sensitivity of liposomal lipid bilayers mixed with poly (N-isopropylacrylamide-co-acrylic acid)." *Journal of biochemistry* no. 121 (1):15-19.
- Kim, Jun-Hyun, and T. Randall Lee. 2004. "Thermo- and pH-Responsive Hydrogel-Coated Gold Nanoparticles." *Chemistry of Materials* no. 16 (19):3647-3651.
- Kim, Sung Wan, You Han Bae, and Teruo Okano. 1992a. "Hydrogels: swelling, drug loading, and release." *Pharmaceutical research* no. 9 (3):283-290.
- Kim, SungWan, YouHan Bae, and Teruo Okano. 1992b. "Hydrogels: Swelling, Drug Loading, and Release." *Pharmaceutical Research* no. 9 (3):283-290.
- Klouda, Leda, and Antonios G. Mikos. 2008. "Thermoresponsive hydrogels in biomedical applications." *European Journal of Pharmaceutics and Biopharmaceutics* no. 68 (1):34-45.
- Ko, Heung Cho, Mark P. Stoykovich, Jizhou Song, Viktor Malyarchuk, Won Mook Choi, Chang-Jae Yu, Joseph B. Geddes Iii, Jianliang Xiao, Shuodao Wang, Yonggang Huang, and John A. Rogers. 2008. "A hemispherical electronic eye camera based on compressible silicon optoelectronics." *Nature* no. 454 (7205):748-753.

- Koetting, Michael C., and Nicholas A. Peppas. 2014. "pH-Responsive poly(itaconic acid-co-N-vinylpyrrolidone) hydrogels with reduced ionic strength loading solutions offer improved oral delivery potential for high isoelectric point-exhibiting therapeutic proteins." *International Journal of Pharmaceutics* no. 471 (1–2):83-91.
- Kokufuta, Etsuo, Hironori Suzuki, and Daisuke Sakamoto. 1997. "On the local binding of ionic surfactants to poly (N-isopropylacrylamide) gels." *Langmuir* no. 13 (10):2627-2632.
- Kokufuta, Etsuo, Yong Qing Zhang, Toyochi Tanaka, and Akira Mamada. 1993. "Effects of surfactants on the phase transition of poly (N-isopropylacrylamide) gel." *Macromolecules* no. 26 (5):1053-1059.
- Kratz, Karl, Thomas Hellweg, and Wolfgang Eimer. 2000. "Influence of charge density on the swelling of colloidal poly(N-isopropylacrylamide-co-acrylic acid) microgels." *Colloids and Surfaces A: Physicochemical and Engineering Aspects* no. 170 (2–3):137-149.
- Kuhn, W, and B Hargitay. 1951. "Muskelähnliche Kontraktion und Dehnung von Netzwerken polyvalenter Fadenmolekülonen." *Cellular and Molecular Life Sciences* no. 7 (1):1-11.
- Kuhn, W, B Hargitay, A Katchalsky, and H Eisenberg. 1950. "Reversible dilation and contraction by changing the state of ionization of high-polymer acid networks."
- L, Vincent, \#233, vesque, J, \#233, r, \#244, me Pasquero, Vincent Hayward, and Maryse Legault. 2005. "Display of virtual braille dots by lateral skin deformation: feasibility study." *ACM Trans. Appl. Percept.* no. 2 (2):132-149.
- Lee, Lay-Theng, and Bernard Cabane. 1997. "Effects of surfactants on thermally collapsed poly (N-isopropylacrylamide) macromolecules." *Macromolecules* no. 30 (21):6559-6566.
- Li, Hua, Teng Yong Ng, Yong Kin Yew, and Khin Yong Lam. 2005. "Modeling and Simulation of the Swelling Behavior of pH-Stimulus-Responsive Hydrogels." *Biomacromolecules* no. 6 (1):109-120.
- Lim, Franklin, and Anthony M Sun. 1980. "Microencapsulated islets as bioartificial endocrine pancreas." *Science* no. 210 (4472):908-910.
- Liu, Danqing, Cees W. M. Bastiaansen, Jaap M. J. den Toonder, and Dirk J. Broer. 2013. "(Photo-)Thermally Induced Formation of Dynamic Surface Topographies in Polymer Hydrogel Networks." *Langmuir* no. 29 (18):5622-5629.

- Liu, Xiaomei, Xianmin Zhang, Jun Cong, Jian Xu, and Kangsheng Chen. 2003. "Demonstration of etched cladding fiber Bragg grating-based sensors with hydrogel coating." *Sensors and Actuators B: Chemical* no. 96 (1–2):468-472.
- Liu, Yonghui, Li Yu, Shaohua Zhang, Jie Yuan, Lijuan Shi, and Liqiang Zheng. 2010. "Dispersion of multiwalled carbon nanotubes by ionic liquid-type Gemini imidazolium surfactants in aqueous solution." *Colloids and Surfaces A: Physicochemical and Engineering Aspects* no. 359 (1–3):66-70.
- Lo, Chi-Wei, Difeng Zhu, and Hongrui Jiang. 2011. "An infrared-light responsive graphene-oxide incorporated poly(N-isopropylacrylamide) hydrogel nanocomposite." *Soft Matter* no. 7 (12):5604-5609.
- Loh, Watson, Luciana AC Teixeira, and Lay-Theng Lee. 2004. "Isothermal calorimetric investigation of the interaction of poly (N-isopropylacrylamide) and ionic surfactants." *The Journal of Physical Chemistry B* no. 108 (10):3196-3201.
- Lowman, AM, NA Peppas, and E Mathiowitz Hydrogels. 1999. "Encyclopedia of controlled drug delivery." *Mathiowitz, E., Ed*:397.
- Lozinsky, V. I., E. S. Vainerman, E. F. Titova, E. M. Belavtseva, and S. V. Rogozhin. 1984. "Study of cryostructurization of polymer systems." *Colloid and Polymer Science* no. 262 (10):769-774.
- Lu, KL, RM Lago, YK Chen, MLH Green, PJF Harris, and SC Tsang. 1996. "Mechanical damage of carbon nanotubes by ultrasound." *Carbon* no. 34 (6):814-816.
- Ma, Huan, Mingxiang Luo, Sriya Sanyal, Kaushal Rege, and Lenore L Dai. 2010. "The one-step Pickering emulsion polymerization route for synthesizing organic-inorganic nanocomposite particles." *Materials* no. 3 (2):1186-1202.
- Ma, Xiaomei, Yanjun Cui, Xian Zhao, Sixun Zheng, and Xiaozhen Tang. 2004. "Different deswelling behavior of temperature-sensitive microgels of poly(N-isopropylacrylamide) crosslinked by polyethyleneglycol dimethacrylates." *Journal of Colloid and Interface Science* no. 276 (1):53-59.
- Mahadevan, L., and S. Rica. 2005. "Self-Organized Origami." *Science* no. 307 (5716):1740.
- Mamada, Akira, Toyochi Tanaka, Dawan Kungwachakun, and Masahiro Irie. 1990. "Photoinduced phase transition of gels." *Macromolecules* no. 23 (5):1517-1519.
- Matsuguchi, Masanobu, Noboru Harada, and Satoshi Omori. 2014. "Poly (N-isopropylacrylamide) nanoparticles for QCM-based gas sensing of HCl." *Sensors and Actuators B: Chemical* no. 190:446-450.

- Meewes, M, J Ricka, M De Silva, R Nyffenegger, and Th Binkert. 1991. "Coil-globule transition of poly (N-isopropylacrylamide): a study of surfactant effects by light scattering." *Macromolecules* no. 24 (21):5811-5816.
- Meitl, M. A., Z. T. Zhu, V. Kumar, K. J. Lee, X. Feng, Y. Y. Huang, I. Adesida, R. G. Nuzzo, and J. A. Rogers. 2006. "Transfer printing by kinetic control of adhesion to an elastomeric stamp." *Nature Materials* no. 5 (1):33-38.
- Molina, M Jesús, M Rosa Gómez-Antón, and Inés F Piérola. 2004. "Factors driving the protonation of poly (N-vinylimidazole) hydrogels." *Journal of Polymer Science Part B: Polymer Physics* no. 42 (12):2294-2307.
- Monti, Sandra, Giorgio Orlandi, and Paolo Palmieri. 1982. "Features of the photochemically active state surfaces of azobenzene." *Chemical Physics* no. 71 (1):87-99.
- Moon, M.-W., S. H. Lee, J.-Y. Sun, K. H. Oh, A. Vaziri, and J. W. Hutchinson. 2007. "Wrinkled hard skins on polymers created by focused ion beam." *Proceedings of the National Academy of Sciences of the United States of America* no. 104 (4):1130-1133.
- Mueller, Mareen, Moritz Tebbe, Daria V Andreeva, Matthias Karg, Ramon A Alvarez Puebla, Nicolas Pazos Perez, and Andreas Fery. 2012. "Large-area organization of pNIPAM-coated nanostars as SERS platforms for polycyclic aromatic hydrocarbons sensing in gas phase." *Langmuir* no. 28 (24):9168-9173.
- Mura, Simona, Julien Nicolas, and Patrick Couvreur. 2013. "Stimuli-responsive nanocarriers for drug delivery." *Nat Mater* no. 12 (11):991-1003.
- Nagai, Yusuke, Larry D Unsworth, Sotirios Koutsopoulos, and Shuguang Zhang. 2006. "Slow release of molecules in self-assembling peptide nanofiber scaffold." *Journal of controlled release* no. 115 (1):18-25.
- Najafi, Ebrahim, Jae-Yong Kim, Song-Hee Han, and Kwanwoo Shin. 2006. "UV-ozone treatment of multi-walled carbon nanotubes for enhanced organic solvent dispersion." *Colloids and Surfaces A: Physicochemical and Engineering Aspects* no. 284–285:373-378.
- Naskar, Jishu, Goutam Palui, and Arindam Banerjee. 2009. "Tetrapeptide-Based Hydrogels: for Encapsulation and Slow Release of an Anticancer Drug at Physiological pH." *The Journal of Physical Chemistry B* no. 113 (35):11787-11792.
- Nge, Thi Thi, Naruhito Hori, Akio Takemura, and Hirokuni Ono. 2004. "Swelling behavior of chitosan/poly (acrylic acid) complex." *Journal of applied polymer science* no. 92 (5):2930-2940.

- Pan, Yongzheng, Hongqian Bao, Nanda Gopal Sahoo, Tongfei Wu, and Lin Li. 2011. "Water-Soluble Poly (N-isopropylacrylamide)–Graphene Sheets Synthesized via Click Chemistry for Drug Delivery." *Advanced Functional Materials* no. 21 (14):2754-2763.
- Panhuis, Marc in het, and Vesselin N. Paunov. 2005. "Assembling carbon nanotubosomes using an emulsion-inversion technique." *Chemical Communications* (13):1726-1728.
- Pantelopoulos, Alexandros, and Nikolaos G Bourbakis. 2010. "A survey on wearable sensor-based systems for health monitoring and prognosis." *Systems, Man, and Cybernetics, Part C: Applications and Reviews, IEEE Transactions on* no. 40 (1):1-12.
- Patel, Vijay R, and Mansoor M Amiji. 1996. "Preparation and characterization of freeze-dried chitosan-poly (ethylene oxide) hydrogels for site-specific antibiotic delivery in the stomach." *Pharmaceutical research* no. 13 (4):588-593.
- Pattanakul, R, N Chomnawang, D Klaitabtim, and A Tuantranont. "Simulation of Metallic MEMS Electrostatic Actuator for Microvalve Applications."
- Peppas, NA, P Bures, W Leobandung, and H Ichikawa. 2000. "Hydrogels in pharmaceutical formulations." *European journal of pharmaceutics and biopharmaceutics* no. 50 (1):27-46.
- Peppas, NA, Y Huang, M Torres-Lugo, JH Ward, and J Zhang. 2000. "Physicochemical foundations and structural design of hydrogels in medicine and biology." *Annual review of biomedical engineering* no. 2 (1):9-29.
- Peppas, Nikolaos A, and Atul R Khare. 1993. "Preparation, structure and diffusional behavior of hydrogels in controlled release." *Advanced drug delivery reviews* no. 11 (1):1-35.
- Peppas, Nikolaos A. 1997. "Hydrogels and drug delivery." *Current Opinion in Colloid & Interface Science* no. 2 (5):531-537.
- Qiu, Yong, and Kinam Park. 2012. "Environment-sensitive hydrogels for drug delivery." *Advanced Drug Delivery Reviews* no. 64, Supplement:49-60.
- Qu, J-B, L-Y Chu, Mei Yang, Rui Xie, Lin Hu, and W-M Chen. 2006. "A pH-Responsive Gating Membrane System with Pumping Effects for Improved Controlled Release." *Advanced Functional Materials* no. 16 (14):1865-1872.
- Ranjha, Nazar Mohammad, Jahanzeb Mudassir, and Sajid Majeed. 2011. "Synthesis and characterization of polycaprolactone/acrylic acid (PCL/AA) hydrogel for controlled drug delivery." *Bulletin of Materials Science* no. 34 (7):1537-1547.

- Razzak, Mirzan T, and Darmawan Darwis. 2001. "Irradiation of polyvinyl alcohol and polyvinyl pyrrolidone blended hydrogel for wound dressing." *Radiation Physics and Chemistry* no. 62 (1):107-113.
- Richter, Andreas, Steffen Howitz, Dirk Kuckling, and Karl-Friedrich Arndt. 2004. "Influence of volume phase transition phenomena on the behavior of hydrogel-based valves." *Sensors and Actuators B: Chemical* no. 99 (2–3):451-458.
- Richter, Andreas, Georgi Paschew, Stephan Klatt, Jens Lienig, Karl-Friedrich Arndt, and Hans-Jürgen P Adler. 2008. "Review on hydrogel-based pH sensors and microsensors." *Sensors* no. 8 (1):561-581.
- Ricka, J, and Toyochi Tanaka. 1984. "Swelling of ionic gels: quantitative performance of the Donnan theory." *Macromolecules* no. 17 (12):2916-2921.
- Roberts, John, Oliver Slattery, David Kardos, and Brett Swope. 2000. New technology enables many-fold reduction in the cost of refreshable braille displays. Paper read at Proceedings of the fourth international ACM conference on Assistive technologies.
- Rogers, John A., Takao Someya, and Yonggang Huang. 2010. "Materials and Mechanics for Stretchable Electronics." *Science* no. 327 (5973):1603-1607.
- Rossi, Giuseppe, and Ken A Mazich. 1991. "Kinetics of swelling for a cross-linked elastomer or gel in the presence of a good solvent." *Physical Review A* no. 44 (8):R4793.
- Ruel-Gariepy, E, G Leclair, P Hildgen, A Gupta, and J-C Leroux. 2002. "Thermosensitive chitosan-based hydrogel containing liposomes for the delivery of hydrophilic molecules." *Journal of Controlled Release* no. 82 (2):373-383.
- Sanyal, Sriya, H Huang, Kaushal Rege, and Lenore L Dai. 2011. "Thermo-Responsive Core-Shell Composite Nanoparticles Synthesized via One-Step Pickering Emulsion Polymerization for Controlled Drug Delivery." *J Nanomedic Nanotechnol* no. 2 (126):2.
- Sasaki, Kotaro, Hideo Naohara, Yun Cai, Yong Man Choi, Ping Liu, Miomir B. Vukmirovic, Jia X. Wang, and Radoslav R. Adzic. 2010. "Core-Protected Platinum Monolayer Shell High-Stability Electrocatalysts for Fuel-Cell Cathodes." *Angewandte Chemie International Edition* no. 49 (46):8602-8607.
- Satoh, Taku, Kimio Sumaru, Toshiyuki Takagi, and Toshiyuki Kanamori. 2011. "Fast-reversible light-driven hydrogels consisting of spirobenzopyran-functionalized poly(N-isopropylacrylamide)." *Soft Matter* no. 7 (18):8030-8034.
- Schexnailder, Patrick, and Gudrun Schmidt. 2009. "Nanocomposite polymer hydrogels." *Colloid and Polymer Science* no. 287 (1):1-11.

- Schild, Howard G, M Muthukumar, and David A Tirrell. 1991. "Cononsolvency in mixed aqueous solutions of poly (N-isopropylacrylamide)." *Macromolecules* no. 24 (4):948-952.
- Schmaljohann, Dirk. 2006. "Thermo-and pH-responsive polymers in drug delivery." *Advanced drug delivery reviews* no. 58 (15):1655-1670.
- Schroeder, Viktor, Till Korten, Heiner Linke, Stefan Diez, and Ivan Maximov. 2013. "Dynamic Guiding of Motor-Driven Microtubules on Electrically Heated, Smart Polymer Tracks." *Nano Letters* no. 13 (7):3434-3438.
- Schwartz, Gregor, Benjamin C-K Tee, Jianguo Mei, Anthony L Appleton, Do Hwan Kim, Huiliang Wang, and Zhenan Bao. 2013. "Flexible polymer transistors with high pressure sensitivity for application in electronic skin and health monitoring." *Nature communications* no. 4:1859.
- Sekitani, Tsuyoshi, and Takao Someya. 2010. "Stretchable, Large-area Organic Electronics." *Advanced Materials* no. 22 (20):2228-2246.
- Sellmer, C., R. Prins, and N. Kruse. 1997. "XPS/SIMS studies of the promoter action in methanol synthesis over silica-supported Pd catalysts." *Catalysis Letters* no. 47 (2):83-89.
- Sershen, SR, SL Westcott, NJ Halas, and JL West. 2000. "Temperature-sensitive polymer–nanoshell composites for photothermally modulated drug delivery." *Journal of biomedical materials research* no. 51 (3):293-298.
- Shinohara, Masami, Yutaka Shimizu, and Akira Mochizuki. 1998. "Three-dimensional tactile display for the blind." *Rehabilitation Engineering, IEEE Transactions on* no. 6 (3):249-256.
- Soll, Sebastian, Markus Antonietti, and Jiayin Yuan. 2011. "Double Stimuli-Responsive Copolymer Stabilizers for Multiwalled Carbon Nanotubes." *ACS Macro Letters* no. 1 (1):84-87.
- Song, Young Min, Yizhu Xie, Viktor Malyarchuk, Jianliang Xiao, Inhwa Jung, Ki-Joong Choi, Zhuangjian Liu, Hyunsung Park, Chaofeng Lu, and Rak-Hwan Kim. 2013. "Digital cameras with designs inspired by the arthropod eye." *Nature* no. 497 (7447):95-99.
- Song, Zeming, Teng Ma, Rui Tang, Qian Cheng, Xu Wang, Deepakshyam Krishnaraju, Rahul Panat, Candace K Chan, Hongyu Yu, and Hanqing Jiang. 2014. "Origami lithium-ion batteries." *Nature communications* no. 5.
- Srivastava, Akshay, Era Jain, and Ashok Kumar. 2007. "The physical characterization of supermacroporous poly(N-isopropylacrylamide) cryogel: Mechanical strength and

- swelling/de-swelling kinetics." *Materials Science and Engineering: A* no. 464 (1–2):93-100.
- Strachotova, B, A Strachota, M Uchman, M Šlouf, J Brus, J Pleštil, and L Matějka. 2007. "Super porous organic–inorganic poly(N-isopropylacrylamide)-based hydrogel with a very fast temperature response." *Polymer* no. 48 (6):1471-1482.
- Strachotova, B., A. Strachota, M. Uchman, M. Slouf, J. Brus, J. Plestil, and L. Matejka. 2007. "Super porous organic-inorganic poly(N-isopropylacrylamide)-based hydrogel with a very fast temperature response." *Polymer* no. 48 (6):1471-1482.
- Stumpel, Jelle E, Bartosz Ziólkowski, Larisa Florea, Dermot Diamond, Dirk J Broer, and Albertus PHJ Schenning. 2014. "Photoswitchable Ratchet Surface Topographies based on Self-Protonating Spiropyran-NIPAAM Hydrogels." *ACS applied materials & interfaces*.
- Sumaru, Kimio, Katsuhide Ohi, Toshiyuki Takagi, Toshiyuki Kanamori, and Toshio Shinbo. 2006. "Photoresponsive Properties of Poly(N-isopropylacrylamide) Hydrogel Partly Modified with Spirobenzopyran." *Langmuir* no. 22 (9):4353-4356.
- Sun, Y. G., W. M. Choi, H. Q. Jiang, Y. G. Y. Huang, and J. A. Rogers. 2006a. "Controlled buckling of semiconductor nanoribbons for stretchable electronics." *Nature Nanotechnology* no. 1 (3):201-207.
- Sun, Yugang, Won Mook Choi, Hanqing Jiang, Yonggang Y Huang, and John A Rogers. 2006b. "Controlled buckling of semiconductor nanoribbons for stretchable electronics." *Nature nanotechnology* no. 1 (3):201-207.
- Sun, Yugang, and John A. Rogers. 2007. "Structural forms of single crystal semiconductor nanoribbons for high-performance stretchable electronics." *Journal of Materials Chemistry* no. 17 (9):832-840.
- Suzuki, A., T. Ishii, and Y. Maruyama. 1996. "Optical switching in polymer gels." *Journal of Applied Physics* no. 80 (1):131-136.
- Suzuki, Atsushi, and Toyochi Tanaka. 1990. "Phase transition in polymer gels induced by visible light." *Nature* no. 346 (6282):345-347.
- Suzuki, Atsushi;Tanaka, Toyochi. 1990. "Phase transition in polymer gels induced by visible light." *Nature* no. 346 (6282):345-347.
- Tanaka, Fumihiko, Tsuyoshi Koga, Hiroyuki Kojima, and Françoise M Winnik. 2009. "Temperature-and tension-induced coil– globule transition of Poly (N-isopropylacrylamide) chains in water and mixed solvent of water/methanol." *Macromolecules* no. 42 (4):1321-1330.

- Tanaka, Fumihiko, Tsuyoshi Koga, and Françoise M Winnik. 2008. "Temperature-responsive polymers in mixed solvents: Competitive hydrogen bonds cause cononsolvency." *Physical review letters* no. 101 (2):028302.
- Tanaka, Toyochi. 1978. "Collapse of Gels and the Critical Endpoint." *Physical Review Letters* no. 40 (12):820-823.
- Tanaka, Toyochi, Izumi Nishio, Shao-Tang Sun, and Shizue Ueno-Nishio. 1982. "Collapse of Gels in an Electric Field." *Science* no. 218 (4571):467-469. d
- Tunckol, Meltem, Jérôme Durand, and Philippe Serp. 2012. "Carbon nanomaterial–ionic liquid hybrids." *Carbon* no. 50 (12):4303-4334..
- Ueki, Takeshi, and Masayoshi Watanabe. 2006. "Upper Critical Solution Temperature Behavior of Poly(N-isopropylacrylamide) in an Ionic Liquid and Preparation of Thermo-sensitive Nonvolatile Gels." *Chemistry Letters* no. 35 (8):964-965.
- Ummadisingu, Amita, and Suresh Gupta. 2012. "Characteristics and kinetic study of chitosan prepared from seafood industry waste for oil spills cleanup." *Desalination and Water Treatment* no. 44 (1-3):44-51.
- Unger, Marc A., Hou-Pu Chou, Todd Thorsen, Axel Scherer, and Stephen R. Quake. 2000. "Monolithic Microfabricated Valves and Pumps by Multilayer Soft Lithography." *Science* no. 288 (5463):113-116.
- Vaisman, L., G. Marom, and H. D Wagner. 2006. "Dispersions of Surface-Modified Carbon Nanotubes in Water-Soluble and Water-Insoluble Polymers." *Advanced Functional Materials* no. 16 (3):357-363.
- Vaisman, Linda, H. Daniel Wagner, and Gad Marom. 2006. "The role of surfactants in dispersion of carbon nanotubes." *Advances in Colloid and Interface Science* no. 128–130:37-46.
- Velazquez, R., E. E. Pissaloux, M. Hafez, and J. Szewczyk. 2008. "Tactile Rendering With Shape-Memory-Alloy Pin-Matrix." *Instrumentation and Measurement, IEEE Transactions on* no. 57 (5):1051-1057.
- Virtanen, Janne, Caroline Baron, and Heikki Tenhu. 2000. "Grafting of Poly(N-isopropylacrylamide) with Poly(ethylene oxide) under Various Reaction Conditions." *Macromolecules* no. 33 (2):336-341.
- Walter, R, J Ricka, Ch Quellet, R Nyffenegger, and Th Binkert. 1996. "Coil-globule transition of poly (N-isopropylacrylamide): a study of polymer-surfactant association." *Macromolecules* no. 29 (11):4019-4028.

- Wang, Wenwu, Toshihide Nabatame, and Yukihiro Shimogaki. 2005. "Interface structure of HfN_x/SiO₂ stack grown by MOCVD using TDEAHf precursor." *Surface Science* no. 588 (1-3):108-116.
- Wang, Xiaojia, Sean Kiluk, Chris Chang, and RC Liang. 2004. "Microcup® Electronic Paper and the Converting Processes." *Advanced Display* no. 3:012.
- Wichterle, O, and D Lim. 1960. "Hydrophilic gels for biological use."
- Winnik, Francoise M, M Francesca Ottaviani, Stefan H Bossmann, Wenseng Pan, Miguel Garcia-Garibay, and Nicholas J Turro. 1993. "Cononsolvency of poly (N-isopropylacrylamide): a look at spin-labeled polymers in mixtures of water and tetrahydrofuran." *Macromolecules* no. 26 (17):4577-4585.
- Winnik, Francoise M, H Ringsdorf, and J Venzmer. 1990a. "Methanol-water as a co-nonsolvent system for poly (N-isopropylacrylamide)." *Macromolecules* no. 23 (8):2415-2416.
- Winnik, Francoise M., H. Ringsdorf, and J. Venzmer. 1990b. "Methanol-water as a co-nonsolvent system for poly(N-isopropylacrylamide)." *Macromolecules* no. 23 (8):2415-2416.
- Wolf, B. A., and G. Blaum. 1975. "Measured and calculated solubility of polymers in mixed solvents: Monotony and cosolvency." *Journal of Polymer Science: Polymer Physics Edition* no. 13 (6):1115-1132.
- Wu, Chia-Jung, Akhilesh K Gaharwar, Burke K Chan, and Gudrun Schmidt. 2011. "Mechanically tough Pluronic F127/Laponite nanocomposite hydrogels from covalently and physically cross-linked networks." *Macromolecules* no. 44 (20):8215-8224.
- Xia, Y. N., and G. M. Whitesides. 1998a. "Soft lithography." *Annual Review of Materials Science* no. 28:153-184.
- Xia, Y. N., and G. M. Whitesides. 1998b. "Soft lithography." *Angewandte Chemie-International Edition* no. 37 (5):551-575.
- Xia, Yonan, and George M. Whitesides. 1998c. "Soft Lithography." *Annual Review of Materials Science* no. 28 (1):153-184.
- Xing, Yangchuan, Liang Li, Charles C. Chusuei, and Robert V. Hull. 2005. "Sonochemical Oxidation of Multiwalled Carbon Nanotubes." *Langmuir* no. 21 (9):4185-4190.
- Xue, Zhongxin, Shutao Wang, Ling Lin, Li Chen, Mingjie Liu, Lin Feng, and Lei Jiang. 2011. "A Novel Superhydrophilic and Underwater Superoleophobic Hydrogel-

- Coated Mesh for Oil/Water Separation." *Advanced Materials* no. 23 (37):4270-4273.
- Yamauchi, Hideo, and Yasushi Maeda. 2007. "LCST and UCST behavior of poly (N-isopropylacrylamide) in DMSO/water mixed solvents studied by IR and micro-Raman spectroscopy." *The Journal of Physical Chemistry B* no. 111 (45):12964-12968.
- Yang, Cheng, Wei Li, and Chi Wu. 2004. "Laser Light-Scattering Study of Solution Dynamics of Water/Cycloether Mixtures." *The Journal of Physical Chemistry B* no. 108 (31):11866-11870.
- Yin, J., Z. X. Cao, C. R. Li, I. Sheinman, and X. Chen. 2008. "Stress-driven buckling patterns in spheroidal core/shell structures." *Proceedings of the National Academy of Sciences of the United States of America* no. 105 (49):19132-19135.
- Yobas, Levent, Dominique M Durand, Gerard G Skebe, Frederick J Lisy, and Michael A Huff. 2003. "A novel integrable microvalve for refreshable braille display system." *Microelectromechanical Systems, Journal of* no. 12 (3):252-263.
- Yokoyama, F, I Masada, K Shimamura, T Ikawa, and K Monobe. 1986. "Morphology and structure of highly elastic poly (vinyl alcohol) hydrogel prepared by repeated freezing-and-melting." *Colloid and Polymer Science* no. 264 (7):595-601.
- Yoo, M. K., Y. K. Sung, Y. M. Lee, and C. S. Cho. 2000. "Effect of polyelectrolyte on the lower critical solution temperature of poly(N-isopropyl acrylamide) in the poly(NIPAAm-co-acrylic acid) hydrogel." *Polymer* no. 41 (15):5713-5719.
- Yoshida, Ryo, Yukinari Okuyama, Kiyotaka Sakai, Teruo Okano, and Yasuhisa Sakurai. 1994a. "Sigmoidal swelling profiles for temperature-responsive poly (N-isopropylacrylamide-co-butyl methacrylate) hydrogels." *Journal of membrane science* no. 89 (3):267-277.
- Yoshida, Ryo, Yukinari Okuyama, Kiyotaka Sakai, Teruo Okano, and Yasuhisa Sakurai. 1994b. "Sigmoidal swelling profiles for temperature-responsive poly(N-isopropylacrylamide-co-butyl methacrylate) hydrogels." *Journal of Membrane Science* no. 89 (3):267-277.
- Yphantis, David A, and Dennis E Roark. 1971. "Equilibrium centrifugation of nonideal systems. Donnan effect in self-associating systems." *Biochemistry* no. 10 (17):3241-3249.
- Yu, Cong, Senol Mutlu, Ponnambalam Selvaganapathy, Carlos H Mastrangelo, Frantisek Svec, and Jean MJ Fréchet. 2003. "Flow control valves for analytical microfluidic chips without mechanical parts based on thermally responsive monolithic polymers." *Analytical chemistry* no. 75 (8):1958-1961.

- Yu, Cunjiang, Yuping Pan, Huan Ma, Teng Ma, Jiaping Zhang, Yanmei Song, M Yashar S Kalani, Lenore Dai, and Hanqing Jiang. 2011. "Thermoresponsiveness of Integrated Ultra-Thin Silicon with Poly (N-isopropylacrylamide) Hydrogels." *Macromolecular rapid communications* no. 32 (11):820-824.
- Zhang, Bo-Yu, Wei-Dong He, Wen-Tao Li, Li-Ying Li, Ke-Ren Zhang, and Hao Zhang. 2010. "Preparation of block-brush PEG-b-P(NIPAM-g-DMAEMA) and its dual stimulus-response." *Polymer* no. 51 (14):3039-3046.
- Zhang, Guangzhao, and Chi Wu. 2001a. "Reentrant Coil-to-Globule-to-Coil Transition of a Single Linear Homopolymer Chain in a Water <math>\langle mi \rangle</mi></math>Methanol Mixture." *Physical Review Letters* no. 86 (5):822-825.
- Zhang, Guangzhao, and Chi Wu. 2001b. "Reentrant coil-to-globule-to-coil transition of a single linear homopolymer chain in a water/methanol mixture." *Physical review letters* no. 86 (5):822.
- Zhang, Guangzhao, and Chi Wu. 2001c. "The water/methanol complexation induced reentrant coil-to-globule-to-coil transition of individual homopolymer chains in extremely dilute solution." *Journal of the American Chemical Society* no. 123 (7):1376-1380.
- Zhang, Jian-Tao, Shi-Wen Huang, Fa-Zhi Gao, and Ren-Xi Zhuo. 2005. "Novel temperature-sensitive, β -cyclodextrin-incorporated poly (N-isopropylacrylamide) hydrogels for slow release of drug." *Colloid and Polymer Science* no. 283 (4):461-464.
- Zhang, Weixia, Yan Li, Changxu Lin, Qi An, Chengan Tao, Yongbing Gao, and Guangtao Li. 2008. "Electrochemical polymerization of imidazolium-ionic liquids bearing a pyrrole moiety." *Journal of Polymer Science Part A: Polymer Chemistry* no. 46 (12):4151-4161.
- Zhang, X. Z., and R. X. Zhuo. 1999. "Synthesis and characterization of a novel thermosensitive gel with fast response." *Colloid and Polymer Science* no. 277 (11):1079-1082.
- Zhang, Xian-Zheng, Yi-Yan Yang, and Tai-Shung Chung. 2002a. "Effect of mixed solvents on characteristics of poly (N-isopropylacrylamide) gels." *Langmuir* no. 18 (7):2538-2542.
- Zhang, Xian-Zheng, Yi-Yan Yang, and Tai-Shung Chung. 2002b. "Effect of Mixed Solvents on Characteristics of Poly(N-isopropylacrylamide) Gels." *Langmuir* no. 18 (7):2538-2542.

- Zhang, Xian-Zheng, Yi-Yan Yang, Tai-Shung Chung, and Kui-Xiang Ma. 2001. "Preparation and Characterization of Fast Response Macroporous Poly(N-isopropylacrylamide) Hydrogels." *Langmuir* no. 17 (20):6094-6099.
- Zhang, Xian-Zheng, and Ren-Xi Zhuo. 2000. "Dynamic Properties of Temperature-Sensitive Poly(N-isopropylacrylamide) Gel Cross-Linked through Siloxane Linkage." *Langmuir* no. 17 (1):12-16.
- Zhang, Xian-Zheng, and Ren-Xi Zhuo. 2001. "Dynamic properties of temperature-sensitive poly (N-isopropylacrylamide) gel cross-linked through siloxane linkage." *Langmuir* no. 17 (1):12-16.
- Zhang, Xianzheng, Daqing Wu, and Chih-Chang Chu. 2004. "Synthesis and characterization of partially biodegradable, temperature and pH sensitive Dex-MA/PNIPAAm hydrogels." *Biomaterials* no. 25 (19):4719-4730.
- Zhao, Bin, and Jeffrey S Moore. 2001. "Fast pH-and ionic strength-responsive hydrogels in microchannels." *Langmuir* no. 17 (16):4758-4763.
- Zhao, Jie, Feng Yan, Zhenzhen Chen, Hanbin Diao, Fuqiang Chu, Shaomei Yu, and Jianmei Lu. 2009. "Microemulsion polymerization of cationic pyrroles bearing an imidazolium-ionic liquid moiety." *Journal of Polymer Science Part A: Polymer Chemistry* no. 47 (3):746-753.
- Zhao, Liping, Yongjin Li, Zhifu Liu, and Hiroshi Shimizu. 2010. "Carbon Nanotube-Conducting Polymer Core-Shell Hybrid Using an Imidazolium-Salt-Based Ionic Liquid As a Linker: Designed As a Potential Platinum Electrode Alternative Material for Large-Scale Solution Processing." *Chemistry of Materials* no. 22 (21):5949-5956.
- Zhou, Xiaosi, Tianbin Wu, Kunlun Ding, Baoji Hu, Minqiang Hou, and Buxing Han. 2009. "The dispersion of carbon nanotubes in water with the aid of very small amounts of ionic liquid." *Chem. Commun.* (14):1897-1899.
- Ziolkowski, Bartosz, Larisa Florea, Jannick Theobald, Fernando Benito-Lopez, and Dermot Diamond. 2013. "Self-protonating spiropyran-co-NIPAM-co-acrylic acid hydrogel photoactuators." *Soft Matter* no. 9 (36):8754-8760.
- Zolfaghari, Reihaneh, Ali A Katbab, Javad Nabavizadeh, Ramin Yousefzadeh Tabasi, and Majid Hossein Nejad. 2006. "Preparation and characterization of nanocomposite hydrogels based on polyacrylamide for enhanced oil recovery applications." *Journal of applied polymer science* no. 100 (3):2096-2103.

APPENDIX A

PYRROLE-BASED POLY(IONIC LIQUIDS) AS EFFICIENT STABILIZERS FOR FORMATION OF HOLLOW MWCNT PARTICLES

1. Introduction

Carbon Nanotubes (CNTs) have been a material of interest in a diverse set of fields because of their remarkable characteristics such as high thermal, mechanical, and electrical properties, low mass density, etc. However, agglomeration of the nanotubes and their incompatibility with polymer matrices encompass some of the major challenges, which limit their employment in the many proposed applications, especially in the field of nano-composites. The fundamental limitations of carbon nanotubes highlight the need to focus on efficient methods for stable CNT dispersion, without reducing their desired thermal, mechanical, and electrical properties.

Broadly speaking, there are two approaches to disperse CNTs: first is the mechanical dispersion method, and the second is the alteration of the surface energy of the CNTs, either physically through non-covalent treatment, or chemically by the means of covalent bonding. Previously, most of work related to dispersion of CNTs (both single walled and multi-walled) have focused on high powered ultra-sonication for dispersing the materials by using a high shear rate. The major drawback of such an approach is the decreased aspect ratio of the nanotubes during the high shear mixing process as well as limited stability (Lu et al. 1996). Chemical methods, particularly the covalent treatment method, offer highly stable dispersions due to the chemical functionalization to increase the surface energy, providing repelling forces in between individual nanotubes (Najafi et al. 2006, Xing et al. 2005). Although this method is efficient, it can cause structural defects in the nanotubes, which significantly affects the performance of the CNTs and their potential applications. This occurs due to the aggressive nature of the chemical method, including high reaction temperatures and long reaction times, as well as the added surface pendant interrupting the

π -electron cloud of the CNTs (Bikiaris et al. 2008). In this context, non-covalent treatment offers an appealing route to disperse CNTs, mitigating the need for harsh thermal or mechanical treatments and allowing the crucial π -electron cloud of the graphitic nanotube structure to remain completely intact.

Non-covalent surface treatment for CNT dispersions generally comprises of utilizing different types of stabilizers, typically surfactants having both a hydrophilic and hydrophobic group, which are known to facilitate the homogenization of CNTs (Lu et al. 1996, Vaisman, Wagner, and Marom 2006, Vaisman, Marom, and Wagner 2006). One of the major drawbacks of surfactant-based stabilization is the need to use of large quantities of the stabilizers to prevent the aggregation of CNTs for any extended period of time. Secondly, most of the known surfactants used for this application do not share the same properties as CNTs, e.g. high conductivity or thermal stability, which interrupts the inherent property of the nanotubes when these molecules wrap around them. A new option to lessen the effect of the above disadvantages is to use ionic liquids (ILs), liquid salts having both organic and inorganic moieties, as an alternative to create stable dispersants of nanotubes. Recently, Fukushima et al. demonstrated this by dispersing CNTs in different ionic liquids (Fukushima et al. 2003). However, the non-covalent wrapping of the CNTs in ILs does not yield very stable dispersions in water or organic solvents.

Polymerized ionic liquids (poly(ionic liquids), PILs) feature a polymer backbone and pendant ionic liquid groups and can offer enhanced stability over ionic liquids for CNT dispersions. This is attributed to the longer chains of the PILs, which are hypothesized to aid in the wrapping of the CNTs and lead to more stable dispersions (Zhao et al. 2010).

Apart from the stability, PILs also offer extraordinary versatility in terms of hydrophilicity/hydrophobicity, a key factor for utilizing CNTs in different liquid systems. The polarity of the PILs can be tuned by simple anion exchange reactions to produce PILs of the same polymer backbone with a variety of anions, thus they can be solubilized in water to many different polar and nonpolar organic solvents corresponding to the polarity of the selected anion. Furthermore, PILs also offer the unique possibility of different functional backbones. In the present work, we demonstrate how intrinsically conducting polymers (or conjugated polymers, ICPs), such as polypyrrole, can be utilized as a functional backbone in PILs to create PIL-ICP hybrids to act as stabilizers for multi-walled carbon nanotubes dispersions in various solvents. Importantly, we expect to overcome the inherent lack of electronic conductivity in a pure ionic liquid-based system and at the same time aid the electronic properties of nanotubes, through the employment of the polypyrrole backbone, unlike the conventional use of nonconductive surfactants. Additionally, incorporating ionic liquid moieties to create the PIL-ICP hybrid system also solves the largest barrier to the use of ICPs alone, which is the lack of solubility in aqueous or many organic solvents, while allowing for the formation of novel CNT dispersions in multiple, differing solvents with stability in the range of several months.

The formed PIL-ICP hybrid stabilized CNT dispersions also offer unique possibilities in terms of applications. One unique usage of such dispersions is in the area of surfactant-free emulsions or Pickering emulsions, formed by adding an oil phase to the dispersion, to create droplets stabilized by MWCNTs. Due to the incorporated flexibility by the virtue of the PIL-ICP hybrids, different emulsions can be proposed with the same PIL-ICP

backbone, such as hexane-in-water or hexane-in-acetonitrile. The Pickering emulsions obtained from this technique demonstrate extended stability and unique characteristics. One of the most unique features of this type of emulsion was the ability to generate hollow conductive shells via the stabilization of the CNTs at the oil-water/acetonitrile interface. The morphology of the CNT particles formed from the emulsion droplets were studied with confocal microscopy and further characterized after drying by scanning electron microscopy (SEM) to view the shell morphology. The hollow particles can therefore be used as a payload carrier, depending on the solubility of the payload in the oil phase of the Pickering emulsion. In the present work, such an idea was demonstrated with silicon nanoparticles, which have limited solubility in the aqueous phase. Overall, this work proposes a new class of efficient PIL-ICP hybrids stabilizers with controllable hydrophilicity offering extended stability of carbon nanotube dispersions with novel applications in hollow particle formation via Pickering emulsion templating and in placing a payload into the shells.

2. Experimental Methodology

2.1. Pyrrole-based PIL Monomer Synthesis

Synthesis of the monomer was carried out according to literature, by first synthesizing the precursor molecule N-(4-bromobutyl)pyrrole, then using it to yield N-(4-butyl-(1-methylimidazole))pyrrole bromide monomer(Dehaen and Hassner 1991, Zhang et al. 2008, Zhao et al. 2009). All materials were used as-in from the suppliers, without further purification. 0.6 g ground potassium hydroxide (Sigma-Aldrich) and 150 mL dimethylformamide (ACROS Organics) were added to a 250 mL round bottom flask, under a nitrogen purge, magnetic stirring, and in an ice bath. 5 mL of 1,4-dibromobutane (ACROS Organics) was added, followed by the addition of 1 mL pyrrole (ACROS Organics) dropwise.

The mixture was stirred for 24 hrs. To purify the reaction mixture, 150 mL HPLC water (Fisher Scientific) was added to the reaction solution and the product was extracted into 300 mL diethyl ether (VWR International). Magnesium sulfate (Alfa Aesar) was used to dry the solution, and then the ether was evaporated under vacuum to yield the precursor molecule, N-(4-bromobutyl)pyrrole. ^1H NMR: 6.62, 6.12 (aromatic C-H); 3.92, 3.37 (C-H near Br); 1.99, 1.83 (alkane C-H). 1.2 g N-(4-bromobutyl)pyrrole and 0.59 g 1-methylimidazole (ACROS Organics) were added to 15 mL acetonitrile (Honeywell), heating at 60 °C under reflux, magnetic stirring, and a nitrogen purge two days. The monomer product, N-(4-butyl-(1-methylimidazole))pyrrole bromide, was then recovered after solvent evaporation. ^1H NMR: 10.32, 7.87, 7.24, 6.65, 6.12 (aromatic C-H); 4.22, 4.07 (C-H near aromatic); 3.95 (C-H on methyl group on imidazole ring); 1.92, 1.83 (alkane C-H).

2.2. Pyrrole-based Hydrophilic and Hydrophobic PIL Synthesis

The synthesis of the hydrophilic pyrrole-based PIL, poly(N-(4-butyl-(1-methylimidazole))pyrrole bromide) (PPy-Br), and the two hydrophobic pyrrole-based PILs, poly(N-(4-butyl-(1-methylimidazole))pyrrole hexafluorophosphate) (PPy-PF₆) and poly(N-(4-butyl-(1-methylimidazole))pyrrole bis(trifluoromethane)sulfonimide) (PPy-Tf₂N), were carried out according to literature (Zhao et al. 2009). 2.3 g of Iron(III) chloride hexahydrate (Fisher Scientific) was used as an oxidant and added to 12 mL HPLC water, under a nitrogen purge and magnetic stirring. 0.78 g of N-(4-butyl-(1-methylimidazole))pyrrole bromide was then added. After addition of the monomer, the solution was stirred for two minutes and then kept at room temperature for 24 hours without further stirring. The polymerization was terminated by pouring the mixture into a great deal of acetone. The black power product was then filtered out and washed with acetone and methanol until the

washing solution became clear, with subsequent drying under vacuum to yield the PPy-Br product. To form the hydrophobic PILs, a simple anion exchange procedure was carried out with PPy-Br and two hydrophobic anion containing salts, potassium hexafluorophosphate to create PPy-PF₆ and lithium bis(trifluoromethane)sulfonimide to create PPy-Tf₂N (both salts being from Sigma-Aldrich). 0.02 g of PPy-Br was dissolved in 10 mL HPLC water, and a solution of 0.04 g of the corresponding salt in 10 mL of water was added dropwise to the first solution, under stirring at room temperature for 24 hours. The resulting hydrophobic precipitate was filtered and washed with HPLC water and dried under vacuum to yield the hydrophobic PIL powders.

2.3. PIL-stabilized CNT Dispersion and Emulsion Formation

For stability testing, CNTs were dispersed in various solvents with and without a PIL stabilizer. 5 mg of CNTs and 5 mg of a pyrrole-based PIL were added to 25 mL of HPLC water. The solution was ultrasonicated for fifteen minutes in an ice bath with a Sonics VibraCell 500W to create a stable, homogeneous black solution. For the control without the PIL stabilizer, 5 mg of CNTs and 25 mL of the solvent were sonicated in an ice bath for the same time. To create the hexane-in-water Pickering emulsion stabilized by the PIL-CNT, 1.5 mL of hexane was added to a solution of CNTs stabilized in water by PPy-Br, according to the procedure above. This was then put on a shaker for 10 minutes. Hexane-in-acetonitrile emulsions with PPy-PF₆ or PPy-Tf₂N as the CNT stabilizer were prepared in an identical fashion. A 2.5% w/w suspension of Silicon (Si) nanoparticles in octane was mixed with the CNT suspension at a ratio of 3:5 by volume. The ratio of the weights of Si nanoparticles to CNT was 1:1.

2.4. Material Characterization and Hollow Particle Formation

^1H Nuclear Magnetic Resonance (NMR) spectra were taken with a Bruker 400 MHz NMR spectrometer in deuterated chloroform (Cambridge Isotope Laboratories). Fourier transform infrared spectra (FTIR) were generated with a Bruker IFS 66V/S FTIR spectrometer, incorporating the samples into potassium bromide pellets. A TA Instruments Thermogravimetric Analyzer (TGA) Q500 was used to analyze the thermal weight loss under nitrogen. The PIL samples were placed in a tared platinum crucible and heated from 25 to 600 °C at a heating rate of 10 °C min⁻¹, while the PIL-CNT emulsion samples were heated from 25 to 900 °C at a heating rate of 20 °C min⁻¹. Microscopic morphologies of the solutions and emulsions were taken using a confocal laser-scanning microscope (Leica TCS SP5), a FEI/Philips XL30 Environmental FEG Scanning Electron Microscope (SEM), and a Philips CM200-FEG Transmission Electron Microscope (TEM). To yield the hollow particles, the emulsion droplets were initially frozen at -18 °C and then freeze dried using a 1L bench top Labconco FreeZone freeze dryer for 24 hours followed by gold sputtering for 100s. The obtained frozen emulsion particles were subsequently studied using the XL-30 SEM for surface morphology.

3. Results and Discussion

3.1. Synthesis and Characterization of Pyrrole-based PILs

The synthesis of the polypyrrole-based poly(ionic liquids) (PILs) was performed following the synthesis of the precursor molecule, N-(4-bromobutyl)pyrrole, and then the creation of the hydrophilic N-(4-butyl-(1-methylimidazole))pyrrole bromide monomer. This monomer was then polymerized with the aid of iron chloride hexahydrate as an oxidant to create the hydrophilic PIL-ICP hybrid, poly(N-(4-butyl-(1-methylimidazole))pyr-

role bromide) (PPy-Br). Simple anion exchanges with the salts potassium hexafluorophosphate and lithium bis(trifluoromethane)sulfonamide, yielded the hydrophobic PIL-ICPs, poly(N-(4-butyl-(1-methylimidazole))pyrrole hexafluorophosphate) (PPy-PF₆) and poly(N-(4-butyl-(1-methylimidazole))pyrrole bis(trifluoromethane)sulfonimide) (PPy-Tf₂N), respectively. Figure A1 shows the FTIR spectra of these three synthesized PILs to show the successful creation of the PILs and anion exchanges. From the FTIR spectra, the characteristic peaks of the poly(pyrrole) (PPy) backbone in the range of 3600 – 3200 and 1700 – 1200 cm⁻¹ can be seen. In addition, absorption bands near 1050 cm⁻¹ (-NH bending deformation) and 950 cm⁻¹ (-CH out of plane bending) can be observed. This indicates that each PIL has the same PPy backbone.

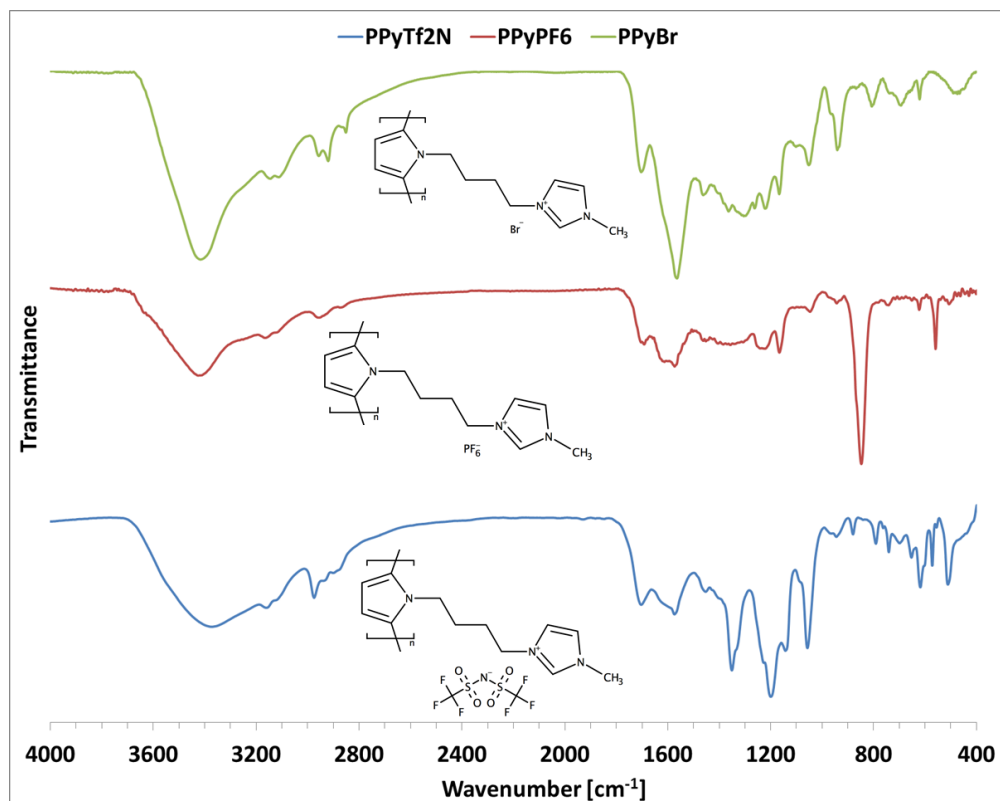


Figure A1. FTIR spectra of the synthesized polypyrrole-based PILs with their respective chemical structures below each curve, from the top down, PPy-Br (green), PPy-PF₆ (red), and PPy-Tf₂N (blue).

The anion exchange of the PILs was done to control the hydrophilicity, as the Br anion is highly polar and hydrophilic and can be easily exchanged with nonpolar and hydrophobic anions to yield hydrophobic PILs as precipitates in water to be easily filtered off and recovered. The anion exchange between Br and PF₆ can be seen in the FTIR spectra through the addition of absorption bands in the PPy-PF₆ spectrum at 1169 cm⁻¹, 841 cm⁻¹, and 559 cm⁻¹ corresponding to the newly present P-F bonds (Zhao et al. 2009). The anion

exchange between Br and Tf₂N is recognized through the appearance of peaks corresponding to the Tf₂N anion, including 1350 cm⁻¹ (SO₂), 1200 cm⁻¹ (CF₃), 1150 cm⁻¹ (SO₂), and 1050 cm⁻¹ (S=N=S))², cm⁻¹(Höfft, Bahr, and Kemper 2008). With the successful synthesis of three PIL-ICP hybrids of varying hydrophobicity, we sought out to take advantage of these characteristics to stabilize CNTs in various solvents, with subsequent emulsion formation and hollow particle generation.

3.2. Polypyrrole-based PIL-stabilized MWCNT Dispersions

Traditional ionic surfactants, such as sodium dodecyl sulfate (SDS), have long been used as a dispersant for carbon nanotubes. However surfactants such as SDS are not thermally stable for many procedures, including large scale melt-blend processing. As far as aqueous dispersions of CNTs are concerned, long-chain ionic liquids (ILs) can be good alternatives to traditional surfactants. Fukushima first described the efficacy of such materials with imidazole-based IL systems (Fukushima et al. 2003). Surfactant-like long-chain ILs such as 1-alkyl-3-methylimidazolium bromides, butyl-a,b-bis(dodecylimidazolium bromide), carbazole tailed ILs (1-n-(N-carbazole)alkyl]-3-methylimidazolium bromide) and imidazolium ion-based ILs with hexadecyl alkyl chains have been found to be quite effective in dispersing CNTs in water. It is also worth mentioning here, that although majority of work utilizes these types of ILs, other combinations are also possible as proposed in literature (Tunckol, Durand, and Serp 2012) and several types of long- and short-chain ILs have been investigated to disperse CNTs in aqueous solvents. However, when using short-chain ILs, the stability of the CNT dispersions is not very long. In the present work, the unique synthesized pyrrole-based PILs were utilized as stabilizers of multi-walled carbon nanotubes (MWCNTs) in order to achieve enhanced emulsion stability, take advantage

of the increased thermal and electrical properties of the pyrrole backbone and the tuning of the hydrophobicity by selection of the PIL anion to disperse the CNTs in varying solvents.

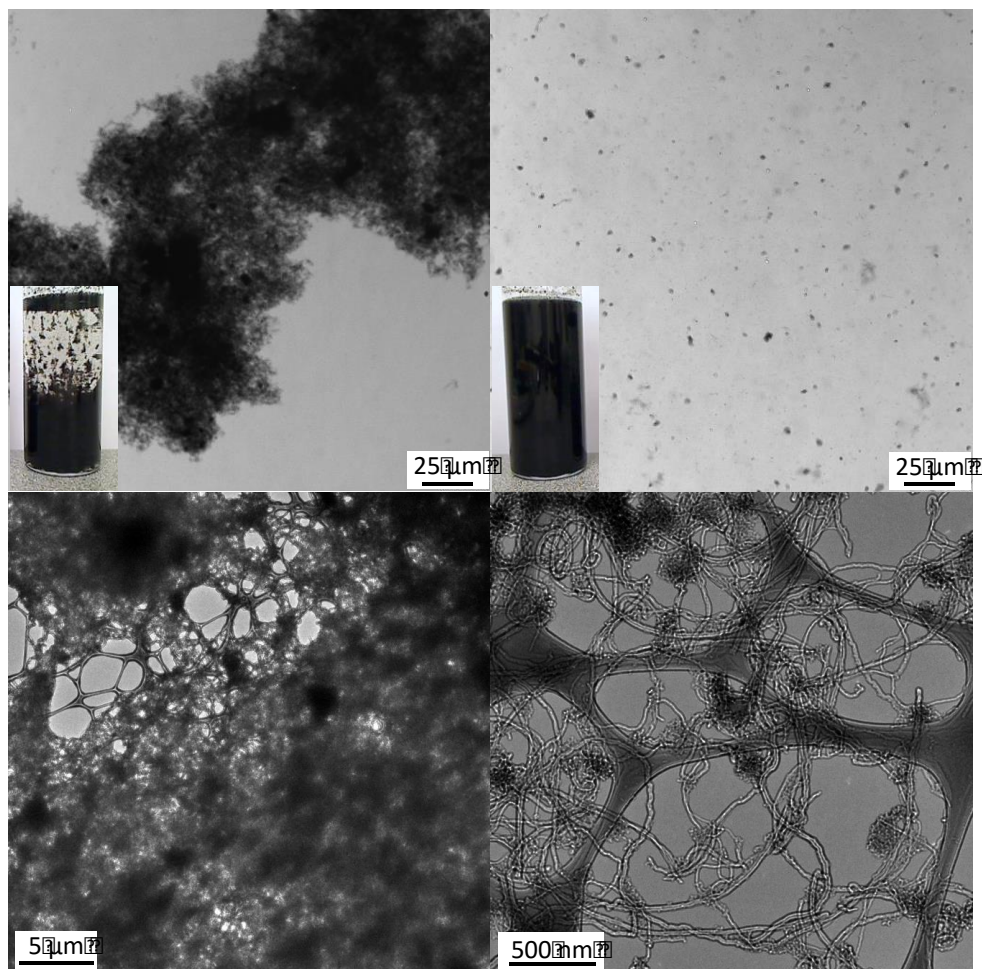


Figure A2. MWCNTs dispersed in water without (a and c) and with (b and d) the PPy-Br stabilizer. a and b: macroscopic stability 8 hr after dispersion (insets left) and corresponding confocal images with 25 μm scale bars, c and d: TEM images of the CNT dispersions with 5 μm and 500 nm scale bars, respectively.

Figure A2 compares the stability and resulting microscopic morphology of CNT dispersions in water with and without the hydrophilic PIL, PPy-Br, as the stabilizer. The macroscopic images of the dispersions in Figures A2a and b (left inset) demonstrate the

efficacy of the PIL as a dispersant, with these images taken 15 min after ultrasonication. It can be clearly seen that the CNT dispersion with no stabilizer has fully destabilized, while the PPy-Br successfully stabilizes the CNTs to create a homogenous black solution. All of the samples prepared here have dispersion stability greater than 6 months. The confocal and TEM images confirm the micro- and nano-stability, respectively, with large aggregates seen for CNT-in-water without a dispersant for both the micro- and nano-regime. For the dispersion with PPy-Br, no large aggregates can be seen in the confocal images and the resulting TEM images clearly show individual nanotubes, which have been spaced away from each other by the PIL. No large aggregates were seen with TEM for the dispersion with PPy-Br.

Like traditional surfactants, the PIL-based stabilizers adsorb on the CNT surface via their hydrophobic polypyrrole backbone and long alkyl chain orienting the cationic imidazolium groups with the corresponding hydrophilic Bromide anion toward the aqueous phase. The positive charges created on the CNTs prevent them from aggregating and give them extended stability due to the enhanced zeta potential caused by their charged nature. The high stability is additionally ascribed to longer chains of the polymerized ionic liquid, which can easily wrap around the nanotubes, as illustrated in Figure A3a. This property of the polymerized ionic liquid is different from other non-covalent methods, in that the molecular weight of the PILs is much higher than a simple surfactant or monomeric IL, which generally lead to lower dispersion stability of CNTs in water or organic solvents. This hypothesis is supported by the fact that the dispersing ability of the surfactants generally increases with the increasing length of the alkyl chain, which is reflected by an increased absorbance on the UV–NIR spectrum (Liu et al. 2010, Dong et al. 2011). For simple ionic

liquids, the effect of different groups at the 3-position of the imidazole ring with a hexadecyl alkyl chain has been investigated in terms of CNT dispersing ability (Di Crescenzo et al. 2009). Through a systematic study, it was found that hydrophobic groups (e.g., phenyl group) increased the affinity of the surfactant toward the CNTs, but too hydrophobic of a group decreased the water solubility of the surfactant, thus favoring micelle self-assembly. Results of this study demonstrated that 1-hexadecyl- 3-phenylimidazolium bromide was the most efficient among the investigated surfactants (Di Crescenzo et al. 2009). Hence, a good balance between the hydrophilic and hydrophobic domains is needed to obtain an effective CNT stabilizer, which is easily obtained by the tunability of the PIL-ICP stabilizers in this work. Liu and co-workers showed that IL-based Gemini (dimeric) surfactants, which consist of two imidazole ring head groups and two hydrophobic chains separated with a spacer, were more effective in dispersing CNTs than the IL-based monomeric surfactants (Di Crescenzo et al. 2009). The long alkyl chain ILs formed aqueous dispersions of CNTs, which remained stable for months. Zhou and co-workers investigated the dispersion of CNTs using very small amounts of short-chain ILs in water and found that ILs bearing both an amino group and imidazolium or pyridinium core are very effective in dispersing CNTs in water. (Zhou et al. 2009). A very small quantity of IL, as little as 1.4 wt%, was sufficient to achieve this. In our work, a 1:1 mass ratio of PIL stabilizer to CNT was used for the dispersions, which is much less than dispersions utilizing conventional surfactants (Hermant, Klumperman, and Koning 2009)

Table A1. PIL-ICP polarity importance in dispersing MWCNT in various solvents (stable dispersion denotes a greater than 6 month stability).

		Polarity of Solvent →		
		SOLVENTS	Acetone	Acetonitrile
Polarity of PIL ↓	PILs			
	PPy-Tf₂N	Stable Dispersion	Stable Dispersion	Unstable Dispersion
	PPy-PF₆	Stable Dispersion	Stable Dispersion	Unstable Dispersion
	PPy-Br	Unstable Dispersion	Unstable Dispersion	Stable Dispersion

Modifying the polarity/hydrophobicity of the overall PIL by simple anion exchange is one of the major advantages of their use as a stabilizer, with Table 1 demonstrating the dispersion capability of the three synthesized PILs for CNTs in varying solvents, forming stable solutions for longer than 6 months. PPy-Br can easily form stable dispersions of CNTs in water, but was unable to form stable dispersions in acetone or acetonitrile due to the hydrophilic/polar nature of the PIL, a direct result of the Br anion.. In contrast, PPy-PF₆ and PPy-Tf₂N were able to form stable dispersions in acetone and acetonitrile, but not water, due to their non-polar hydrophobic nature, with Tf₂N being a more hydrophobic anion than PF₆ (Chiappe and Pieraccini 2005).

Thermogravimetric analysis (TGA) can be used to probe the interaction between the PIL stabilizer and the CNTs. Figure A3b shows the TGA scans for the neat PIL stabilizers, with PPy-Br possessing less stability, with PPy-Tf₂N possessing the most before the decomposition step around 330 C, where the trend switches and PPy-Tf₂N possesses the least stability with PPy-PF₆ being the most stable. These differences in stability are directly related to the differences in the stability of the anion, with the hydrophobic PF₆ and Tf₂N stabilizing the PPy backbone, until there is a drastic degradation of the many function groups in the Tf₂N anion, with the PF₆ anion remaining the most stable to thermal loss. The quantity of the grafted IL moiety can be determined from TGA. Under air atmosphere, the onset decomposition of pristine MWCNT is between 873K to 973 K (600-700C) depending on the sample and the heating rate. For the CNTs associated with the PIL stabilizers, there are two onset temperatures, as seen in Figure A3c. This suggests that the stabilized nanotubes demonstrated higher stability than pristine CNT. Interestingly, the CNT decomposition is also determined by the PIL counterion. The stability of PF₆- ion was found to higher than the TF₂N and Br ions.

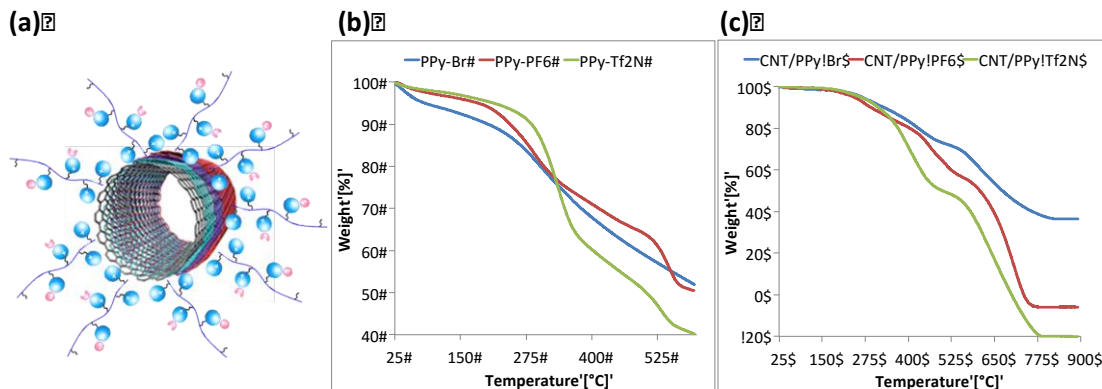


Figure A3. (a) Schematic showing the proposed interaction between the PIL-ICP hybrid stabilizers and the surface of a MWCNT. (b) TGA scans showing the comparative degradation of the synthesized PIL-ICP hybrid powders. (c) TGA scans showing the comparative degradation of the respective dried PIL-CNT dispersions with the pristine MWCNTs, showing the interaction between the two materials.

3.3 Oil in water emulsion stabilized by PIL-MWCNT

The poly-ionic liquids synthesized in the previous section demonstrated superior ability of carbon-nanotube stabilization. Along with a conductive backbone the present method of CNT stabilization offers the unique capability of dispersing and stabilizing the CNT for extended period of time in various conditions; both aqueous and organic. The latter ability of utilizing versatile dispersion solvent is credited to possibility of facile exchange of anions. The replacement of ions has a strong influence on the hydrophilic/hydrophobic character of the PILs. In the present section we explore the idea of utilizing such dispersions as template for stabilizing two immiscible phases, e.g. water and hexane. The present approach of utilizing nanotubes as the stabilizing agent could be bracketed under novel “pickering emulsion” technique.

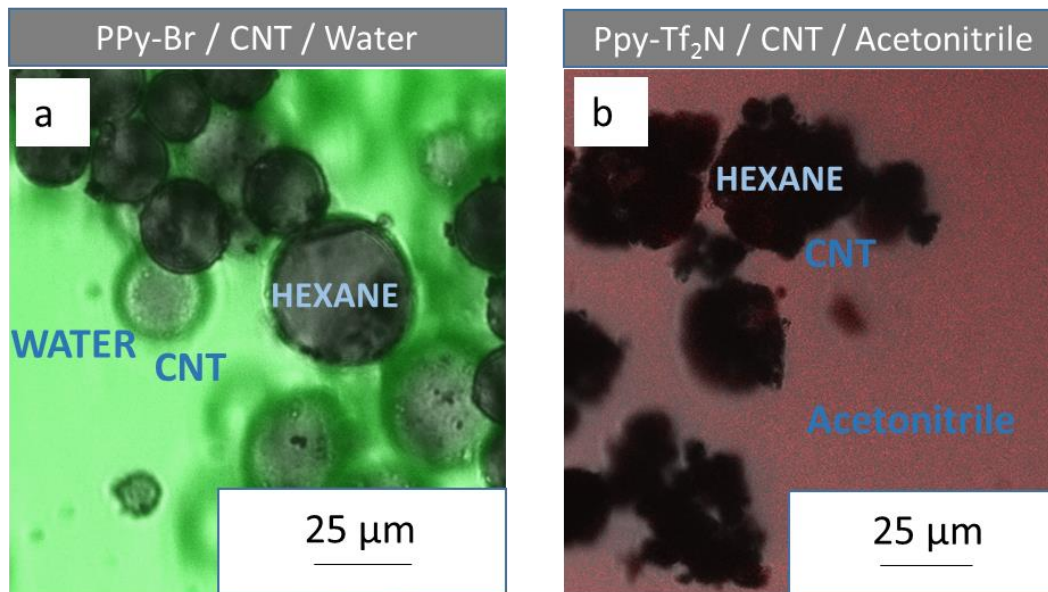


Figure A4. Confocal images of the Pickering emulsions showing the CNT-stabilized droplets. (a) PPy-Br / CNT / water(green)/hexane, (b) PPy-Tf₂N / CNT / acetonitrile(red)/hexane.

Figures A4a, A4b are images from a confocal microscope clearly depicting the ability of utilizing these nanotubes for formation of emulsion with uniform droplet size in two immiscible phase combinations; water-hexane and acetonitrile-hexane. On homogenizing the CNT laden water or acetonitrile phase with an immiscible solvent- hexane and acetone respectively, there is quick movement of CNT to the oil and water interface. Specifically, the aqueous/acetonitrile phase became very clear and transparent, demonstrating that the CNTs have completely transferred to the oil/water interface of the emulsions. Specifically, both the vials contain equal volumes of water and hexane with PIL and CNT being 3 mg each. The emulsion phase accounts for ~40% volume fraction of the total liquid. The obtained emulsion was very stable during storage under ambient conditions, as shown in inset

of figure 4. The droplet size remained almost unchanged over 100 h. As gradual evaporation of the organic solvent, some of the CNTs transferred to the wall of the vial and the total volume of emulsion was reduced. Importantly, both these emulsions show good coverage and have considerable homogeneity in terms of droplet size.

To visualize the droplets better, the water was dyed with a hydrophilic compound, sodium fluorescein (Figure A4a). Similarly, in figure A4b the organic phase- acetonitrile has rhodamine b incorporated for the distinctive pink coloration. The dyeing also elucidates that the first emulsion could be clubbed under oil in water system determined by the dye solubility test by tracing the colors of the emulsion droplets and the continuous phase after adding the above mentioned green water-soluble dye (fluorescent Na salt) appearing outside the droplets and no coloration appearing in the continuous phase. Importantly, apart from the visual appearances, the crucial CNT stabilizing molecule is different in both these experiments-PPyBr (right) and PPyTf₂N (left). The studies clearly reveal that both these previous CNT dispersions are compatible enough for emulsion formation. Moreover, such studies acquire novelty in terms of ease of formation and stability (greater than 100 hours) in versatile media. Such diversity and tunability has not been achieved previously by other methods and thus possesses the possibility of expanding the utilization of these emulsion for diverse applications. Previously, certain pure ionic liquids have tried to demonstrate similar capability of being used as dispersant and replacing surfactant for formation of novel “Pickering emulsions”. However, these studies require addition of certain additives or particles; e.g. silicon to aid in stabilizing the immiscible phases (Gao et al. 2011) and therefore cannot be classified as pure CNT stabilized emulsions. Furthermore, studies were

undertaken to probe the ability of the above synthesized PILs as dispersant by themselves. However, they showed limited ability to do so.

Among, the other studies in this field, Gao et al. utilized acid treated dispersions of CNT along with pure ionic liquid as a similar template for pickering emulsion process (Gao, Yin, and Wang 2010). They suggested that the ionic liquids can be used to stabilize two immiscible phases, water and cyclohexane with the aid of acid treated nanotubes. The hydrophobic ionic liquid, e.g. 1-butyl-3-methylimidazolium hexafluorophosphate, is useful in helping to tune the highly hydrophilic character of the acid treated nanotubes to mix the nanotubes with the oil phase which was cyclohexane in their case study. Although, such studies clearly indicate the efficacy of ionic liquids as good dispersant; the nanotubes still need prior treatment before their use as Pickering emulsion stabilizers. Therefore, the present use of poly(ionic) liquid could be considered superior to the method proposed by Gao and co-workers as it allows the option of utilizing various solvents. Moreover, the use of acid treatment for previous methodology is expected to decrease the aspect ratio of the CNT, a fact which has been verified before. (Lu et al. 1996). Also Figures A4a, A4b demonstrate that the PILs stabilized nanotubes are considerably more efficient than their ionic liquid alternative is able to form the emulsion droplets of considerable uniform size. Importantly, ratio of the CNT to poly(ionic-liquid) is 1:1 to form these emulsions droplets which considerably lesser than the surfactants required (> 5 times) for similar purposes. The microscopic image taken for the liquid droplets acquired from the emulsion phase shows that the average emulsion droplet sizes appear to be around 3-20 μm , tens of times smaller than those prepared by only MWNT.

3.4 Formation of hollow droplets

The emulsions in section 3.3 demonstrated that ability of using different PILs for formation of different emulsions with the help of nanotubes. The nanotubes are dispersed only at the interface due to the effect of PILs which are wrapped on the surface of the CNT. Figure A5, elucidates a facile method of hollow particle creation using the same pickering emulsion as discussed above. The method relies on the controlled evaporation of the water and hexane phase with the CNT particles clubbed carefully at the interface. Unlike the previous work of Panhuis et al. which suggested the cross-linking of emulsion by glutaraldehyde for formation of hollow CNT particles, the present method does not rely on chemical cross-linking (Panhuis and Paunov 2005). Instead the self-assembly nature of the CNT allows the formation of homogenous droplets. To understand the morphology of the droplets better, continuous phase was carefully dried with help of freeze-drying and then studied under the SEM. The SEM studies reveal presence of good stability of the emulsion, as the droplet diameter was uniquely uniform in the experiment.

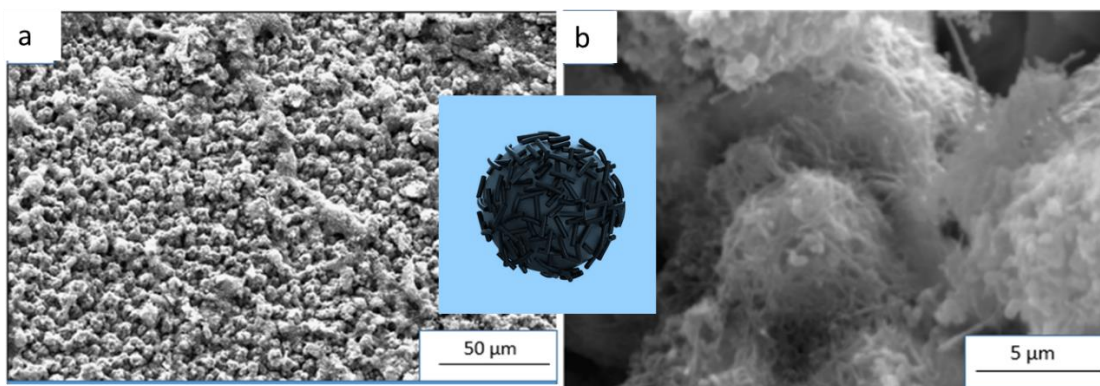


Figure A5. a, b: SEM images of the formed hollow particles from the PPy-Br / CNT / water Pickering emulsions. Inset is a schematic showing the morphology of the CNT shell.

The hollow nature of such particles present a unique possibility of incorporating functional particles. One such example demonstrated here, is the encapsulation of silicon nanoparticles. Figure A6c, A6d is a confocal microscopy of such hybrid structure in wet phase. The above reported method offer a simple emulsion-templated directed assembly technique for forming silicon carbon composite particles, which could be further investigated for energy application. Using this method, we are able to confine the Si nanoparticles to regions that are surrounded by a porous carbon black cage and an interconnected conductive carbon black network.

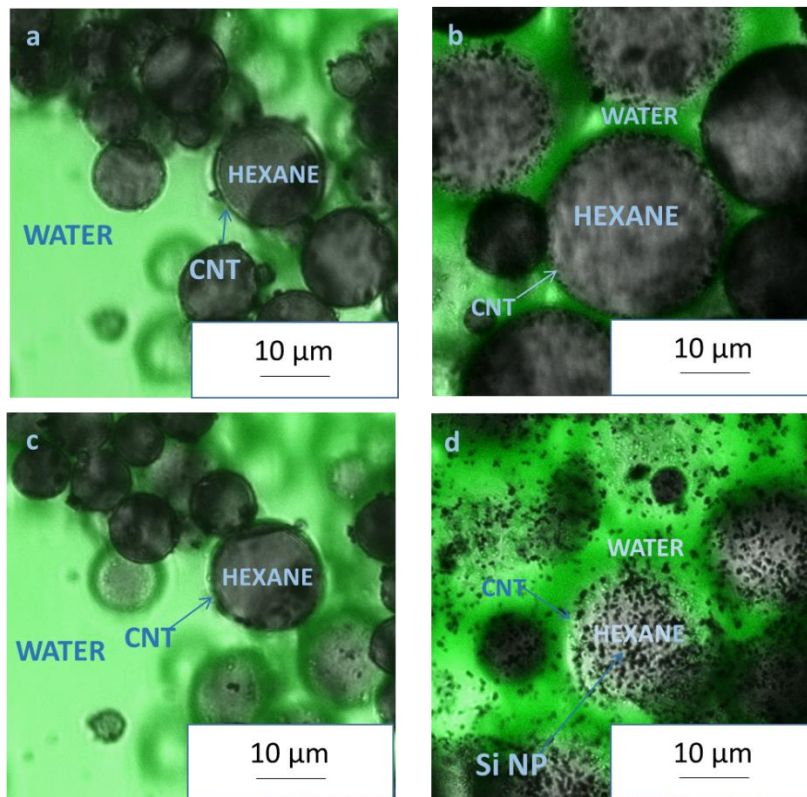


Figure A6. Confocal images depicting Si incorporation in the CNT stabilized hexane droplets, (a),(c) Hexane droplets in water phase, (c),(d) Silicon dispersed in hexane phase.

4. Conclusion

Overall, the present work proposes a new class of efficient ICP-IL hybrid with controllable hydrophilicity and overcomes the inherent challenges of classical ICPs of low electronic conductivity of IL by using conducting polypyrrole as the polymer backbone. Importantly, such unique dispersions demonstrated high degree of stability ranging over months even with low amounts of dosage. Using the concept of pickering emulsion, the PILs stabilized dispersions were then used to form different emulsions, such as water-hexane and acetonitrile-hexane. Such a versatile template of emulsion is then utilized for formation of unique hollow CNT shells with the capability of loading hydrophobic materials into them.